

Table of Contents

Introduction:	1
Different types of flying wings:	2
Advantages of flying wings:	2
Disadvantages of flying wings:	3
The purpose of design UAV system	3
Comparison between the flying wing aircraft and the conventional aircraft:.....	4
The flying wing design Process:	5
Mission specifications:	6
Chapter 1: Initial Design	7
Step 1: Wing Geometry	7
Step 2: Airfoil Selection.....	8
Step 3: Washout	8
Step 4: Lift distribution	11
Step 5: Elevon Design.....	11
Step 6: Flap Design.....	12
Step 7: Centre of Gravity.....	13
Chapter 2 Design optimization	15
What's optimization?	15
Steps for the optimization process	15
1 st optimization problem (Maximize local lift coefficient)	16
2 nd optimization problem (Minimize induced drag)	17
Chapter 3 Propulsion system	19
Motor:	20
Rimfire motors	21
RimFire .60	21
RimFire .80	22
RimFire 1.20	22
Electronic speed controller:	24
The power source (battery):	25

ii Flying wing Design and Manufacturing project

Chapter 4 Aerodynamics.....	31
Design Stage	31
Wing Profile.....	31
Wing Aerodynamics	38
II. Analysis Stage	41
2D Analysis:.....	41
3D Analysis.....	46
Solution at the Design Point.....	47
Chapter 5 Structural Design:.....	56
Introduction:	56
Flying Wing Geometry:	57
Material Selection:	57
Introduction to composite materials:	57
Choice of materials:	59
Aircraft Loads:	59
The aircraft Structural components:.....	59
Wing Structural design:.....	59
Fuselage structural design:	63
Finite Element Analysis (FEA):.....	64
General:.....	64
Preliminary Decision:	66
The Preprocessing:.....	67
The post processing:	78
Conclusion:.....	81
Chapter 6 Aircraft Geometric model	82
The Solid model:	82
The wing solid model:	82
The Fuselage solid model:.....	84
Nose part:.....	85
Tail part:	85
The control surfaces:.....	88
Wing Flap:	88

Wing Elevon:	89
The wing structure:	90
The upper skin:	90
The Lower Skin:	92
Wing Ribs:	92
The Fuselage Structure:	93
The fuselage Skin:	93
The fuselage Frames:	94
The Flying wing views:	95
Chapter 7 The Flying Wing mass model:	97
Structural Component:	97
Propulsion Components:	98
Control elements:	98
The aircraft center of mass:	99
The aircraft moment of inertia (Kg m^2):	99
Chapter 8 Aircraft Simulation:	100
Introduction:	100
The Equation of motion for the rigid aircraft:	100
The force equations from the linear momentum:	101
The moment equations from the angular momentum:	101
The Euler angles:	101
The Aircraft position X, Y, Z:	101
MATLAB simulink:	102
Euler angle representation of six-degrees-of-freedom equations of motion:	103
The input variables:	106
Atmospheric Parameter	106
Flight conditions	106
The Aircraft Geometry	106
Lift Coefficient	106
Drag Coefficient	106
1.1.1 Coefficient of the Y-D force	106
1.1.2 Rolling moment coefficient	106

Pitching moments coefficient	107
Yawing moment coefficient	107
Moment of inertia.....	107
The final results:.....	109
The angle of attack:.....	109
The Aircraft velocity:	109
Theta VS Time:	110
The angular velocity:.....	110
Chapter 9 Performance Analysis:.....	111
Steady flight performance	111
Accelerated flight performance	111
Steady flight performance	112
Accelerated flight performance	120
Chapter 10 Stability and Control.....	123
Longitudinal Stability	123
Lateral stability.....	124
Directional stability	126
Sizing of Control Surfaces	127
Sizing to Longitudinal Motion (Steady & level Flight) and Take Off	127
Cruise	127
Take Off.....	127
Calculating Coefficients of Flap, Elevator and Aileron	127
Elevator & Flap.....	128
Aileron.....	130
Control Surface Size & Data	130
1.1. Cruise	131
1.2. Take off	131
Stability Study	132
1. Longitudinal stability study	132
Lateral Stability Study	133
Chapter 11 Manufacturing.....	136
Master Mold.	136

Laser cut:	136
Fix the Jig:.....	137
Fix the ribs into the jig:	137
Fix the spars along the ribs:	138
Cover the upper surface of the construction by Balsa wood Sheets:.....	138
Cover the upper skin by Fiber Glass:.....	139
7. Break the connection between the ribs and the jig.....	140
8. Invert the Body to repeat the previous process to the lower surface.....	140
9. Sanding the Master Mold.....	140
10. Fill the Master Mold with Poly-Fiber Putty and Paint it.....	141
Female Mold	141
Construct a frame	141
Fill the empty space	142
Isolate the surface.....	142
Make an AEROSIL Fillet	143
Cover Master Mold with Fiber Glass.....	143
Separate the frame	144
Make a check	144
Wing Body:.....	145
Put the Carbon Fiber	145
3K, 2 x 2 Twill Weave Carbon Fiber Fabric	146
Construct the internal structure	146
Install the structure inside the wing skin	147
Use carbon fiber tape	148
Spray paint the wing.	148
Control Surfaces:.....	148
Cut the control surfaces.....	148
Install the servos.	149
Install the control surfaces.....	150
Fuselage:	151
Make the Master Mold	151
Make the female mold.....	151

Make the fuselage body.....	152
Spray Paint the fuselage.	153
Installing motor and all other devices:	153
Mount the motor	153
Fix the landing	153
Fix the Instruments	153
Appendices:.....	154
Appendix A: The ANSYS Report for model 1:.....	154
Appendix B: The ANSYS Report for mode 2	177
Units	177
References:	200
• Karl Nickel, Michael Wohlfahrt, “Tailless Aircraft”	200
• John D. Anderson, “Aircraft Performance and design”	200
• John D. Anderson, “Introduction to Flight”	200

Introduction:

Airplane design means the intellectual engineering process of creating on paper a flying machine to meet certain specifications and requirements, Pioneer innovative new idea and technology. **In our project** we desire to design a **Flying wing**; flying wing means aircraft with one surface only simply it is a tailless aircraft. Theoretically the flying wing is the most efficient aircraft configuration from the point of view of aerodynamics and structural weight. It is argued that the absence of any aircraft components other than the wing should naturally provide these benefits. However in practice an aircraft's wing must provide for flight stability and control; this imposes additional constraints on the aircraft design problem. Therefore, the expected gains in weight and drag reduction may be partially or wholly negated due to design compromises needed to provide stability and control. Alternatively, and more commonly, a flying wing type may suffer from stability and control problems.



Figure 1- Flying Wing

Different types of flying wings:

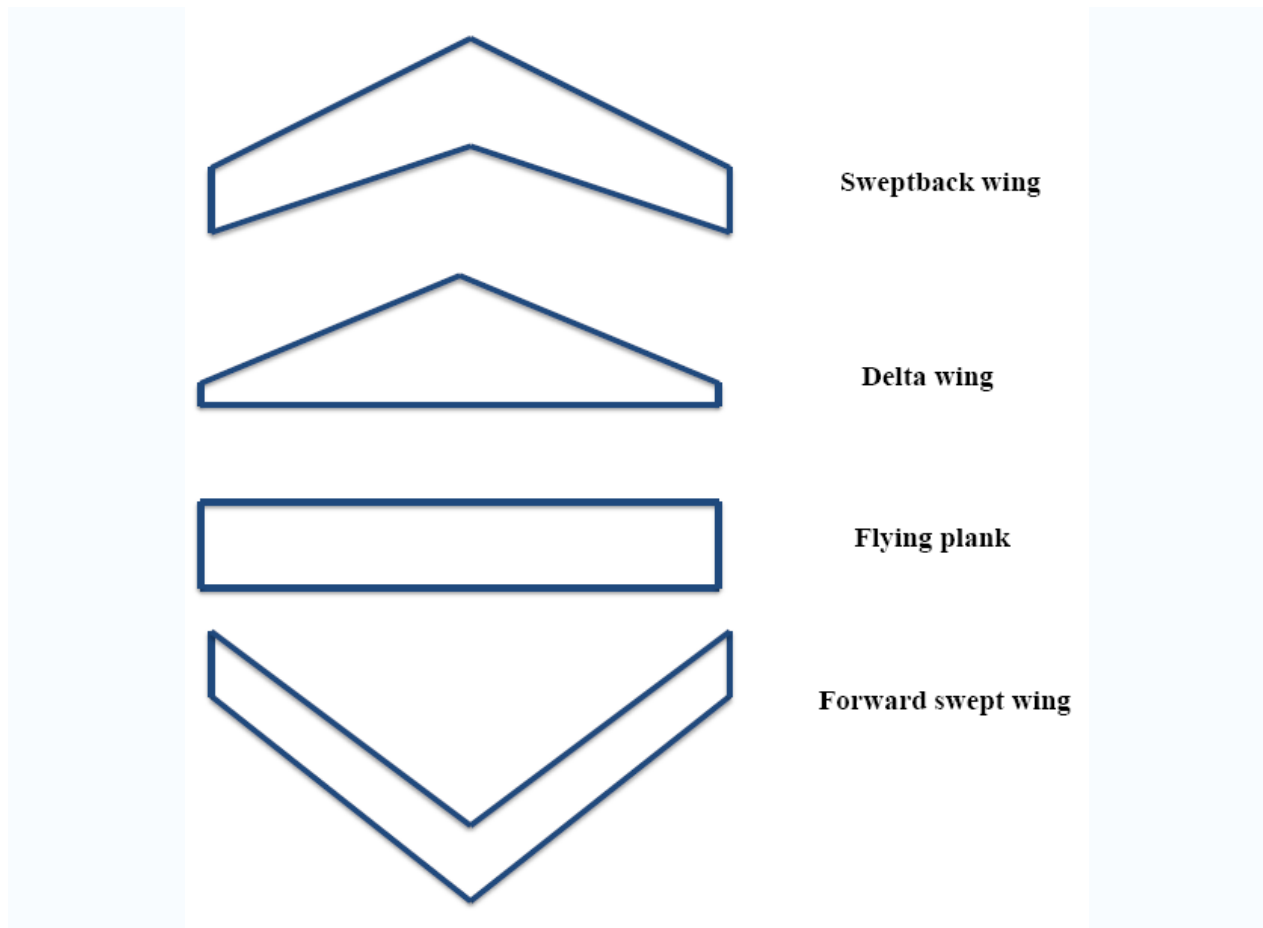


Figure 2-Types of flying wings

In our project we desire to design a **sweptback flying wing**, there for the wing give the function of flap, elevator and rudder (Stabilized and control the airplane).

Advantages of flying wings:

- The weak directional stability gives spiral stability.
- Flying wings are stable while circling, i.e. they hold attitude with constant degree of bank without pilot movement of control stick.
- Normally the stall behavior is good and the tendency to spin is low.
- A low drag coefficient is expected but not always attained.
- A pusher propeller and turbines are easier to install.
- Theoretically, a flying wing should be less expensive to construct.
- Flying wings are attractive in the sky and air shows.

Disadvantages of flying wings:

- The flight performance is often inferior. This stems from the desire to improve the stability and maneuverability.
- The permissible CG-limits are smaller.
- Elevator deflection alters the lift distribution and increase the induced drag.
- The adverse yawing moments due to aileron deflection can often not be compensated fast and easily because of weak rudder efficiency.
- The weak pitch damping and the small moment of inertia around the pitch axis may induce alpha-oscillations.
- Cross-wind take offs and landings are difficult.
- In case of motorized flying wings the propeller slipstream over the rudder is absent during take-off, therefore it is difficult to maintain directional control.

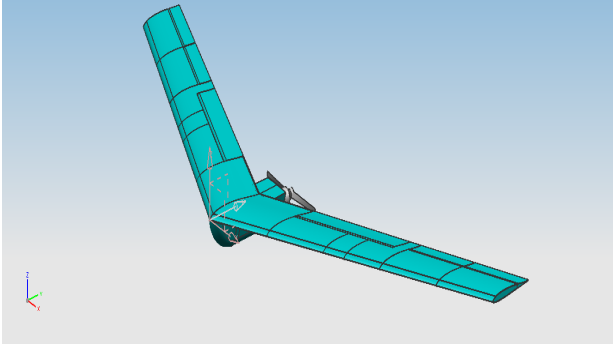
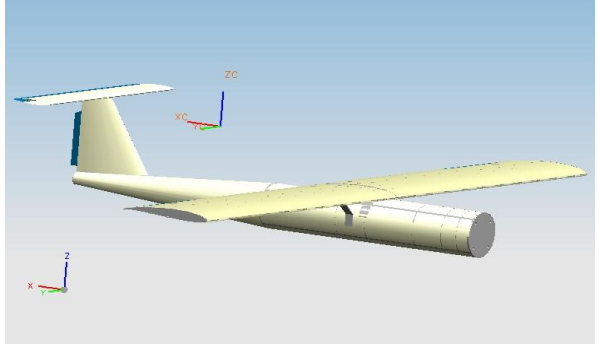
The purpose of design UAV system

Generally we can use the flying wing UAV in many purposes for example

1. Surveillance.
2. Reconnaissance.
3. Picturing and Registration

Comparison between the flying wing aircraft and the conventional aircraft:

Table 1 Comparison between the flying wing and the conventional aircraft

The Flying wing aircraft	The conventional aircraft
	
Aircraft without horizontal tail and sometimes without vertical tail.	Aircraft with horizontal and vertical tail.
Theoretically the flying wings give low drag coefficient and should be less expensive.	Give relatively high drag (not always) and more expensive.
A pusher Propeller easier to install.	A pusher Propeller more difficult to install.
The permissible CG-limits are smaller.	The Permissible CG-limits higher.

The flying wing design Process:

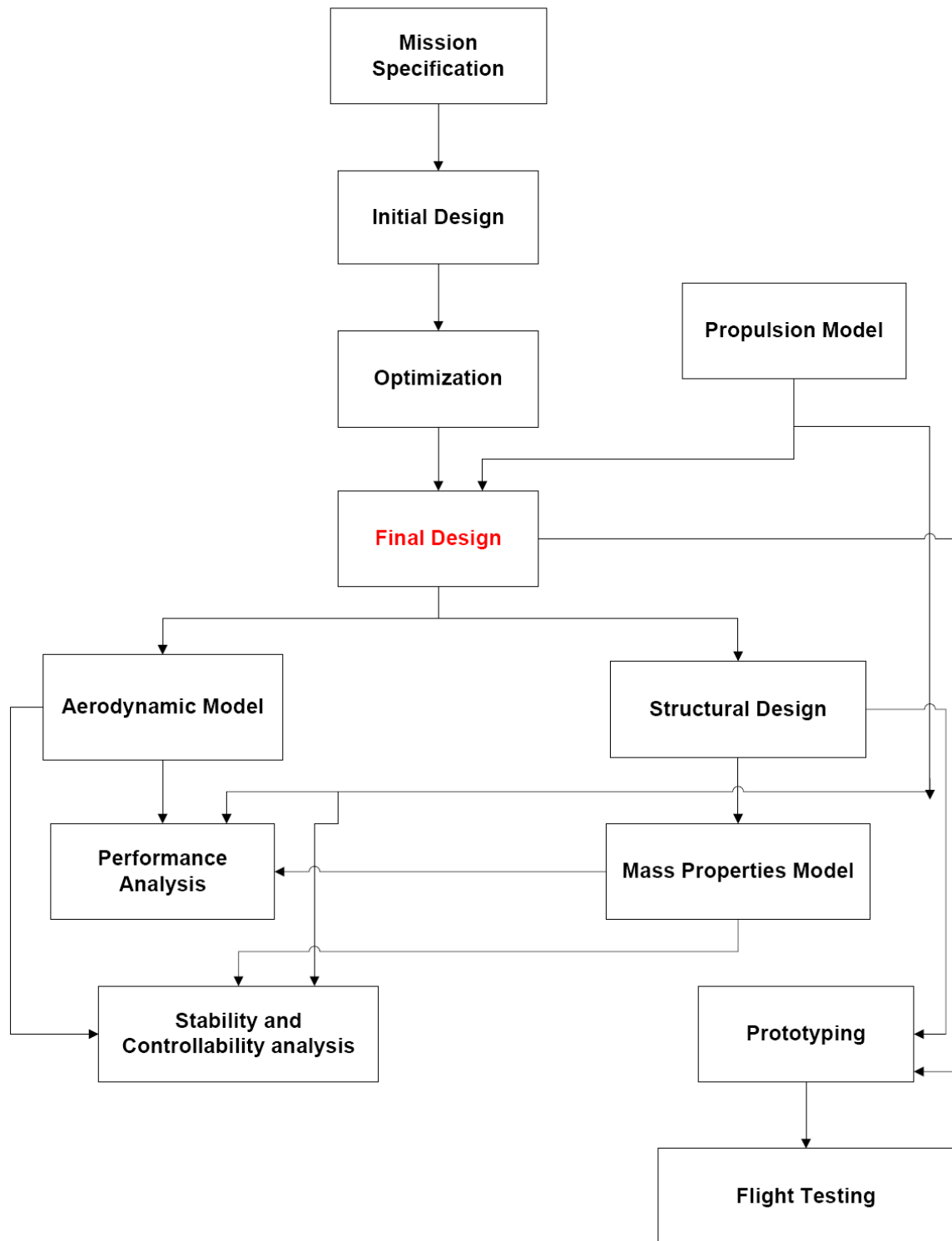


Figure 3: The design procedure

Mission specifications:

Table 2: Mission Specifications

Range class	close range
Airframe	flying wing with propeller
Propulsion	electric
Maximum payload weight	0.5 Kg
Endurance	1 hour
Range	5-10 Km
Cruise speed	20 m/sec
Maximum speed	30 m/sec
Service ceiling	500 m

Chapter 1: Initial Design

This is the first step of the project, in this step it is required to:

- Find a wing which can perform the required mission specifications this includes
 - choosing the geometric properties of the planform
 - the airfoil/s to be used along the wing sections
 - geometric washout (if needed)
- choose the size of the control surfaces to be used
- calculate the lift distribution on the chosen wing
- check that the center of gravity of this suggested wing lies on the c-point

Step by step procedure for initial design

Step 1: Wing Geometry

In this step we are required to choose the geometric properties of the wing planform that will satisfy the required mission specifications.

There are three main independent parameters for the wing planform:

Taper ratio: it determines the maximum lift (value and position) provided by the wing

Aspect ratio: it determines the position of the center of lift on the

Wing; this position changes with speed, so the aspect ratio directly affects the range and endurance the wing can perform

Sweepback angle: it determines the degree of stability of the wing

So we will choose the wing span, root chord, tip chord, and lever arm that will give a combination of the aspect ratio, taper ratio and sweepback angle that satisfy the mission requirements.

Based on mission specifications and existing database for flying wings we will choose:

- Maximum weight (w)
- Wing span (b)
- Root chord (C_r)
- Tip chord (C_t)

8 Flying wing Design and Manufacturing project

Then, we will calculate other geometric properties

- Wing aspect ratio (AR)
- Wing taper ratio (Z)
- Wing area (S)
- Sweep back angle (ϕ)
- Lever arm of the leading edge sweep (H)

The results for existing flying wings database are summarized in table in the next page

Step 2: Airfoil Selection

In this step we want to check weather size and planform will work properly

- Estimate the value of the maximum lift coefficient C_{Lmax} ;

$C_{Lmax} = 0.7-1.0$ for airfoils 8% to 12 % thickness

- Calculate the minimum speed

$$V_{stall} = \sqrt{\frac{2W}{\rho S C_L}}$$

- Calculate the lowest Reynolds number

$$Re_{min} = \frac{\rho V C_t}{\mu}$$

- Choose a suitable airfoil

Any airfoil is defined by two parameters:

- Camber distribution:

it determines the lift and moment that the airfoil can give.

- Thickness distribution:

it determines the drag that the airfoil gives.

In selecting a suitable airfoil for tailless aircraft we are very much concerned with the pitching moment coefficient (C_{mo}) ;there is a well known fact that says:

For tailless aircrafts only airfoils with a small pitching moment should be used. if possible a zero pitching moment is preferable

Step 3: Washout

In this step it is required to calculate the required washout of the wing

The problem is what amount and what form of washout is to be chosen.

Required amount of washout:

To determine the required washout you must first determine what is called **design lift coefficient** (C_L^*), it is that lift coefficient at which the aircraft flies with neutral elevators.

- Now, to determine the design lift coefficient of the aircraft you must look at the **operational profile** of your aircraft. This tabulates how long (on average) each flight condition appertains for a typical flight. The operational profile differs from one type of aircraft to another and from one mission to another as follows:
- **Special aircraft:** in this case the operational profile consists of one single point; the aircraft flies (nearly) always with the same value of C_L , so the design lift coefficient is taken directly equal to the operation C_L
- **Long range airliners and touring aircrafts:** although these types of aircrafts use different values of C_L during takeoff and climbing, and, on approach and landing. But compared to the overall flight time these specific periods are negligible. Hence on this case also can be treated as the above case and the design lift coefficient is taken equal to the operation C_L during cruise.
- **Sailplanes and hang gliders** on cross-country soaring using thermals are quite different. Here the operational profile consists of two completely different flight conditions which last approximately the same length of time, namely, slow slow circling in the thermals and high speed straight and level flight in between. During circling the lift coefficients used lie well above the value $C_L = 1$. In the second flight phase small values till $C_L = 0.1$ are typical. Hence the question occurs which value of the design lift coefficient C_L^* should you choose.
- Strictly speaking our aircraft type and mission is the third one and the design lift coefficient is to be chosen as small as possible.

The Panknin twist formula :

This formula can be used to calculate the required washout for our wing

There are six variables which influence the amount of required geometric wing twist:

➤ **Taper ratio:**

The greater the taper ratio, the more twist will be required. This is due to the loss of airfoil efficiency as the wing tip chord gets smaller.

➤ **Aspect ratio:**

The greater the aspect ratio, the less twist is required. However, as aspect ratio increases, and the wing chord gets proportionally smaller, it becomes more difficult to build a strong stiff wing.

➤ **Sweep back angle:**

The greater the sweep back angle, the less twist will be required. However, angles of sweep back in excess of 20 degrees adversely affect air flow over the wing and may lead to control problems.

➤ **Airfoil moment coefficients:**

10 Flying wing Design and Manufacturing project

The moment coefficient of the whole aircraft must be positive for stability. While some of this moment is derived from the down force generated by the wing tips, it is also greatly influenced by the pitching moments of the airfoils used. Sections used on contemporary swept wing tailless aircraft have near zero pitching moments.

➤ Desired static stability value:

Increased static stability (CG further ahead of the neutral point) dictates increased wing twist.

➤ Design coefficient of lift:

The greater the design coefficient of lift, the more wing twist will be required. The design coefficient of lift should be the coefficient of lift at cruise speed so that trim drag is minimized. Some amount of up trim is expected to be necessary for thermalling.

➤ Airfoil zero lift angles:

The zero lift angles of the root and tip airfoils influence the geometric wing twist required.

$$\alpha_{\text{total}} = \frac{(K_1 \cdot C_{M\text{root}} + K_2 \cdot C_{M\text{tip}}) - \bar{C}_L \cdot St}{1.4 \cdot 10^{-5} \cdot \lambda^{1.43} \cdot \gamma}$$

$$\alpha_{\text{geo}} = \alpha_{\text{total}} - (\alpha_{L=0\text{root}} - \alpha_{L=0\text{tip}})$$

b = wingspan

t_{root} = root chord

t_{tip} = tip chord

\bar{t} = mean chord = $(t_{\text{root}} + t_{\text{tip}})/2$

λ = aspect ratio = b/\bar{t}

γ = angle of sweepback, as measured at 1/4 chord line

Γ = taper ratio = $t_{\text{tip}}/t_{\text{root}}$

$K_1 = 1/4 \cdot (3 + 2\Gamma + \Gamma^2)/(1 + \Gamma + \Gamma^2)$

$K_2 = 1 - K_1$

$\alpha_{L=0\text{root}}$ = root section zero lift angle

$\alpha_{L=0\text{tip}}$ = tip section zero lift angle

$C_{M\text{root}}$ = moment coefficient of root section

$C_{M\text{tip}}$ = moment coefficient of tip section

\bar{C}_L = design lift coefficient

St = stability factor (static margin)

For our wing there is no aerodynamic twist, so the root and tip sections have the same airfoils

So $\alpha_{\text{geo}} = \alpha_{\text{total}}$

➤ **Optimum Washout spanwise distribution:**

Now the desired design lift coefficient C_L^* can be produced with infinitely many forms of wash-out. Hence the question arises, which one of these wash-out distributions is optimum, the word 'optimum' here can have many different meanings e.g an induced drag which is as low as possible for the design lift coefficient, favorable stall behavior. Therefore the problem is:

wanted is the washout distribution of the wing, which generates on one hand a prescribed design lift coefficient and which on the other hand guarantees a lift distribution which is as optimum as possible over the entire C_L area

We can make linear or quadratic washout distribution

Step 4: Lift distribution

In this step it is required to calculate the optimum lift distribution on the wing which is a combination of the bell-shaped lift distribution and elliptical lift distribution. This is obtained by suitable choice of the 'washout curves'

After choosing the wing planform we can now get the lift distribution on the wing by solving the second basic problem, namely given the wing shape (planform and washout) you can get the lift distribution and its induced drag.

Step 5: Elevon Design.

- Elevon Chord.
 - 50% of local chord near wingtip.
 - 18% for modern airfoils or 25% for older airfoils of local chord at the other side .
- Elevon Length.
 - $AR > 10$;
Elevator length of up to 70% half span.
 - $AR \leq 10$;
Elevator length for about only 40% half span.

It is strongly recommended to use parted elevons so as we can get elevator, aileron, and rudder functions.

- For Swept Back Flying Wings:

The deflection of the elevator changes in general both the profile moment M_p and the wash-out induced pitching moment M_w . Depending on the flap arrangement on the wing it may be possible that both moments have the same pressure effect or, that they are weakening each other. There are even configurations possible where there is no change of balance with elevator deflection at all.

And there are the following three arrangements

- Outboard elevators: Usually, on swept back flying wings the designers prefer to put the elevators as far out as possible as number (a) in the figure. Thus they get the largest available distance to the cg, so an upward deflection increases the wash-out which produces an additional positive moment M_w . Also the profile moment M_p is increased in the area of the elevators. Both moments have, thus, the same pressure sign and reinforce each other.
The wash-out induced pitching moment M_w increases approximately linearly with the sweep angle.
- This means that for wings with a large sweep angle only small deflection of the elevator is needed. Hence the (still unavoidable) constriction of the flight polar becomes less and less severe with increasing sweep angle when comparing it with the flying plank.

The effectiveness of the elevator, however, it is not influenced much by an increase of the sweep angle. This stems from the fact that there are two different influences which largely cancel each other out: on the one hand for the large sweep angle the elevator has also a large lever-arm and therefore high turning moment. On the other hand, however, a wing with high sweep also has a large moment of inertia and therefore turns more slowly. Hence the pilot has more or less the same elevator control with a flying plank as with highly swept flying wing.

An important advantage of outboard elevators is the favorable stall characteristics.

Step 6: Flap Design

- Flap Chord.
 - At wing center (inner chord)
 - $(30 \div 50)\% C_r$
 - At outer chord (outer chord)
 - $(18 \div 25)\% C_o$
- Flap length
 - Moment free flap
 - $S_F(AR; \varphi_{1/4})$
- Systems of camber flaps:

Many tailed aircrafts have camber flaps at the trailing edge. These flaps are normally installed in the centre part of the wing, between the ailerons. In extreme cases they stretch over the entire wingspan. With these flaps the aircraft polar is shifted towards larger or smaller values of drag. In other words one can say that such flaps should adapt the airfoil camber to the respective flight simulation.

On Tailless aircraft the usable lever arm of the elevator is usually smaller than that of tailed aircraft. It is extremely interesting that this balancing of the additional pitching moments of camber flaps can be performed automatically by design means, at least for sweptback flying wings. Such flaps have the property that their deflection does not change the trimming of the aircraft in question. No elevator movement is necessary with them. They are called trimming free or moment neutral.

Step 7: Centre of Gravity

The center of gravity will be estimated then.

Compared with the location of the center of lift for the combined bell shaped and elliptical lift distribution:

- If CG is not on the C-point; either to shift the CG to the desired point or consider the degree of loss of the Flying Wing performance
- If the neutral point is used as a point of reference for a rectangular or slightly tapered wing then: if a cg position of, say 10% in front of the neutral point is chosen then the cg lies at least by the same value ahead of the C point. Hence one is safe firstly to look after the neutral point with this kind of wing.

For strongly tapered wings the opposite is true: with them it is advisable to use the C-point as the point of reference. If for example, a cg position of 10% in front of the C-point is chosen, then the cg already automatically lies the same distance ahead of the neutral point.

➤ For Nose Heaviness:

A forward position of the centre of gravity must be compensated for by down lift at the wingtips, behind the cg. This aerodynamic force is produced by elevons up which generate

Flying wing UAVs:

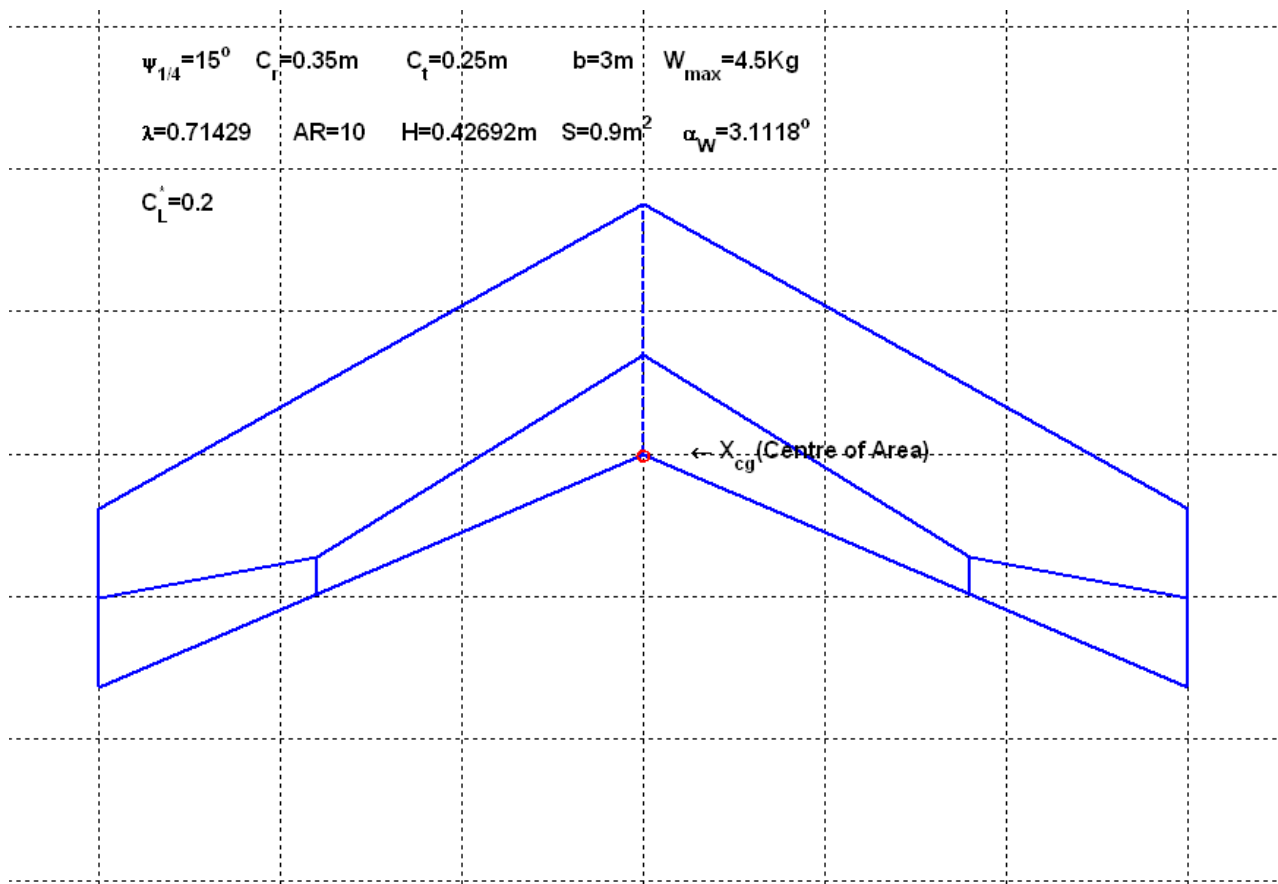


Figure 5 : Initial Design

Chapter 2 Design optimization

What's optimization?

It's the problem of finding an optimal output (minimum or maximum) for a given function (objective) without violating (satisfying) a certain constraints.

It seems from the first sight that it's a problem of finding only the local (or global) maximum or minimum of a function of single variable by finding the signs of its 2nd derivative, but if the dimension of the problem increases (**Euclidean Space**) it's not the simplest way like that.

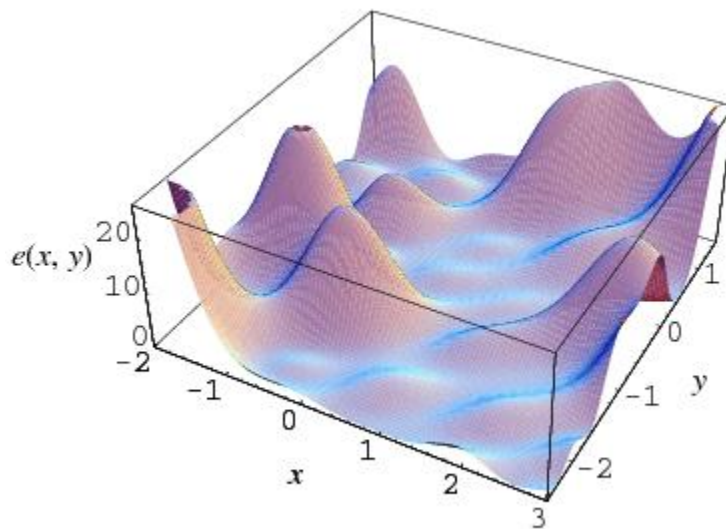


Figure 6

Steps for the optimization process

- Defining the problem (objective function or cost function (**the problem must be well posed**))
- Defining the design variables:
 - All design variables must appear implicitly or explicitly in the objective function, i.e. must fully define the objective function.
 - All design variables must be completely independent (not dummy variables).
- Imposing the constraints of the problem (physical & geometrical constraints).

1st optimization problem (Maximize local lift coefficient)

C_{Lmax} This value is reached when one of the local lift coefficients reach it's maximum

$c_{lmax} \rightarrow objective$

$AR(Aspect\ ratio), \lambda(taper\ ratio) \rightarrow Design\ variables$

$Value, Position\ of\ c_{lmax} \rightarrow Constarints$

- Design variables
 - Aspect Ratio (AR)

$$C_{Lmax} = \frac{c_{lmax}}{\sqrt{1 + \left(\frac{c_{lmax}}{\pi AR}\right)^2} + \frac{c_{lmax}}{\pi AR}}$$

For a chosen stall speed get the value of C_{Lmax} (max.lift coeff. on wing) , and by choosing AR , we can predict the value of local max. lift coeff. (c_{lmax})

- Taper ratio(λ)

If $\lambda = 1$ (rectangular wing) $\eta_{c_{lmax}} = 0$

If $\lambda = 0$ (Arrow wing) $\eta_{c_{lmax}} = 1$

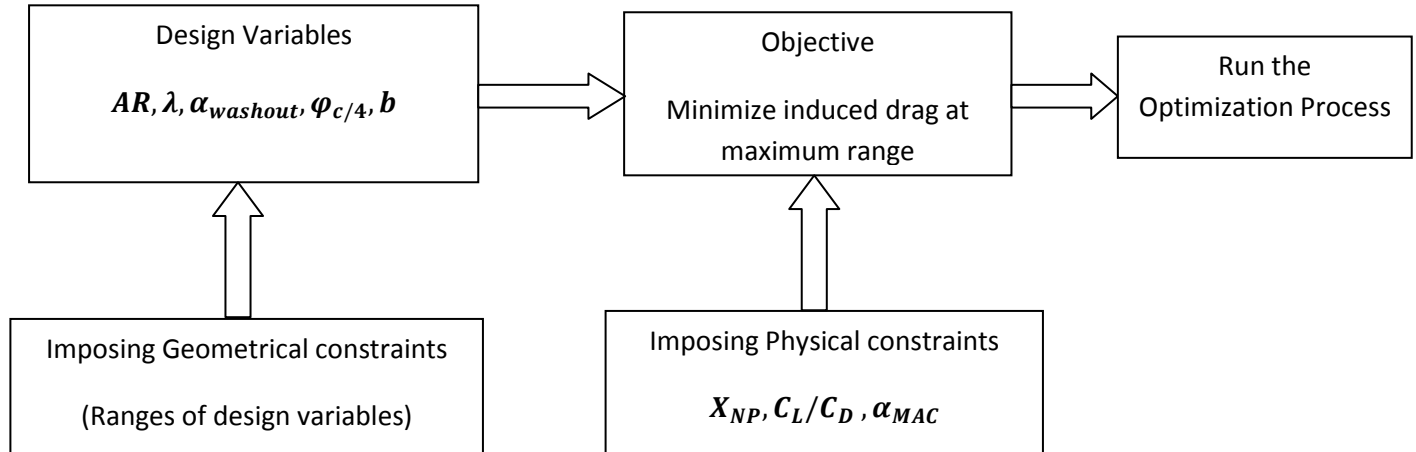
From these two results one can suggest a linear relation between $\lambda, \eta_{c_{lmax}} \rightarrow \eta_{c_{lmax}} = 1 - \lambda$

Conclusion \rightarrow From the relation between λ, AR and c_{lmax} , we see that we can control its position and value by appropriate chose λ, AR

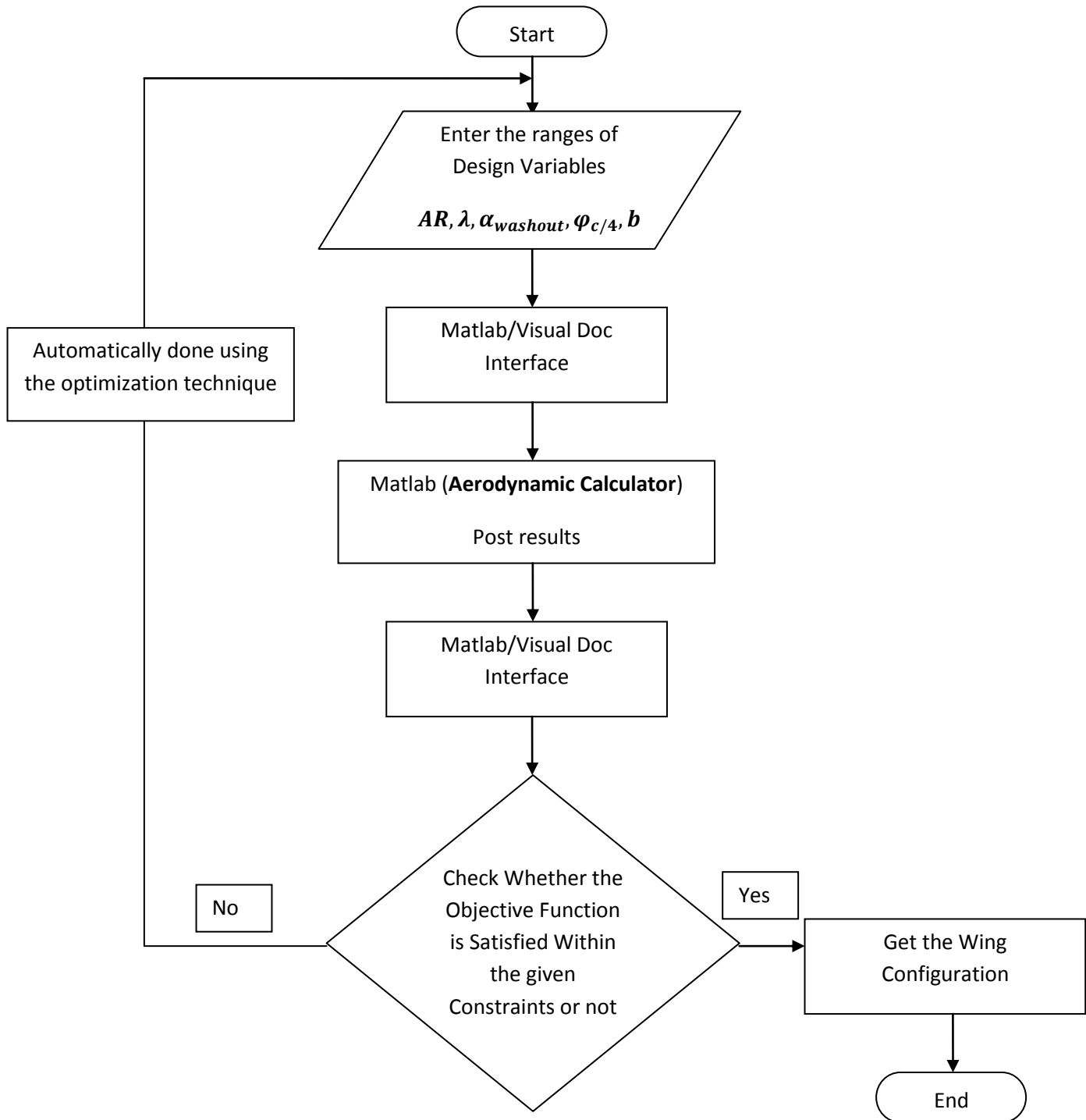
For our first problem we don't need an optimization problem, just chose the values of λ, AR

2nd optimization problem (Minimize induced drag)

Our problem → Aerodynamic optimization of a wing from the point of view of induced drag at a given flight condition (Range, Endurance, etc....).



- Design Variables
 - $9 < AR < 13$
 - $0.65 < \lambda < 0.75$
 - $-2 < \alpha_{washout} < -5 \rightarrow$ Amount of twist at tip section
 - $15 < \varphi_{c/4} < 30$
 - $2.5 < b < 3$
- Objective
 - Minimize C_{Di}
- Constraints
 - $0.9C_r < X_{NP} < 1.1C_r$
 - $15 < V_{(C_L/C_D)} < 20$
 - $1 < \alpha_{MAC} < 5 \rightarrow$ Angle of attack at Mean Aerodynamic Chord



Chapter 3 Propulsion system

We have two choices for the propulsion model for the aircraft, either electric engine propulsion or gasoline (nitro) engine. Here is a comparison between the advantages and disadvantages of the two propulsion models at the same power.

Point of comparison	Electric engine	Nitro engine
Power source	The electric motor requires electricity in the form of a battery pack as the fuel	The nitro engine is fuelled by a methanol-based fuel that contains nitro methane.
Engine components		Nitro engines have carburetors, air filters, flywheels, clutches, pistons, <u>glow plugs</u> (similar to spark plugs) and crank-shafts just like full-size gasoline-powered cars and trucks do. There is also a <u>fuel system</u> that includes a fuel tank and exhaust.
Chassis material	Plastic or carbon fibre	Light weight anodized aluminum
Drive train	plastic	metal
Center of gravity	All the components in an electric RC are stationary and don't shift at all giving it a stable center of gravity	The center of gravity changes due to the movement of the fuel in the tank
Power to weight ratio	High	lower
pollution	Clean source of propulsion	
noise	Low	Higher due to muffler
Run time	The runtime is dependent both on how long the battery lasts and how long it takes to recharge the battery pack.	The runtime is dependent on how much fuel the tank holds and how long it takes to refuel.
Engine start	Direct easy start	There are multiple ways to <u>start a nitro engine</u> , some of which require additional accessories or parts.
After –run maintenance	No after run maintenance is required	after-run maintenance on a nitro engine that's not necessary on an electric RC includes draining the fuel tank, <u>cleaning and oiling the air filter</u> , and <u>adding after-burn oil</u> .

After this comparison it is decided to use an electric brushless motor for the propulsion system for the aircraft.

The propulsion system components are:

- Brushless motor
- Engine accessories (engine mount, propeller adaptor, bullet connectors....)
- Lithium polymer (LIPO) battery
- Electronic speed controller (ESC)
- Pusher propeller
- High torque servos
- Battery charger

Brief explanation of each component in the power system:

Motor:

Brushless vs brushed motors:

A **brushless motor** consists of stationary coil and a rotating magnet connected to the output shaft. In a brushless motor electric controller is required to keep the motor running, less maintenance is required due to absence of brushes, the motor efficiency is high because there is no voltage drop across brushes, also the electric noise generation is low in brushless motors.

A **brushed motor** uses stationary metallic contacts that brush against moving metallic contacts, these brushes transfer electrical energy to coils on the rotating armature. In brushed motors no controller is required for fixed speeds. brushed motors operate in extreme environments due to lack of electronics, brushed require periodic maintenance, Brush Arcing generates noise.

Out-runner vs in-runner motors:

An **out-runner** motor has stationary coils at the center and rotating magnet on the outside. Out-runner motors, in general, have low KV rating i.e they rotate at relatively low rpm (but they give high torque) which means that they can be directly used to drive relatively large propellers without the need for gearbox Out-runners have a rotating magnet-lined bell, spinning around a wire-wound fixed stator. Generally out-runners are much lower Kv (ex. 300-1500Kv) and higher torque (in part because of the larger rotating mass of magnets and bell), and so can be used as direct drive with large props. Some higher Kv out-runners can be geared

An **in-runner** motor has stationary coils which surround rotating magnet at the center. In general in-runner motors give lower torque at very high rpm, that's why they are used in helicopters because they need gearbox to reduce the engine high speed. In-runners have a rotating, wire wound, armature spinning within a magnet-lined can. Generally in-runners are high Kv designed

for high rpm 50,000rpm- they can be used in direct drive with small props, but are often geared to drive bigger props.

The engine to be used will be brushless out-runner motor.

So the first step is to choose the brushless out-runner motor that provides the suitable power to the aircraft, and satisfy the required power loading, keeping in mind that you will need to take factor of safety. Then the speed controller and the battery suitable for this motor are chosen.

There are so many types of engines manufacturers, the most popular of which is hacker and rimfire. The following table shows a comparison between some engines in the range of power required for our aircraft to make our choice easier.

Rimfire motors

RimFire .60

Description	Stock No.	Diameter	Length	kV	Constant Watts	Burst Watts	Weight	Shaft Diameter (mm)	Voltage Range	Sport	3D	Power System Recommendation		
												ESC	LiPo	Prop
RimFire .60	GPMG 4745	50 mm (2.0 in)	55 mm (2.2 in)	650	1200	2200	298 g (10.5 oz)	8 mm (0.31 in)	18.5 - 22.2 V / 5-6S LiPo	4705 g (10.5 lbs)	2950 g (6.5 lbs)	60 Amp	6S	12x6 to 13x4 Electric

RimFire .80

Description	Stock No.	Diameter	Length	kV	Constant Watts	Burst Watts	Weight	Shaft Diameter (mm)	Voltage Range	Sport	3D	Power System Recommendation		
												ESC	LiPo	Prop
RimFire .80	GPMG4740	50 mm (2.0 in)	55 mm (2.2 in)	500	1300	2200	298 g (10.5 oz)	8 mm (0.31 in)	18.5 - 22.2V / 5-6S LiPo	5215 g (11.5 lbs)	3175 g (7 lbs)	60 Amp	6S	15x6 to 15x8 Electric

RimFire 1.20

Description	Stock No.	Diameter	Length	kV	Constant Watts	Burst Watts	Weight	Shaft Diameter (mm)	Voltage Range	Sport	3D	Power System Recommendation		
												ESC	LiPo	Prop
RimFire 1.20	GPMG4770	50 mm (2.0 in)	65 mm (2.6 in)	450	1800	2300	400 g (14.1 oz)	8 mm (0.31 in)	18.5 - 22.2V / 5-6S LiPo	6520 g (14.5 lbs)	80 Amp	6S	16x6 to 17x8 Electric	

Hacker motors

A50-10S

Prop	13x6,5 APC-E	14x7 APC-E
LiPo	5 S	5 S
Volt	17,5 V	17,5 V
Amp.	47,5 A	58,4 A
RPM	9291	9064
Power	832 W	1022 W
Contr.	X70-SB-Pro	X70-SB-Pro
KV rating	588	
Shaft diameter	6 mm	
Shaft length	21.4 mm	
Can diameter	48.8 mm	
Can length	63 mm	
weight	395 g	

For Airplanes up to 7,0 lbs and Gliders up to 20 lbs with Prop up to 14 inch

A50-12S

Prop	13x10 APC-E	14x7 APC-E
LiPo	5 S	6 S
Volt	17,5 V	21,0 V
Amp.	44,4 A	54,0 A
RPM	7851	9302
Power	777 W	1134 W
Contr.	X70-SB-Pro	X70-SB-Pro
KV rating	492	
Shaft diameter	6 mm	
Shaft length	21.4 mm	
Can diameter	48.8 mm	
Can length	63 mm	
weight	395 g	

For Airplanes up to 7,0 lbs and Gliders up to 20 lbs with Prop up to 14 inch

Motor specifications:

The motor used for the UAV is Great Planes Rimfire .80 50-55-500 Outrunner Brushless

The technical specifications given by the motor manufacturer are:

- Engine dimensions; Can diameter: 50 mm
Can length: 55 mm
Shaft length: 20 mm
Shaft diameter: 8mm
- Motor weight : 298 gram
- Power; Maximum continuous power the motor can supply: 1300 watt
Motor burst power: 2200 watt
- KV rating: 500 rpm/volt
- (it is the number of rpm per volt i.e multiplying the KV rating by the battery voltage we get the motor rpm for no load) therefore the rpm for no load at full throttle is 500×22.2 i.e about 11000 rpm
However, this high rpm is only at the full throttle position (at take off only), but at cruise (partial throttle) the rpm will be lower.
- Current rating; Maximum constant current: 50 amp
Maximum surge current: 65 amp

This means that the speed controller to be used with this motor must be a 70 amp speed controller or more so that it can withstand the maximum current provided by this motor.

Electronic speed controller:

An ESC is basically a device that controls the motor through the radio system i.e it is used to vary the speed of the motor. There are brushed ESC and brushless ESC; but since the Rimfire motor used is brushless then a brushless speed controller must be used with it. The ESC is connected between the motor and the battery, it receives a signal from the RC receiver and controls the power supplied to the motor from the battery based on this throttle signal. There are speed controllers with break electronic circuit (BEC) and others without BEC, the function of the BEC is to provide a regulated voltage for the receiver (and servos) i.e it lowers the battery voltage to 4.8 Volt (the voltage required to operate the servos), also the BEC prevents the battery from being deeply discharged (it allows the battery to be discharged up to the voltage cut-off value only).

ESC specifications:

The ESC used for the UAV is **Hacker X-70 SB Pro Brushless Motor Speed Controller ESC 70A**

- Dimensions; length: 75mm
Width: 28mm
Height: 10mm
- Weight: 55 g
- Current rating: 70 amp (it is the maximum continuous current the ESC can withstand; the ESC current rating must be greater than or at least equal to the motor current rating.)
- Cell rating: the maximum number of battery cells that can be used with the ESC
- Voltage cut-off: this is the limit for how deeply the battery can discharge. For LIPO batteries we are usually interested in low voltage cut-off value.
- BEC Current: 3 amp (and this current is sufficient to operate our servos).
In case the speed controller doesn't have BEC, a separate battery should be used to provide electricity for the servos.
This speed controller is programmable (it can be programmed using a programming kit), the parameters that can be adjusted are: number of cells, cut-off voltage, timing adjustments ...

The power source (battery):

Provide the required electric energy to operate all electronic equipments on the UAV (through the speed controller; which adjusts the battery voltage according to the signal send by the RC to the receiver). There two types of batteries that can be used to provide power for the motor, namely, LIPO, NiCad/LiMH. The battery used will be LIPO battery because it is light and reliable.

Battery technical specifications:

The battery used in the UAV is **Thunder Power RC G4 Pro Power 30C 5000mAh 22.2V 6 Cell LiPo 6SP30 5000 Lipo**

- Battery dimensions; length: 160 mm
Width: 54 mm
Height: 44 mm
- Battery weight: 792 gram
- Voltage: 22.2 volt (no. of cells x voltage per cell i.e 6x3.7)
(Based on the chosen motor, the battery is chosen so as to provide the required voltage input to the motor)
- Number of cells: 6 cells

The LIPO batteries consist of cells (each cell provides 3.7 volt) if the cells are connected in series their voltage is added (e.g if the motor requires 22.2V input voltage then the battery used should be 6 cells connected in series). Arranging the batteries in parallel will give you more duration (more capacity).

- Capacity: 5000 mAh

The battery capacity is measured in mAh, As the capacity of the battery increase its endurance increase but its weight also increase.

- Maximum continuous discharge: 30 C



It is the maximum rated discharge that must not be exceeded or the battery will be damaged (e.g 20C, 30C...). if we multiply this number by the battery capacity this gives us the maximum current that can be drawn by the engine. therefore for this battery with maximum discharge 30C, capacity 5000 mAh, the discharge rate (current draw of the motor) must not be more than $30C \times 5000mAh = 150$ amp (which is satisfied as the motor maximum current as far less than 150 amp; it is only about 50 amp). If your power system draws more than the maximum current that can be provided by your battery, the batteries will have to be connected in parallel to increase the capacity or another battery with higher capacity is to be used.

- Maximum continuous current: 150 amp

The charger used to charge this battery is: **Thunder Power RC TP610C Li Poly A123 (with balancer)**, Also a DC power supply is needed: **Thunder Power RC 12V 5A Power Supply for TP-425, TP-535, or TP-610C LiPo**

Note that charging and discharging a battery is a dangerous process, that's why all the safety precautions provided by the manufacturer must be strictly followed to protect yourself and your battery.

The power system components pictures

Component	picture
Out-runner brushless motor	 A gold-colored out-runner brushless motor with a yellow and red flame pattern on its side. The word "RIMM" is printed vertically in large black letters. A silver metal shaft extends from the right side.
battery	 A Dragonfly Pro Power 30C battery, which is a 3S LiPo battery. It has a blue and silver casing with red and black wires extending from the top. The text "Dragonfly" is visible in the top left corner of the image area.

Power supply

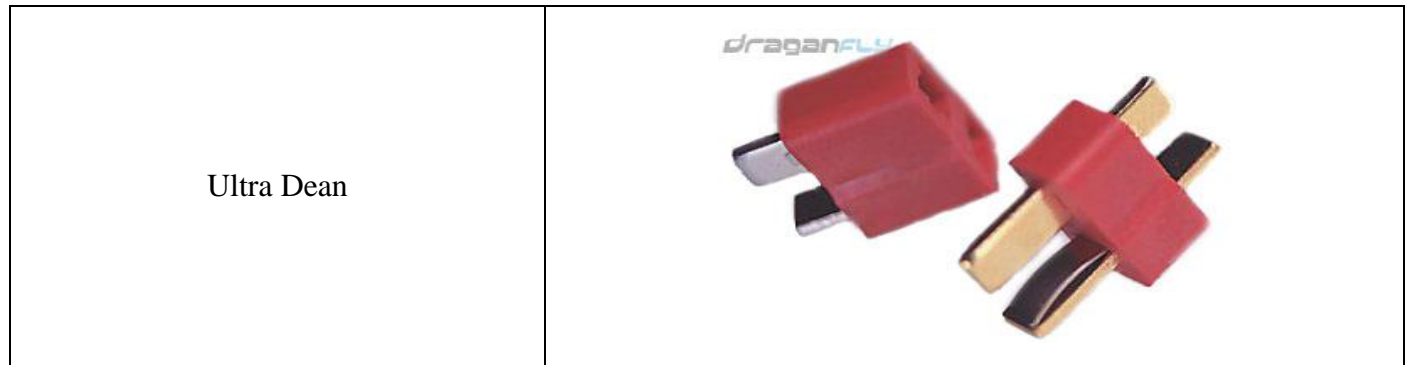


USB user interface



Bullet connectors





All these components were bought from: www.rctoy.com & www.towerhobbies.com

Control system

The control system components are:

- RC
- Receiver
- Servos

Chapter 4 Aerodynamics

The Aerodynamics of the wing includes calculating the aerodynamic forces and moment on the wing as well as the load distributions that results from it for a wing of arbitrary planform.

- This Includes Two Stages:
 - 1- Design Stage
 - 2- Analysis Stage

Design Stage

Wing Design parameters include the following:

- 1- Wing Profile (Airfoil)
 - Airfoil Selection
 - Possible Airfoil Spline(multiple airfoil sections across span)
- 2- Wing Planform
 - Span
 - Aspect Ratio
 - Taper Ratio
 - Sweep-Back Angle
- 3- Geometric Twist
 - Angle of Twist
 - Twist Distribution

Wing Profile

➤ Airfoil Selection

For Tailed Aircrafts not much attention is paid to the airfoil pitching since it can always be compensated for by Horizontal Stabilizer (using size and lever arm) to balance the pitching moment, other more important aspects such as stall characteristics and performance criteria.

For Flying Wing this pitching moment coefficient is much more important. For Sweptback wing a negative (nose down) pitching moment can be compensated with suitable combination of sweep back and wash out.

For Tailless Aircrafts only airfoils with small pitching moment should be used. If Possible zero moment is preferable.

Several Candidates were picked for this end:

	Airfoil	Cm0	C _{lmax}	Re	Max(t/c)
Eppler Series	E 325	0.05	0.89	7X10 ⁵	12.63
	E 327	0.005	1.1		13.1
	E 330	0.05	0.89		11.03
	E 332	0.005	1.1		11.53
MH Series	MH60	0.014	1.19	2X10 ⁵	10.12
	MH61	0.0175	1.0		10.28
	MH62	-0.006	1.1		9.30

From these Candidates, The Martin Hippler Airfoil (MH Series) “MH60” was chosen since it has

- Comparatively high maximum lift coefficient.
- Low moment coefficient of cm c/4 = +0.0140.
- Lower max(t/c) which means lower drag

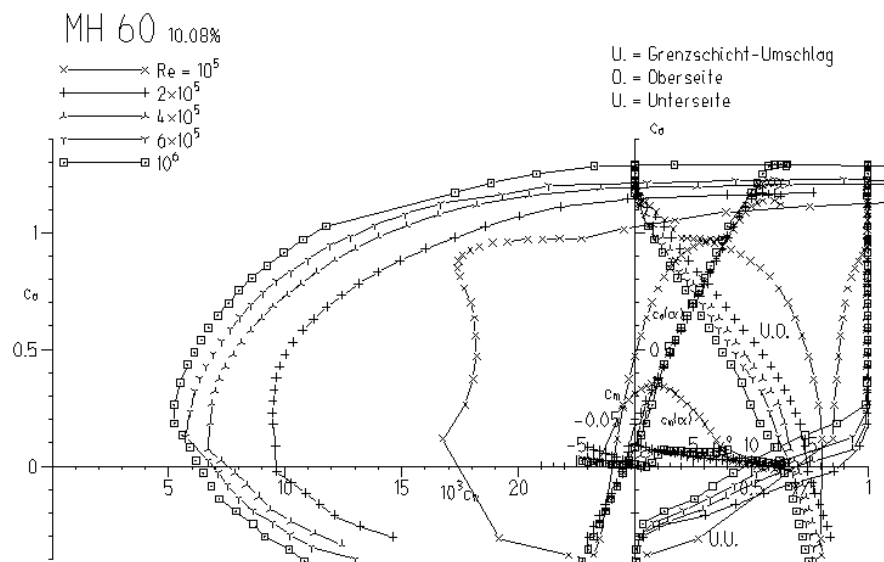


Figure 8-Airfoil Data using Xfoil Code

- Unfortunately, The Experimental Data of the Airfoil were not given by Martin Hippler, The Airfoil Data given are numerically calculated by Two Different Codes Eppler Code (Profil),Drela Code (Xfoil).
 - The Two Results are quite different especially the lift at high angle of attacks and stall prediction, but the results predicted by Xfoil showed agreement with the experimental Data of many airfoils so we decided to use it during the design until further analysis is done during “Analysis Stage”.
- Possible Airfoil Spline(changing airfoil sections across span)

Some of the Flying Wings has a reflexed airfoil at the root which is quite thick with high camber and at the tip a much thinner one which seems to have less camber.

Such Successive Airfoils are called “Airfoil Splines”.

Reason for Airfoil Spline is mainly to:

- Eliminate C_{MP} by using nose up and nose down airfoils combined in a suitable spline.
- Prevent wing tip stall by using high lift airfoils at the outer wing parts but the deflection of the elevators must be taken into account(if as usual the elevators are located at the wing tip) depending on the location of the c.g and the resulting elevator deflection the C_{Lmax} of those control surface profiles is changed considerably

The Choice of different airfoils which vary along the wing seems to have more disadvantages than advantages.

Considerations to be taken into Account in Flying Wing Design

Sweepback Effect

Large Sweepback means large distance from the elevator to the cg provided that the control surfaces are as normal attached to the wing tips. Therefore The Large sweep back should have the following:

- a) Give good “ pitch maneuverability”
- b) Permit the cg to be long way forward
- c) Ensure positive longitudinal Stability by virtue of the forward cg position.

On the other hand there are construction difficulties because of large Sweep Back

Small Sweepback avoids these (real or imaginary) disadvantages:

These wings are aerodynamically clean and differ little constructionally from the usual.

However, such wings look quite “wobbly” at first sight and there is the question of longitudinal stability and control.

Tapering Effect

A strong tapering of the wing (Z small) has only advantages for a flying wing, but there are two grave disadvantages.

Advantages:

- 1) Aesthetics. They looked beautiful in flight (elegant, sleek, lovely, striking...).
- 2) Volume at wing root: A strongly tapered wing has much more usable volume in the wing center than a rectangular wing.
- 3) Spar height: If the wing tapering is increased then the absolute thickness of the wing root increases as well.
- 4) Spar bending moment: The lift center at each half-wing lies closer to the wing root and therefore produces smaller bending moments.
- 5) Wing torsion. Torsion of each half-wing is introduced into the root rib in the wing center which is exceptionally large.
- 6) Centering of masses. Wing masses are oriented toward the wing center.

Disadvantages:

- 1) Induced drag. If the wing is designed with strong tapering then it is far away from being optimum.
- 2) Wingtip Stall. The danger of wingtip stall is high with strongly tapered wing. Actually, it is possible to eliminate this danger, or at least alleviate it, as it will be discussed during optimization.

Conclusion:

Any sweptback Flying Wing with a taper ratio which is stronger than $Z=0.7$ has either no optimum lift distribution or critical wingtip stall behavior.

Wash-Out

Wash-Out is composed of two main parts:

Distribution:

Usually taken Linear for its simplicity but it can also be taken parabolic or even tailored to satisfy or obtain a certain lift distribution.

But Complex Wash-out Distribution means more complex manufacturing process and more complex problem to solve.

Wash-out Angle:

To Fly at the design lift coefficient with neutral elevator and zero pitching moment (trimmed)

For sweptback flying wing, it is advisable to keep the design lift coefficient small and to reach high values with elevator deflections or by using camber flaps.

- The required value for the wash-out angle α_w is determined from:

1. Condition for the balance of pitching moment.

$$C_{MW} + C_{MP} - C_L \cdot \delta = 0$$

δ = The Static Margin

Then, C_{MW} is influenced by the Sweep angle (ϕ) and aspect ratio (AR) and Calculated using the Approx. Method or using one of the wing theory methods such as the Lifting Surface Method.

Parasite Drag Model

- The subsonic wing zero lift drag coefficient may be computed from:

$$C_{Dow} = (R_{wf})(R_{LS})(C_{fw}) \frac{S_{wett}}{S} \left\{ 1 + L(t/c) + 100(t/c)^4 \right\}$$

Where:

1. R_{wf} : wing/fuselage interference factor
This value was taken as 1 since during design process the effect of a possible fuselage was not taken into account
2. R_{LS} = lifting surface correction
For $\Lambda t/c = 26$ [deg]
 $R_{LS} = (1.34 * M^{0.18} * \cos(\Lambda t/c))^{0.28}$;
3. C_{fw} = flat plate friction coefficient of the wing
To judge whether the flow is a turbulent or a laminar one the wings Reynold's number should be firstly calculated.

$$R_{ew} = \rho U \bar{C}_w / \mu$$

Where

\bar{C} Mean geometric chord

The flow is assumed to be mainly laminar since $U_{cruise} \leq 20$ m/s and $\bar{C} < 0.5$

Therefore the laminar flow friction coefficient is valid and is given by:

$$F_w = \frac{1.33}{\sqrt{R_{ew}}}$$

- t/c = thickness ratio defined at mean geometric chord
= 0.1012 for MH60
- L' = airfoil thickness location parameter
 $L' = 1.2$ for $t/c)_{max}$ at $x_t \geq 0.3C$
 $L' = 0.6/(x_t)$; for $t/c)_{max}$ at $x_t < 0.3C$
For MH60 $x_t = 0.277 C$
 $L' = 2.16$ is valid
- $S_w/S = 1.9767 + 0.5333 * t/c)_{max}$

By Substituting in the Equation above The Wing Zero Lift Drag is obtained

$$C_{Dow} = (R_{wf})(R_{LS})(C_{fw}) \frac{S_{wett}}{S} \left\{ 1 + L(t/c) + 100(t/c)^4 \right\}$$

Stall Characteristics Model

- Wing Stall characteristics are obtained by comparing the spanwise wise distribution of c_l with the spanwise distribution of $c_{l_{max}}$. The $c_{l_{max}}$ distribution will not be constant owing to the changing Reynolds Number across wing and hence the stall may not start at the point where C_l is greatest.
- The procedure embraces plotting both the c_l distribution and $c_{l_{max}}$ distribution on one sheet and increasing wing C_L progressively until the c_l curve touches that of the $c_{l_{max}}$.
- The spanwise location of the tangency is then the spanwise location of the start of the stall.
- In General it's desirable to have the stall start somewhat out from the root but inboard of the innermost part of the aileron so the lateral control remains good. A stall that is too strong at the root may cause undesirable tail buffeting.
- The above Method has not been very successful for sweptback wing since it makes no provision for the three dimensional effect of the boundary layer flow
- Currently no solution to this problem has been advanced, other than general experience to the effect that the stall usually appears earlier than calculated.

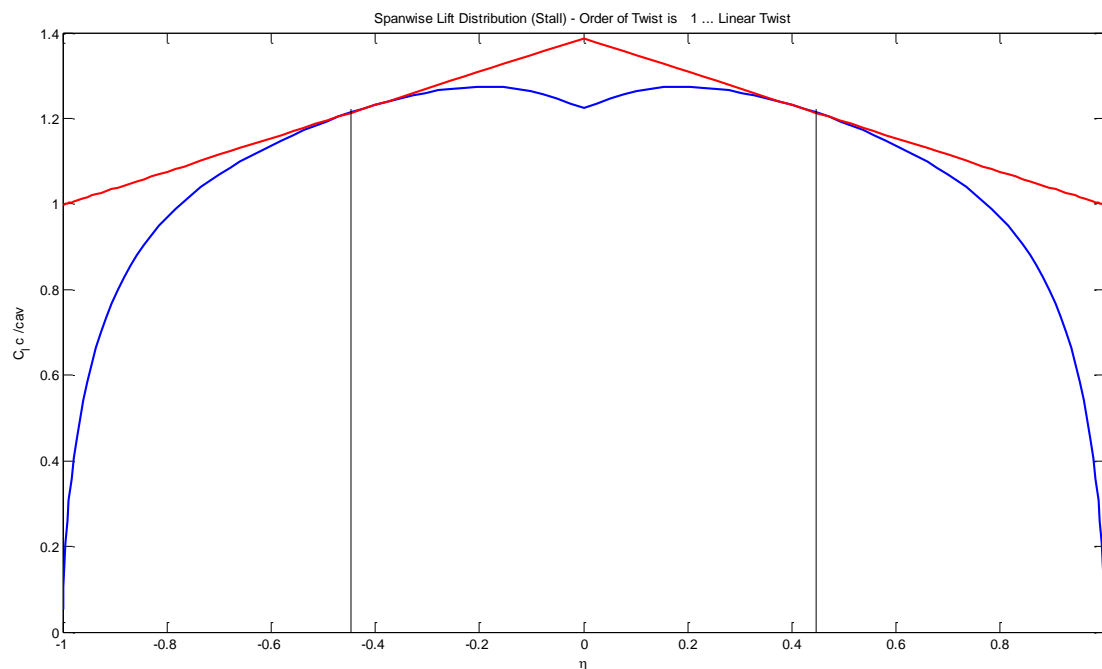


Figure 9: Stall Characteristics

Wing Aerodynamics

For Design purposes a reliable and fast method to calculate the aerodynamic parameters of a planar wing of arbitrary planform is required.

Many methods are available for this end however they differ with respect to accuracy and limitations but most of them are based on Prandtl Lifting Theory.

This Theory has the Following Limitations:

- Inviscid Flow which means that:
 - Separation effect is not taken into account and so stall prediction may be incorrect and lift at high angles of attack may incorrect
 - Parasite Drag cannot be calculated.
- Subsonic Flow

Some of these methods are the following:

- 1- Lifting Surface Method
- 2- Lifting Line Method
- 3- Extended Lifting line Method

1) Lifting Surface Method

- Vortex Distribution on the surface varies over the chord and span.
- Applies to any wing of any Planform
- Gives the lift distribution over the span and over the chord.
- The Following Coefficients can be Calculated :
 - 1- The Total Lift
 - 2- The Induced Drag
 - 3- The Rolling Moment
 - 4- The Induced Yaw Moment(Yaw from Induced Drag)
 - 5- The Pitching Moment
 - 6- The line of local N.P
 - 7- The Wing Neutral Point.
 - 8- The Centre of Pressure

2) Lifting Line Methods

- Vortex Distribution Representing the wing is concentrated on one line (quarter-chord line).
- Applies to unswept wings and gives good results for wing with aspect ratio larger than 3
- Gives the lift distribution over the span.
- The Following Coefficients:
 - 1) The Total Lift
 - 2) The Induced Drag
 - 3) The Rolling Moment
 - 4) The Induced Yaw Moment(Yaw from Induced Drag)
- However the Following Coefficients cannot be Calculated:
 - 1) The Pitching Moment
 - 2) The line of local N.P
 - 3) The Wing Neutral Point.
 - 4) The Centre of Pressure
- And these coefficients are of practical importance to the design process of flying wing.

3) Extended Lifting Line Methods(Weissenger Method)

- This Method is also called the “three-quarter point” Method.
- Line of Control Points is on the three-quarter chord point measured from Leading Edge.
- Applies to swept wings and gives good results for any planform.
- Gives the lift distribution over the span.
- The Following Coefficients:
 - 1) The Total Lift
 - 2) The Induced Drag
 - 3) The Rolling Moment
 - 4) The Induced Yaw Moment(Yaw from Induced Drag)
 - 5) The Pitching Moment (approximately)
- However the Following Coefficients cannot be Calculated:
 - 1) The line of local N.P
 - 2) The Wing Neutral Point.
 - 3) The Centro of Pressure.

- In all above methods, the effect of the control surfaces can be introduced and their effect on the coefficients can be calculated.
- For the Design Needs of the Flying wing the method must satisfy the Following needs:
 - Accurate Calculation of the lift and drag, pitching moment
 - The Wing Neutral Point which is very critical for swept back wings and especially flying wings that are naturally swept to compensate for the need of horizontal tail.
- So the only method that can satisfy these needs is the” Lifting Surface Method” which was used during the design and optimization process.
- Multhopp and Truckenbrodt independently developed methods for numerical evaluation of the method .Multhopp puts two control points at 34.5% and 90.5 % of the local chord and Truckenbrodt puts two control points at $c/4$ line and trailing edge of the Wing.
- The Method used during my Design is “Multhopp Subsonic Lifting Surface Method”.
- The Method is Easy to understand as numerical procedure and provide acceptable results.

II. Analysis Stage

The Analysis Stage is Composed of Two Levels:

- 1- 2D Analysis
- 2- 3D Analysis

2D Analysis:

Our Chosen Airfoil for The Wing is Martin Hippler MH60, However due to the fact that no Experimental Data are available for the airfoil, we had no choice but to rely on the data obtained by numerical solutions

Many Software are available from which the Numerical Solution of the Airfoil, however they differ especially in the viscous (Boundary Layer) Model used to predict the Drag and The Separation (Stall Prediction).

Panel methods :

- 1- Drela Code "Xfoil"
- 2- Eppler Code

CFD Methods :

They Required special to the Choice of the viscous model and the construction of the mesh otherwise unaccurate solution is obtained.

Many Packages are available from which This problem can be Solved such as Fluent and Ansys CFX.

Drela Code "Xfoil"

- The analysis module consists of a 2nd order panel method (linear varying velocity), which cannot achieve the accuracy of Eppler's panel module.
- But in contrast to Eppler's simple boundary layer method Drela has implemented a more sophisticated method, which takes the boundary layer into account while solving for the flow field.
- Thus the interaction between boundary layer and external flow is modeled quite realistic and the code can also handle small to medium sized separated regions.
- When the separation is getting larger or extends into the wake, the results are getting worse, but usually are still acceptable for an impression of the airfoil behavior.
- The transition prediction, which is of utmost importance for low Reynolds number airfoils, is based on a so called e^n method, which is used as a simplified

envelope method. In some cases, the errors introduced by this envelope method can be quite large though.

- A transition value of $N_{cirt}=9.0$ was chosen for the analysis.
- The Results are Presented in Figure (1a),(1b)

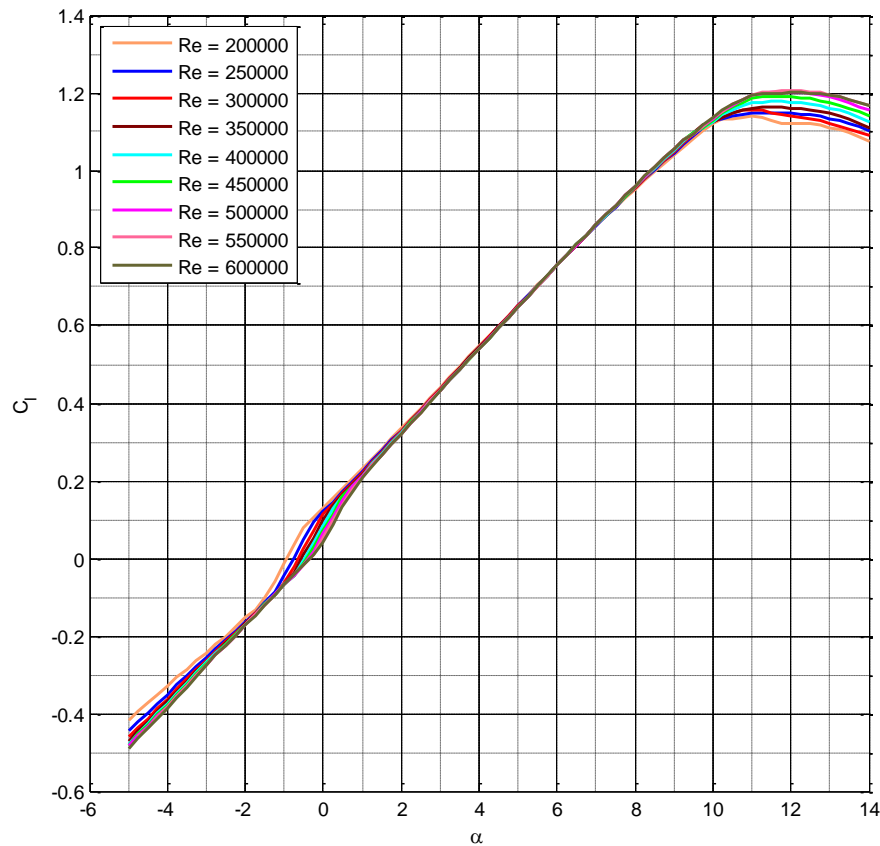


Figure 10: Lift Curve Results using XFOIL CODE

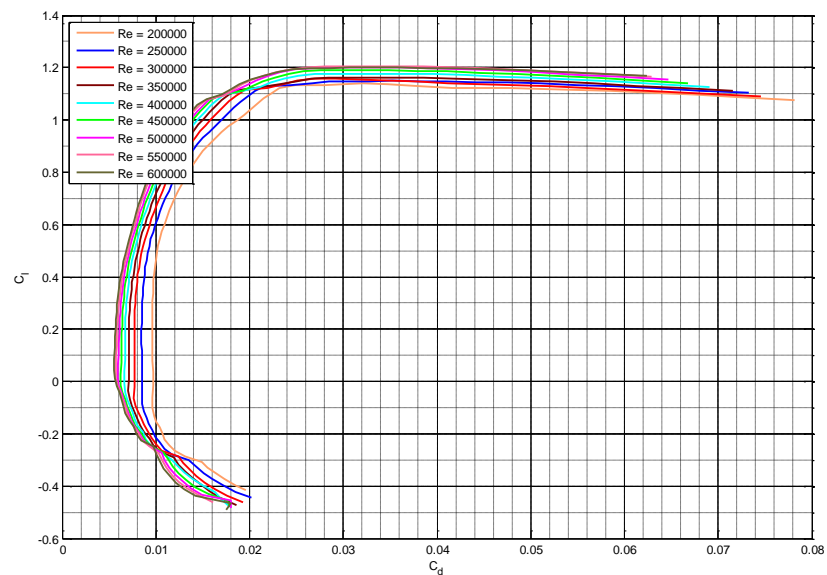


Figure 11: Drag Polar Results using XFOIL CODE

CFD Analysis

Fine Mesh was created using Gambit with Number of Nodes = 24810 and Number of Elements = 24300

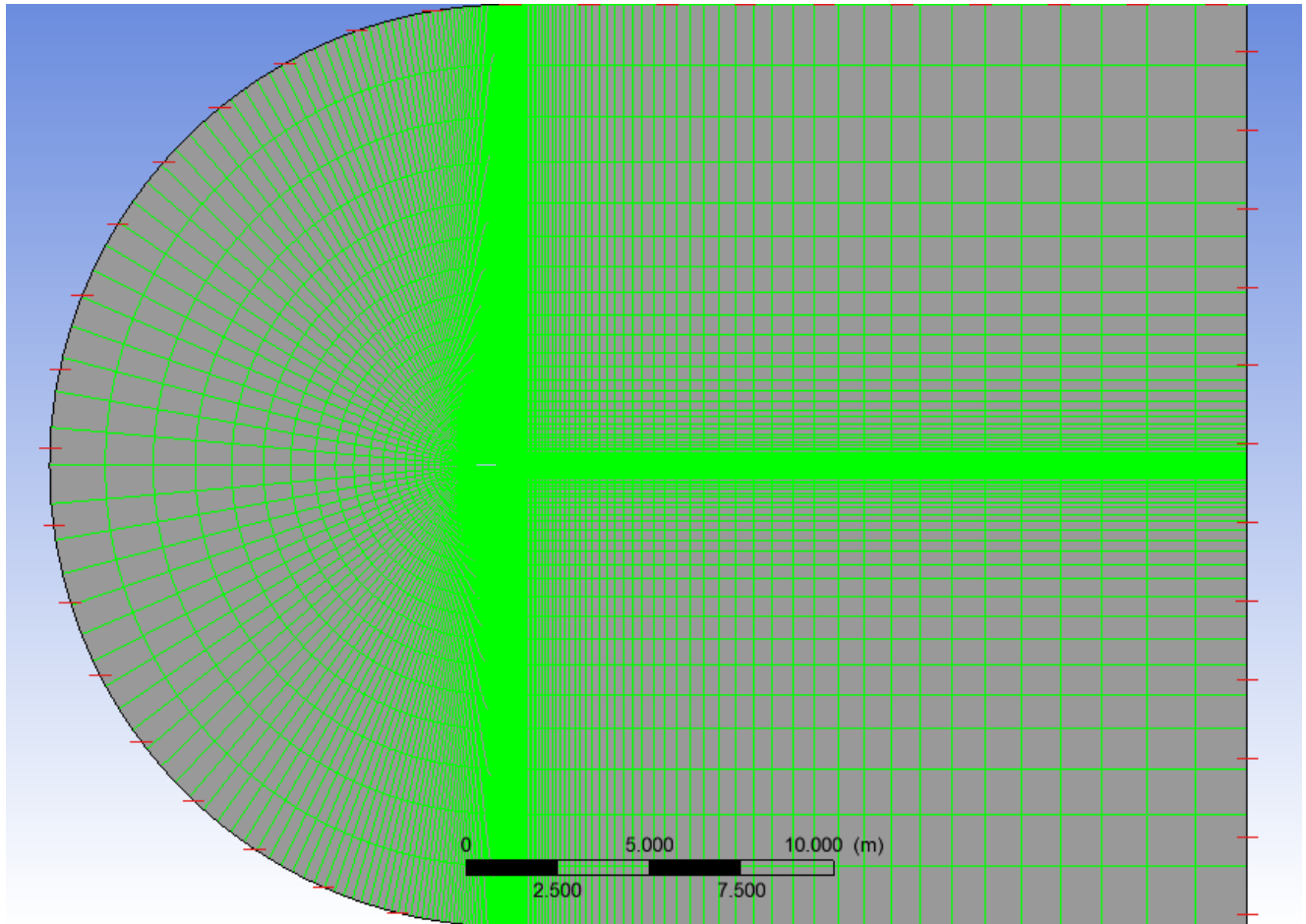


Figure 12: Domain Mesh

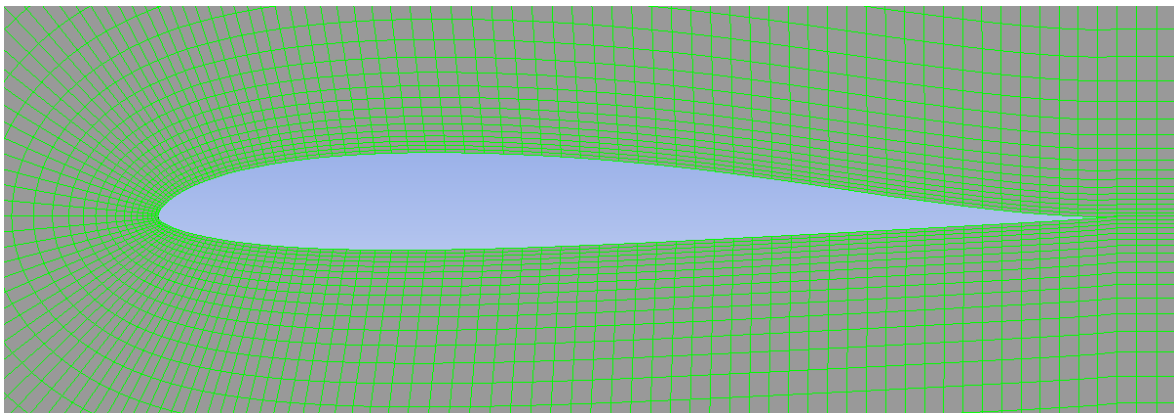


Figure 13: Zoom on the Airfoil Mesh

- Ansys CFX was used to solve the Problem
- Our viscous model is the k- ϵ which is popular of giving accurate results for Airfoil Analysis at Low Reynolds Number.
- Standard operating conditions
- Due to the Tedious nature of the analysis and the fact that it takes a long time solution was only done at $Re = 3 \times 10^5$
- Convergence to an RMS Error of $1e-6$ was reached after 40 time steps.

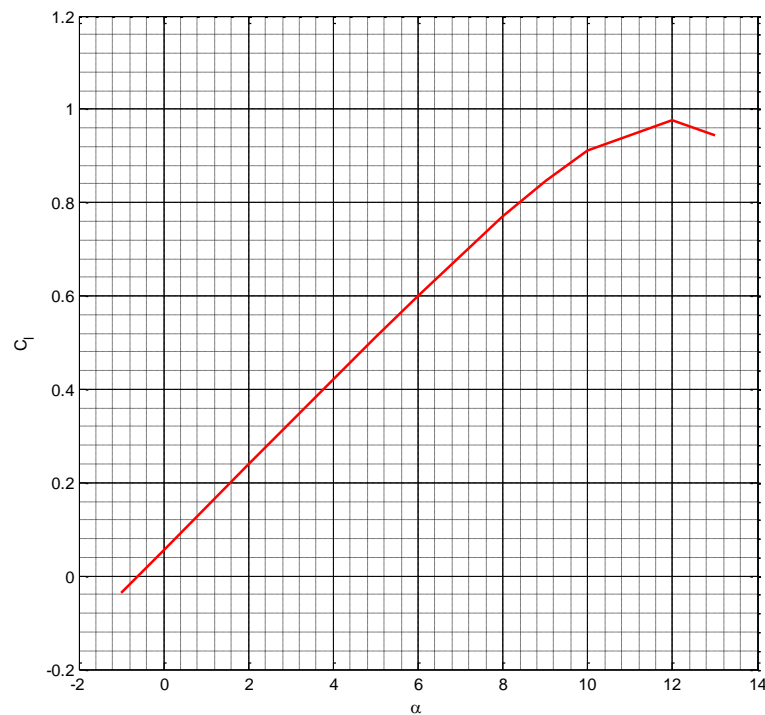


Figure 14: Lift Curve obtained by Ansys CFX

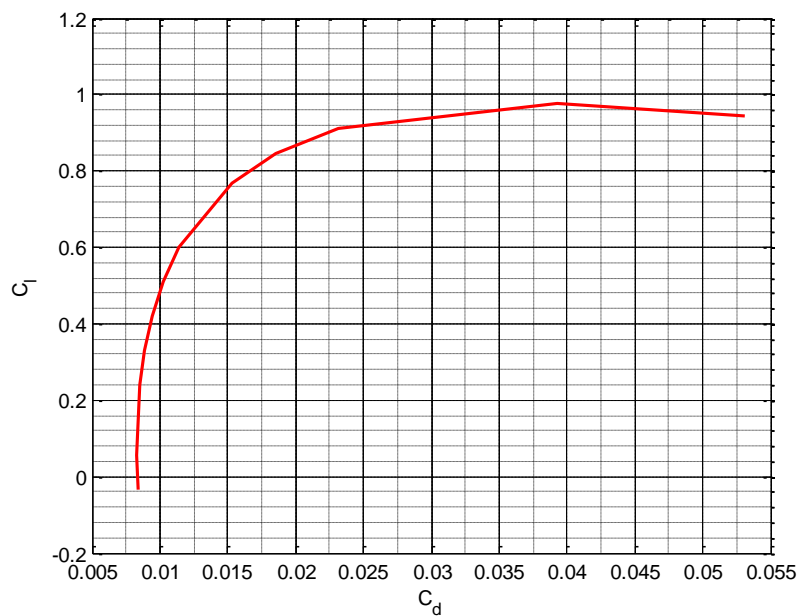


Figure 15: Drag Polar obtained by Ansys CFX

Discussion:

- The Predicted Lift Curve and Drag Polar are almost the same in both methods which shows the Power of the Xfoil Code.

Results:

- $\alpha_0 = -0.62$, $C_{Lmax} = 1.19$

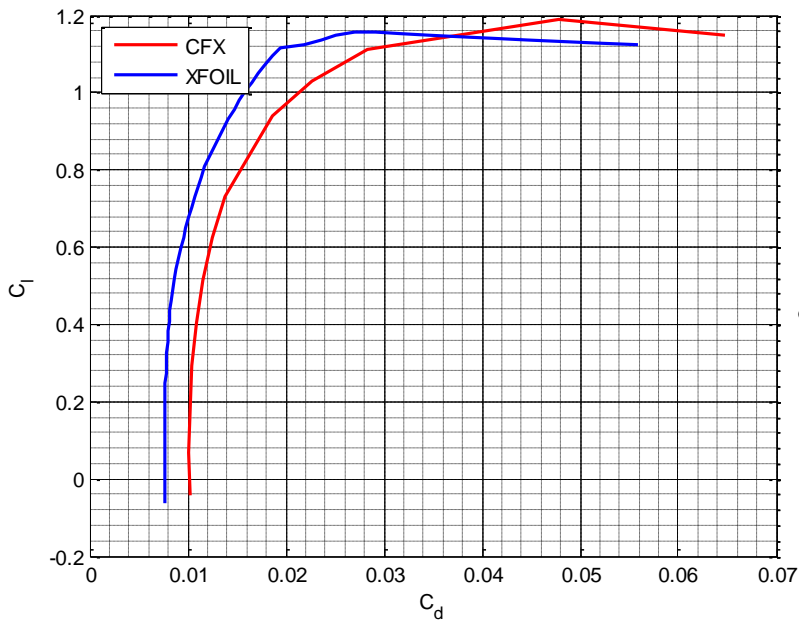


Figure 17: Comparison Between Drag Polars at Re=3E5

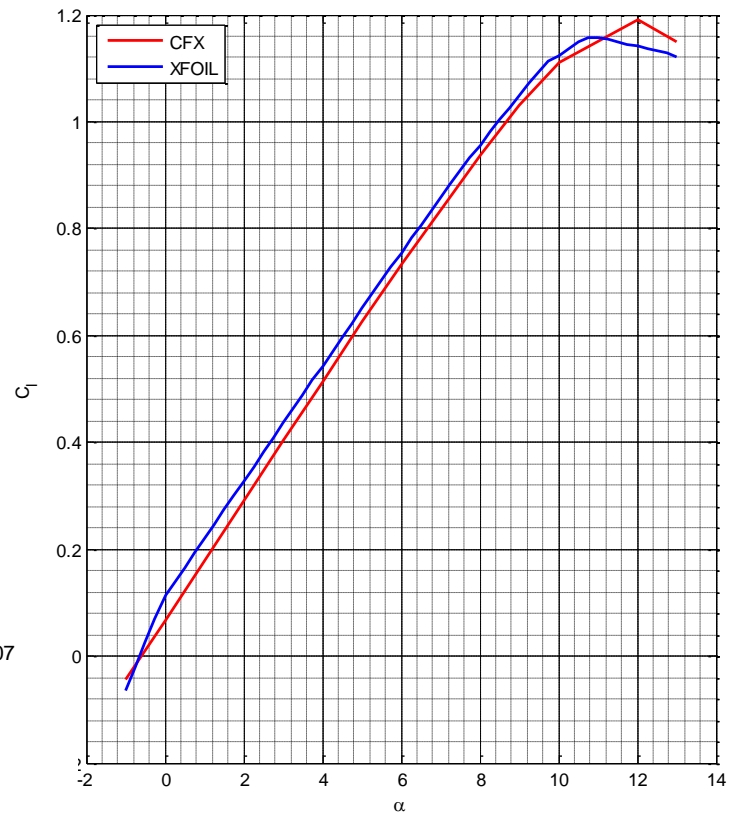


Figure 16: Comparison Between Lift Curves at Re=3E5

3D Analysis

The Final Design of the Wing Obtained after Aerodynamic Optimization of the wing is the Following:

Aspect Ratio	10
Taper Ratio	0.724
Span	2.5
Sweep Back Angle at c/4 line	26[deg]
Washout Angle	-2.5 [deg]
Wash-Out Distribution	Linear
Airfoil	MH60
Airfoil Spline	None

Design Point:

Design Angle of Attack	4.3 [deg]
Design Speed	17.5 [m/s]

- Analysis will be mainly performed at the Design Point.

3D Analysis of the wing will be performed by the Following Methods:

1. 3D Panel Method
2. Multhopp Subsonic Lifting Surface Method
3. CFD Solution

- A Comparison of the Aerodynamic Parameters of the Wing will be made between the following three Methods.

Solution at the Design Point

3D Panel Methods

The 3D panel method has been implemented with the following objectives:

- Refine the LLT and VLM results by a more sophisticated full 3D method, taking into account the wings' thickness, whereas the VLM only considers the mean camber line.
- provide insight in the C_p distributions over the top and bottom surfaces of a wing
- provide a method capable of modeling fuselages

The principle of the 3D Panel Method is to model the perturbation generated by the wing by a sum of doublets and sources distributed over the wing's top and bottom surfaces. The strength of the doublets and sources is calculated to meet the appropriate boundary conditions, which may be of the Dirichlet or Neumann type.

Results

Cp Distribution over the Wing

C_L	0.3577
C_{Di}	0.0040
C_{D0}	0.0083
$C_D = C_{Di} + C_{D0}$	0.0123
C_{M_LE}	-0.4695
C_{M_COG}	-0.0146
kfactor	1.03241
C_L/C_D	29.0813

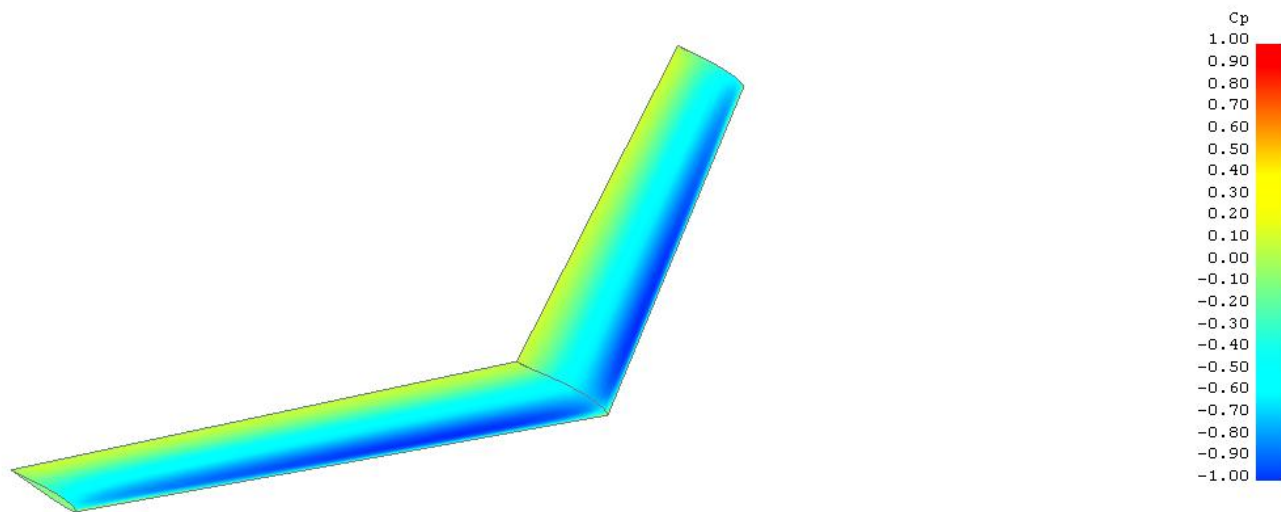


Figure 18: Cp Distribution using 3D Panel Methods at Design Point

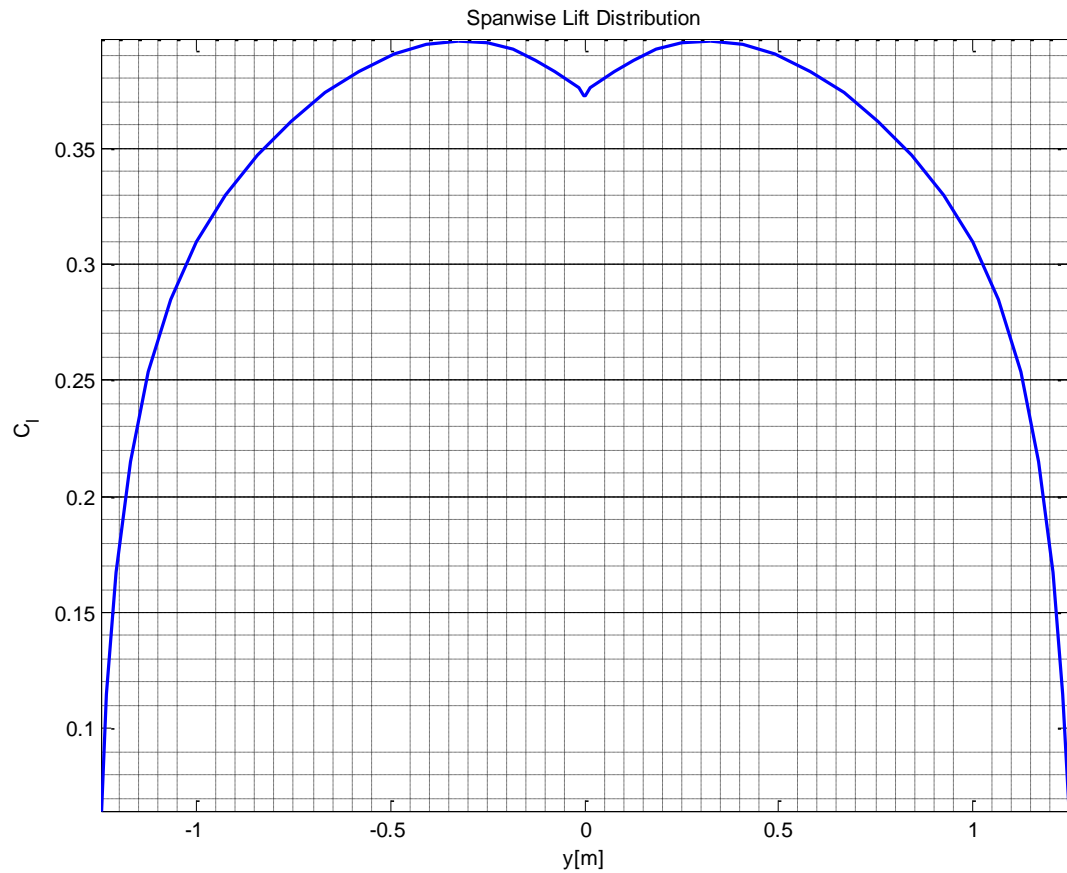


Figure 19 : Spanwise Lift Distribution using 3D Panel Methods at Design Point

Discussion:

The Induced Drag is calculated using the Panel Method, however the Parasite Drag is calculated by calculating the Reynolds number at every spanwise station and using the value of the spanwise lift distribution to get the corresponding drag value using the airfoil Drag Polar to obtain the spanwise drag distribution then integrating over the span we get the wing Parasite Drag.

Multhopp Subsonic Lifting Surface Method

The Method is explained extensively before so we get right down to the results.

Results

C_L	0.35
C_{Di}	0.0039
$C_{D0}(\text{Laminar})$	0.0046
$C_D = C_{Di} + C_{D0}$	0.0085
C_{M_LE}	-0.4544
C_{M_COG}	-0.0146
kfactor	1.0066
C_L/C_D	40.9426

At the Design Point

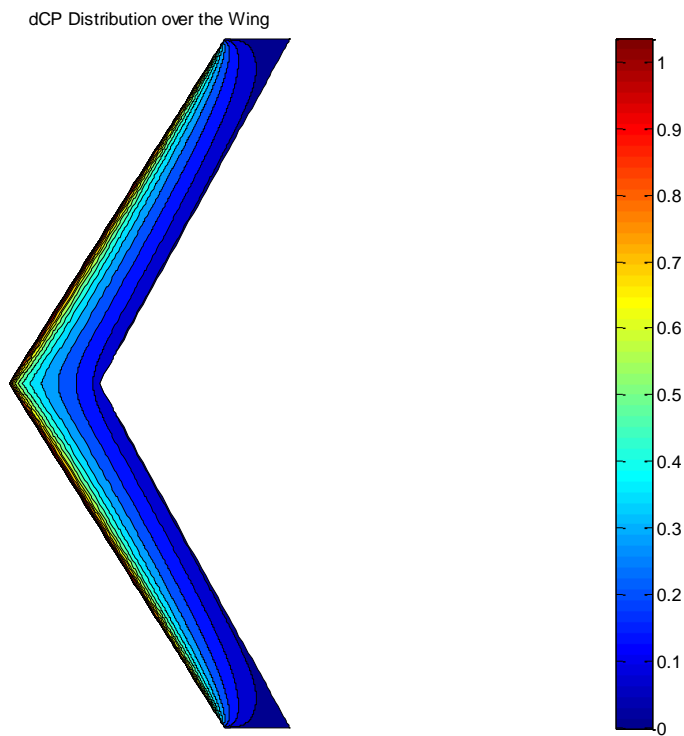


Figure 20 : Cp Distribution using Lifting Surface Method at Design Point

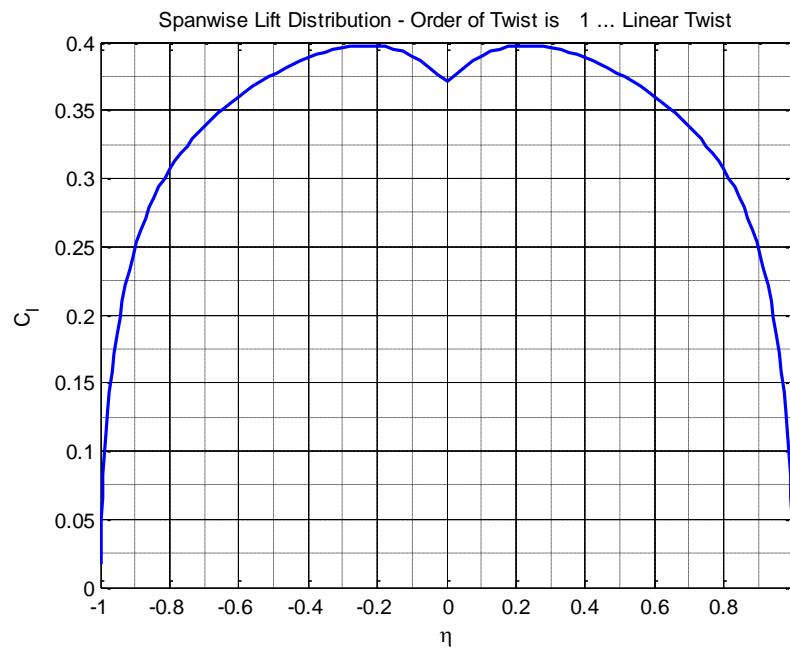


Figure 21: Spanwise Lift Distribution using Lifting Surface Method at Design Point

Discussion:

- The Model used to evaluate the Wing parasite Drag is Empirical Model Stated in “Aircraft Design” by Roskam with the assumption that flow is entirely Laminar over the wing.
- The effect of Possible Turbulence could not be introduced which explains the high Gliding Ratio or The Low Drag of the Aircraft.
- Possible Turbulence effect will be introduced in the CFD Analysis.

CFD Solution

A CAD model was constructed in Solidworks and a Coarse and Fine Mesh was used to model the problem in

Ansys CFX and The Following Results were obtained at The Design Point

Wing

Coarse Mesh

Mesh Statistics:

Total Number of Nodes = 438259

Total Number of Elements = 2502996

Results:

C_L	0.393369
C_D	0.0298481
C_{M_LE}	-0.538934
C_{M_COG}	-0.0380026
C_L/C_D	13.188

Cp Distribution over the Wing

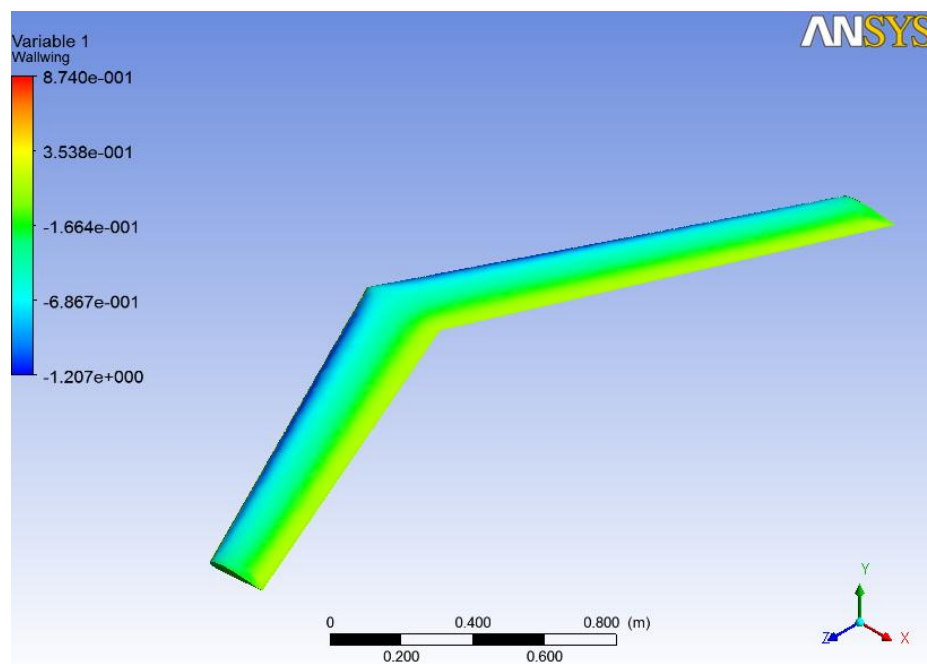


Figure 22 :Cp Distribution using CFD (Coarse Mesh) at Design Point

*Fine Mesh*Mesh Statistics:

Total Number of Nodes = 111934

Total Number of Elements = 643025

Results:

C_L	0.37207
C_D	0.022396
C_{M_LE}	-0.49742
C_{M_COG}	-0.0242
C_L/C_D	16.613

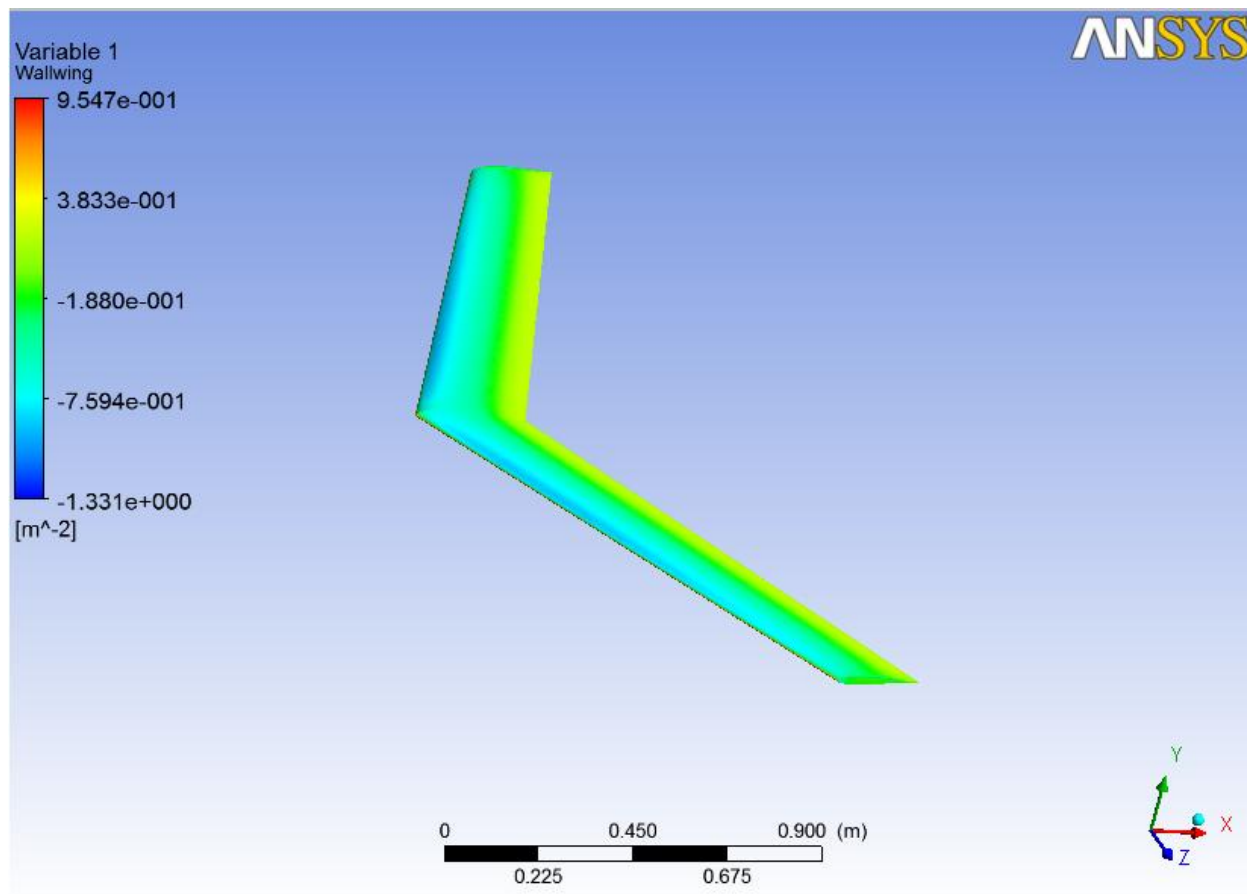
Cp Distribution over the Wing

Figure 23 : Cp Distribution using CFD (Fine Mesh) at Design Point

Discussion:

1. The Difference in values of lift is considerably small between the two meshes, but quite for the moment and drag.
2. The k- ϵ Turbulence Model was used to predict any possible effect of Turbulence in the Flow over the wing which explains the high Drag value.
3. The Error in the Lift Calculation with respect to the other two methods is relatively low but the error in moment is higher but still good enough to validate the results obtained by the two previous Methods.

Comparison between the Three Types of Analysis

Comparison will be done with respect to the following:

1- $C_L - \alpha$ Curve

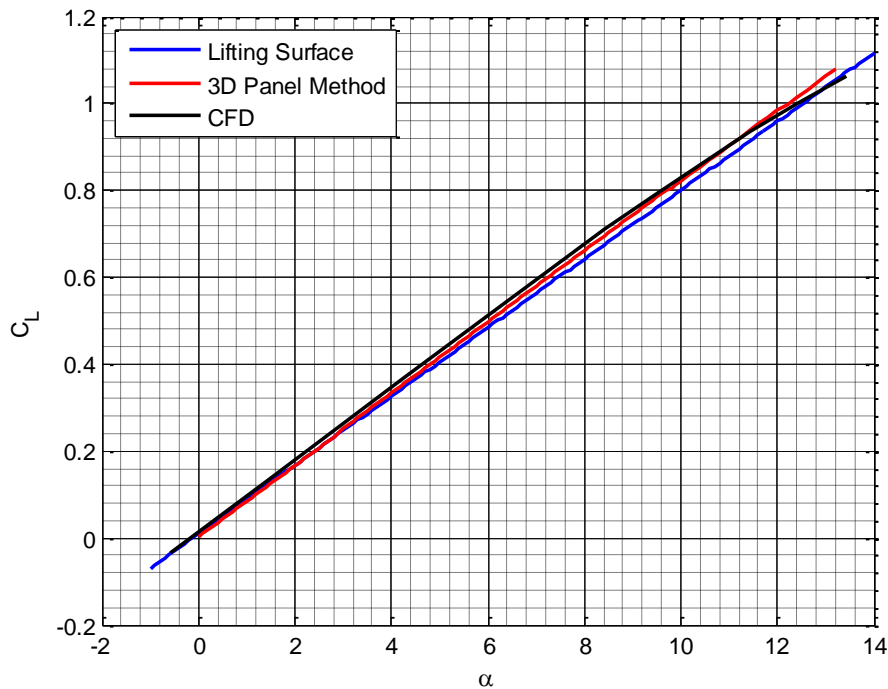


Figure 24 : Comparison between Lift Curves obtained by the Three Methods

2- $C_{mCOG} - \alpha$ Curve

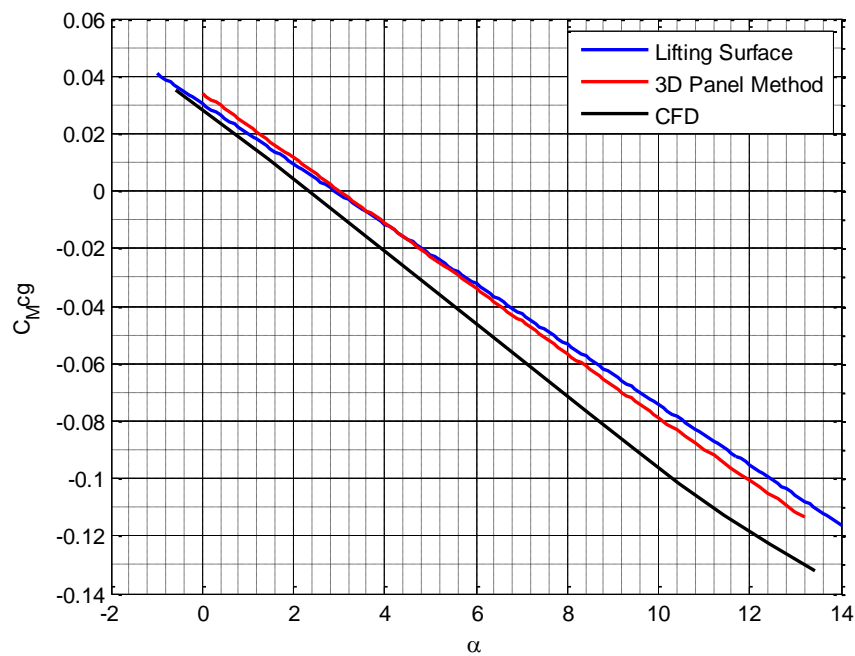


Figure 25 : Comparison between Moment Curves obtained by the Three Methods

Conclusion:

The 3 Methods presented very close results especially the Lift, however for the moment the error between the 3D Panel Method and Lifting Surface Method with respect to the CFD Solution which could mean that either the mesh was not good enough to get accurate calculation of the pitching moment or the error is in the method used in the 3D Panel Method and Lifting Surface Method to evaluate the pitching moment

Full Aircraft CFD Simulation

Fine Mesh Was Constructed for Ansys CFX and only half the Aircraft was solved .

Mesh Statistics:

Number of Nodes = 197153

Number of Elements = 1112635

Results:

C_L	0.33207
C_D	0.0313
$C_{M_{LE}}$	-0.39016
C_L/C_D	11.0212

C_p Distribution of the Aircraft

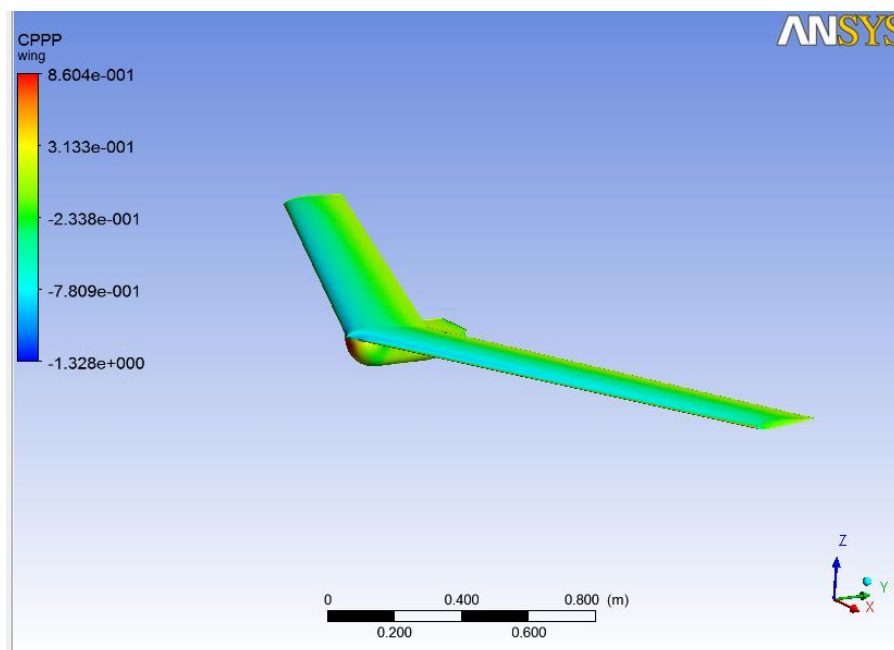


Figure 26 : C_p Distribution using CFD (Full Aircraft) at Design Point

Chapter 5 Structural Design:

Introduction:

Structural design is the process of determine ribs, skin (shape and dimensions) and materials to find the best structural configuration to carry specific load and perform specific tasks. There are many aspects of design of aircraft structures, we can say that the structural design of our aircraft (flying wing) is determine by;

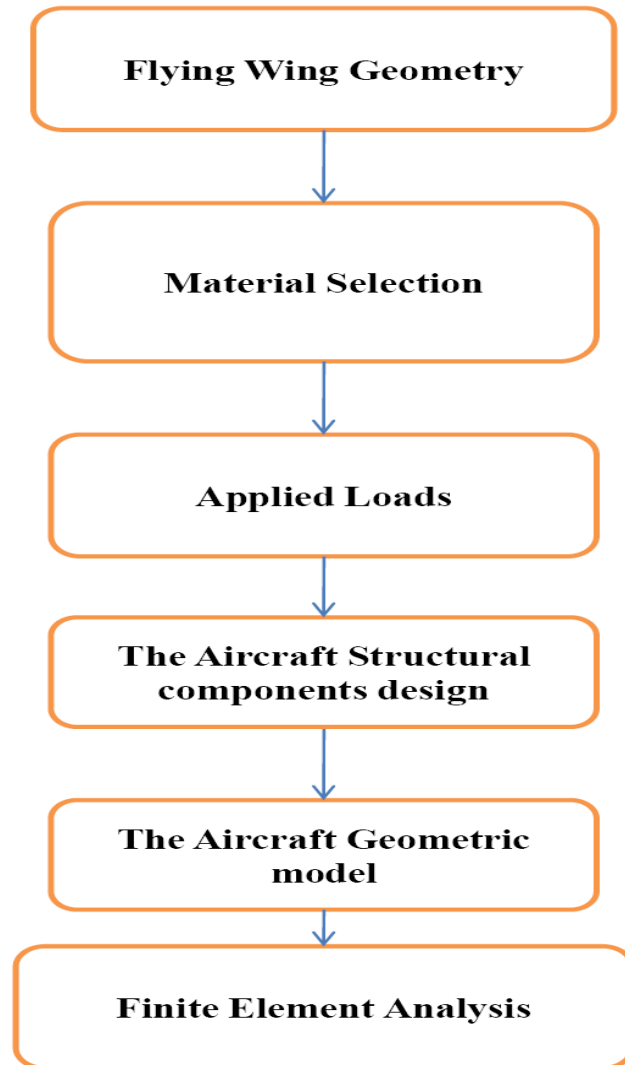


Figure 27-Flow chart to Structural design procedure

Flying Wing Geometry:

Aspect Ratio (AR)	10
Taper Ratio (Z)	0.724
Wing Area (S)	0.625
Sweep back angle (φ)	26°
Washout (α_w)	-2.5
Root chord (C_r)	0.29 m
Tip chord	0.21 m

Material Selection:

Introduction to composite materials:

A composite material is formed by the combination of two or more distinct materials to form a new material with enhanced properties. The composite materials used for aircraft structure belong to the class known as “fiber composites” comprising continuous fibers

embedded in a resin matrix. The prime reason for using composite materials is that substantial weight savings (of order 25% because fibers and the polymers used as matrices have low density) can be achieved because of their superior strength-to-weight and stiffness-to-weight ratios, as compared with the conventional materials of aircraft construction such as the aluminum alloys. The key features of composites are that they have high strength with low weight, and they are corrosion resistant and last a long time. Fibers cannot be used alone, because fibers cannot sustain compression or transverse loads. A binder or matrix is thus required to hold the fibers together. The usual practice is to write the name in the format “fiber/matrix”.

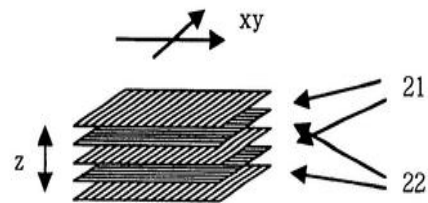


Figure 28-Composite material

FIBERS:

Fibers are used in composites because they are lightweight, stiff, and strong. Fibers are stronger than the bulk material that constitutes the fibers. There are many types of fibers used for aircraft structure applications, e.g. Glass fibers and Carbon fibers.

Glass fibers:

They are flexible, lightweight, and inexpensive. These properties make glass fibers the most common type of fibers used in low-cost industrial application. All glass fibers have similar stiffness but different strength values and different resistance to environmental degradation.



Figure 29-Glass fiber

Carbon fibers:

Also called **graphite** fibers, are lightweight and strong fibers with excellent chemical resistance. They dominate the aerospace market. Unlike glass fibers, carbon fibers are available with a broad range of stiffness values.

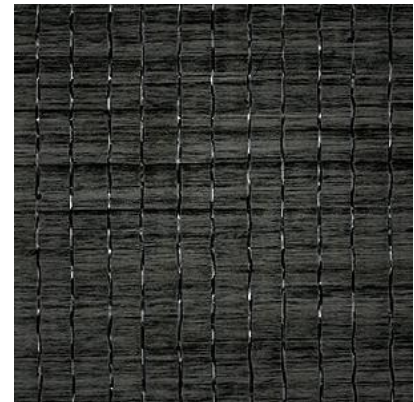


Figure 30-Carbon fiber

Matrices:

The matrix material holds the fibers together, thus transferring the load between fibers and between the composite and the supports. It also protects the fibers from the environment and mechanical abrasion and carries some of the loads, particularly transverse stress and inter-laminar shear stress. It separates the fibers to prevent failure of adjacent fibers when one fails.

The selection of a matrix is guided by the mechanical properties, the corrosion resistance and the flammability of the polymer matrix in the composite

Advanced composite materials usually refer to more expensive and high performance composites targeted to aerospace applications, mostly carbon/epoxy or carbon/thermoplastic systems.

Choice of materials:

There are wide ranges of choice for both the reinforcement and the resin materials of the composite. The most common combination for aerospace applications is an epoxy resin with carbon-fiber fabric reinforcement and we will use them.

Why we used carbon/Epoxy?

- High rupture resistance
- Very good fatigue strength
- Very good heat and electricity conductor
- High operating temperature (limited by the resin)

But it is more delicate fabrication.

Aircraft Loads:

Aircraft loads are those forces and loading applied to the airplane structural components to establish the strength level of the complete airplane. These loading may be caused by air pressure, Inertia forces, Propulsion, and weight.

The aircraft Structural components:

In this section we desire to determine the aircraft structural components design.

Wing Structural design:

The wing is essentially a beam which transmits and gathers all of the applied air-load to the central attachment. The term design is related to the design of composite wing structures refer to the process of establishing an appropriate laminate configuration to perform the given function. Our wing is completely composite material, and consists of skin, ribs, and spar (all composite structure; as well as having graphite/epoxy skin, it also has a graphite/epoxy ribs) then we required to design wing skin, ribs and spar.

Skin Design:

Skin is the most common wing cover. The skin is primarily required to carry direct stresses in the span wise direction due to the wing bending more or less as a cantilever beam and shear stresses caused by the wing twisting; there will be also generally smaller direct stresses in the chord-wise direction due to forward and after bending. The simplest design approach is to use a laminate pattern (defined with respect to a reference axis in the span-wise direction) consisting of 0° plies to carry the span-wise direct stresses, $\pm 45^\circ$ plies to carry the shear stresses, and 90° plies to carry the chord-wise direct stresses. The laminates have been designed so that the

interaction between the direct loads and the shear strains reduces the wing twist to an acceptable level.

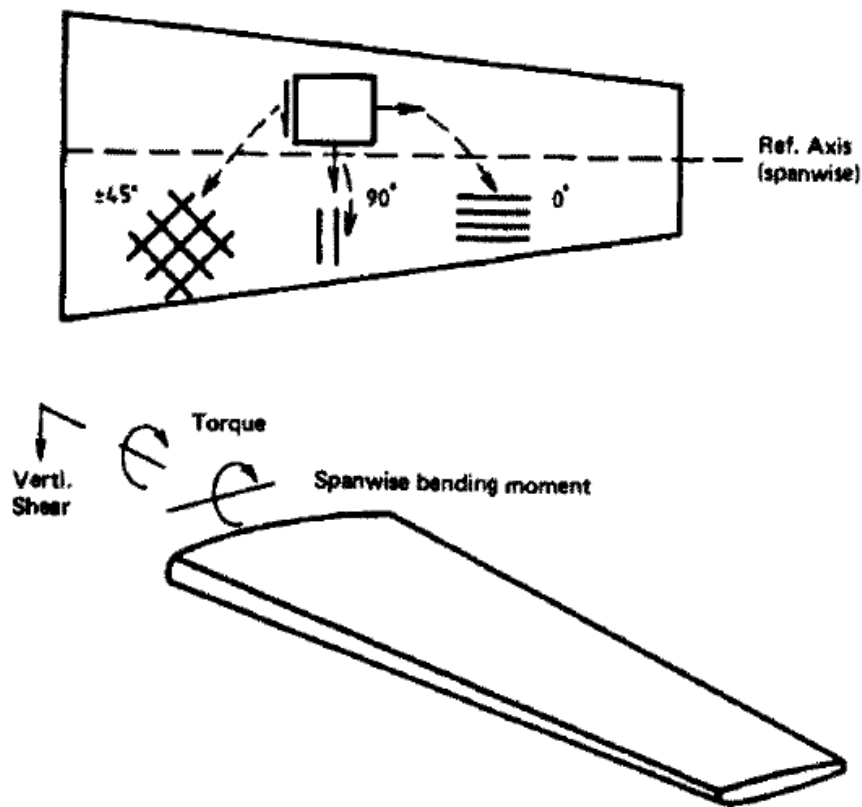


Figure 31-Tailoring of fiber directions for the applied loads in a composite wing skin (ply orientation).

Where the load distribution decreasing in the span wise direction, then we can design the wing skin as consists of two parts

The inboard skin:

Consists of four layers with angles 0, 90, -45, +45 with thickness $t = 0.6096 \text{ mm}$

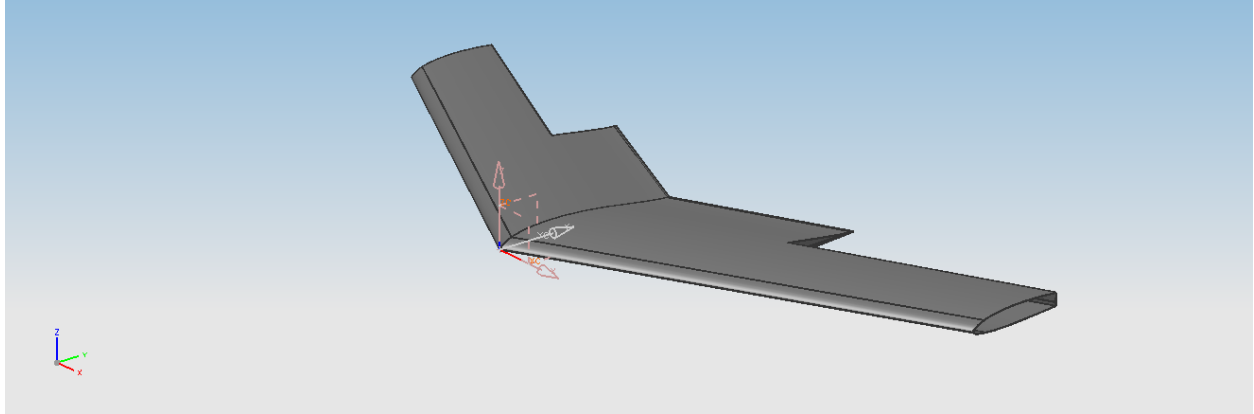


Figure 32-The inboard skin

The outboard skin:
Consists of two layers with orientation ∓ 45 with thickness $t = 0.3048$ mm.

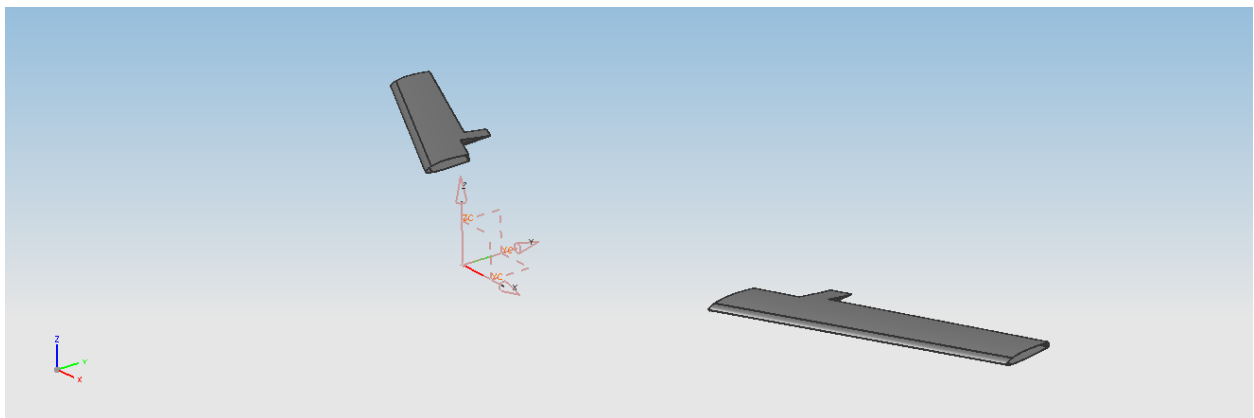


Figure 33-The outboard skin

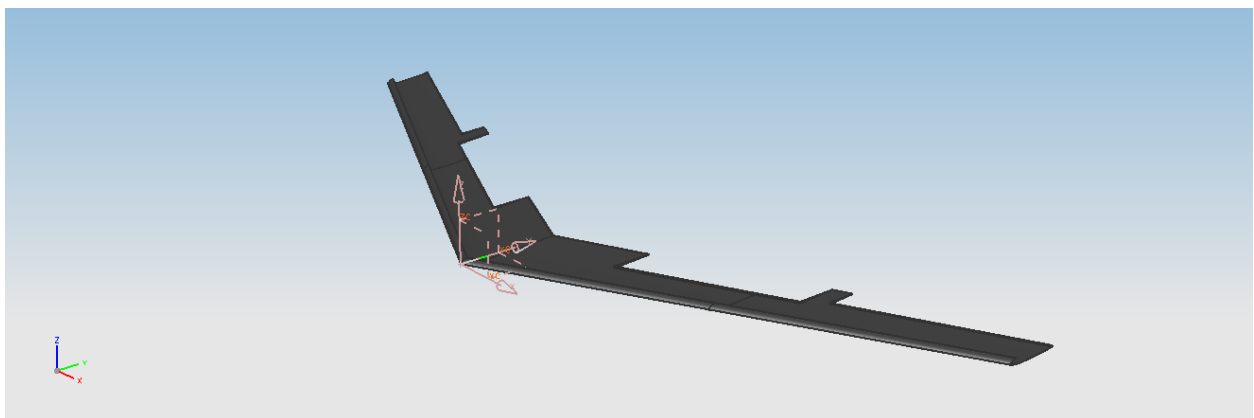


Figure 34-The lower skin

Ribs Design:

Ribs are structural components that are repeated at regular intervals span-wise in an aircraft wing. For aerodynamic reasons the wing contour in the chord direction must be maintained without appreciable distortion. Therefore, ribs are used to hold the cover panel to contour shape. The rib also has another major purpose, to act as a transfer or distribution of loads. Usually ribs incorporate the airfoil shape of the wing, and the skin adopts this shape when stretched over the ribs. The optimum wing structure would have variable rib spacing with the maximum spacing at the inboard end, to make the design simple we will construct a constant rib thickness with 8 layers carbon fiber with thickness $t = 1.2192 \text{ mm}$ and rib spacing = 250 mm.

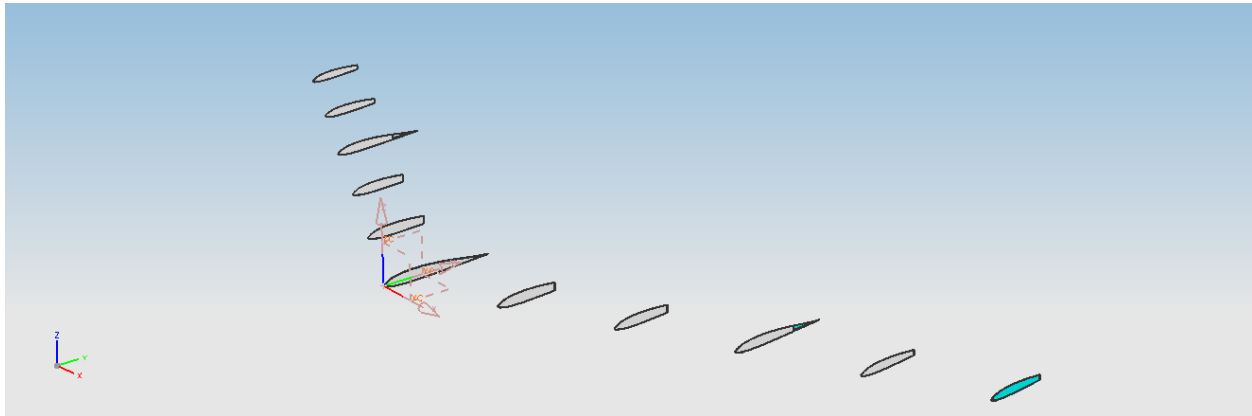


Figure 35-Wing Ribs

Spar design:

Most airplane wings use a so-called torque-box (wing-box) as the main load carrying component. The torque box should be located to take maximum advantage of the structural height available within the airfoil contours. This will save weight. The torque box is normally closed off by a front spar, a rear

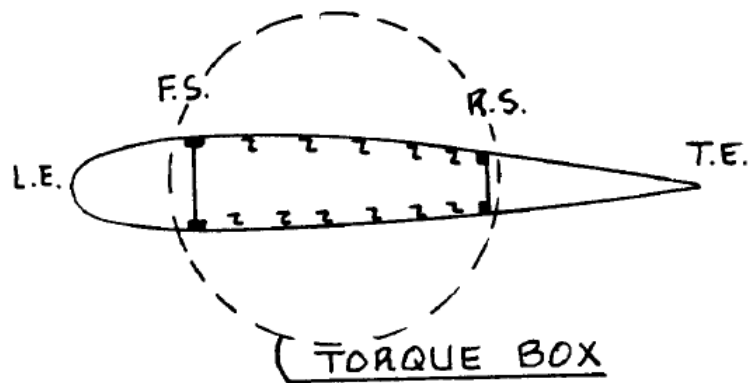


Figure 36-Spar design

spar and an upper and lower skin. The spar locations are often constrained by requirements for high lift devices, where the spar carrying the main aircraft loads (Bending moment and shear force). In our aircraft the maximum wing thickness relatively small then we will design a front spar only;

Spar component	Number of layers	thickness
Shear web	16	2.4384
Upper and lower flanges	32	4.8768

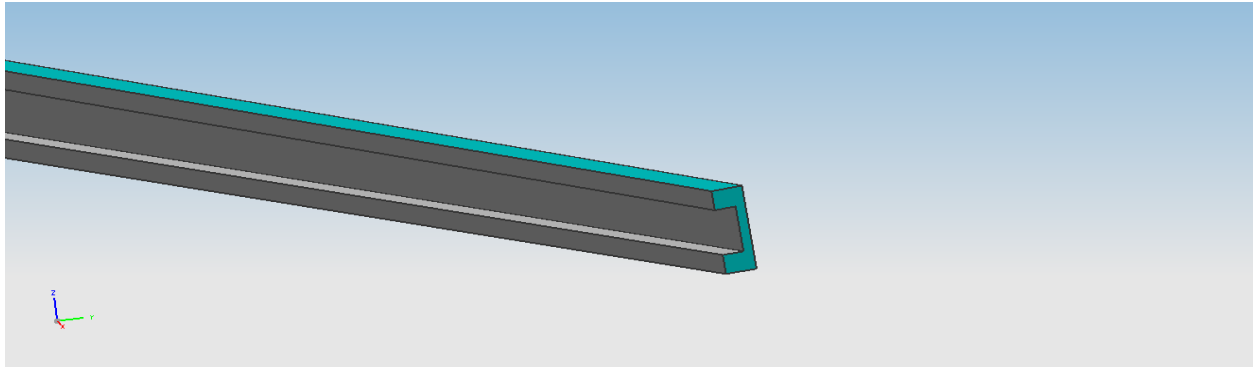


Figure 37-The wing spar

Fuselage structural design:

Skin design:

Consists of three layers with thickness $t = 0.9144$ mm.

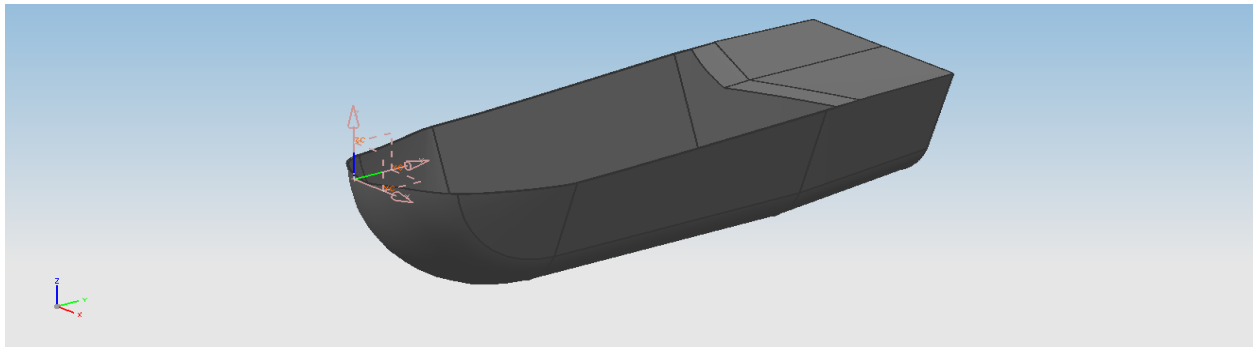


Figure 38-The fuselage skin

Frames design:

Frames are designed with 8 layers carbon fiber with suitable holes to hold the propulsion components and to make wing fuselage joint based on it, with thickness $t = 1.2192$ mm.

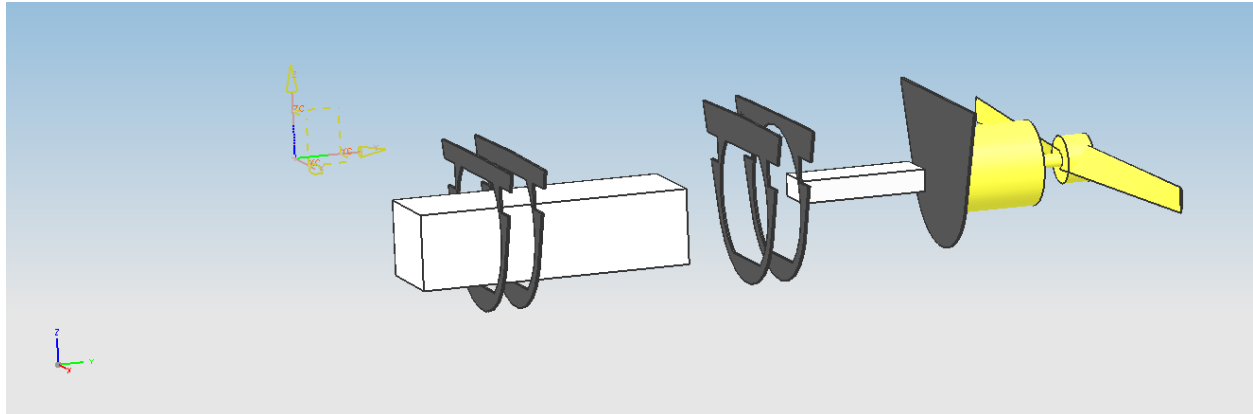


Figure 39-The Frames

Finite Element Analysis (FEA):

General:

The Finite Element method is the computational tool most widely used to validate the performance of structures. It provides the analysis required for the design process. Typically it can be used to define the displacements, stresses, Vibration, and buckling characteristics of a structure composed of metal or composite materials under a defined set of loads and displacement boundary conditions. The FEA involves dividing the structure into discrete elements (panels). Each panel becomes an assembly of non-overlapping plate or brick elements that are connected at discrete points called nodes. The behavior of each element is defined by a relation between force and displacement at the nodes that are usually located on the boundaries of the element. The elements are then assembled into the structure by satisfying the equilibrium of the forces. This process is equivalent to pinning the elements together at the nodes. Constraint of the deformation on the element ensures an appropriate level of continuity of displacement and slope is maintained on the element boundary. The results are a set of linear algebraic equations that are solved to determine the displacements at the nodes. The purpose of analysis is usually to determine the response of a system based on some type of excitation or loading where;

- CAD geometry is an idealization of the physical model.
- The mesh is mathematical representation of the CAD model.
- The accuracy of answers is determined by
 - How well the physical model is represented depends on the assumptions.
 - Numerical accuracy is determined by the mesh density.

Then we can make the FEA with the following procedure:

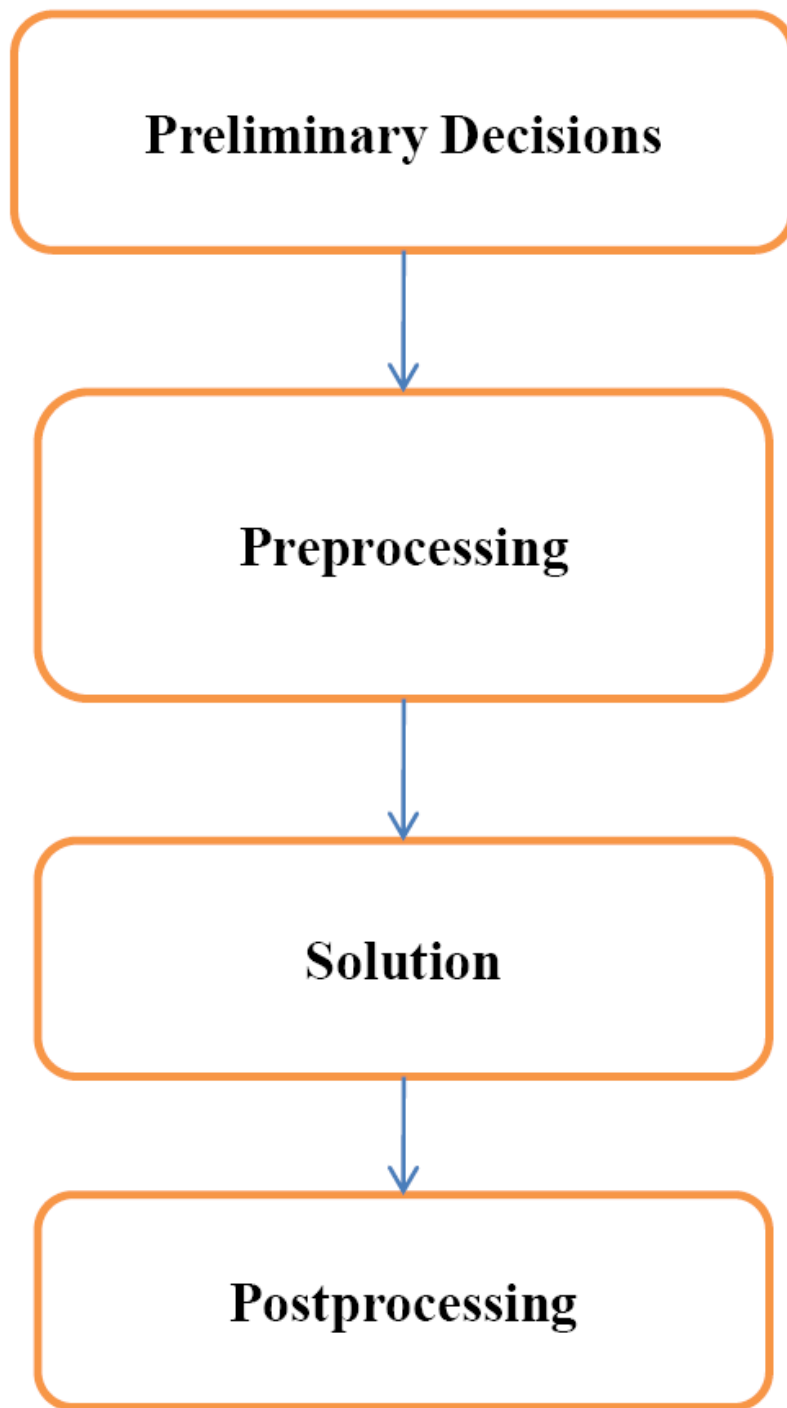


Figure 40-FEA procedure

Preliminary Decision:

The preliminary decision is that we will make a static structural analysis using **ANSYS** program and by importing the aircraft geometry from the UG-NX5 program and we will make two models for the aircraft.

Model 1:

The wing only¹

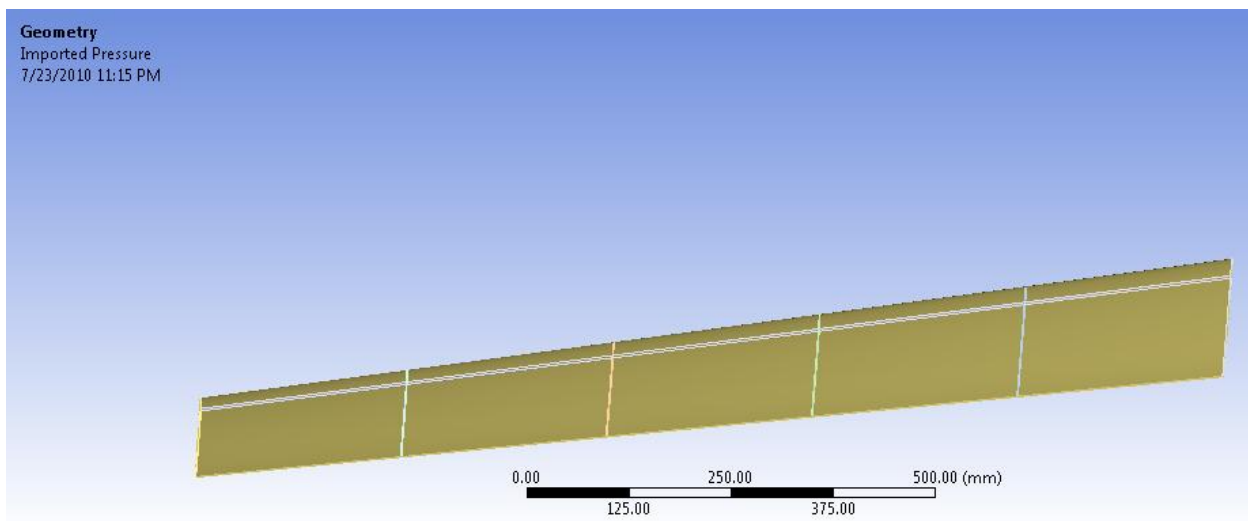


Figure 41 - the left half wing

Model 2:

The complete aircraft²

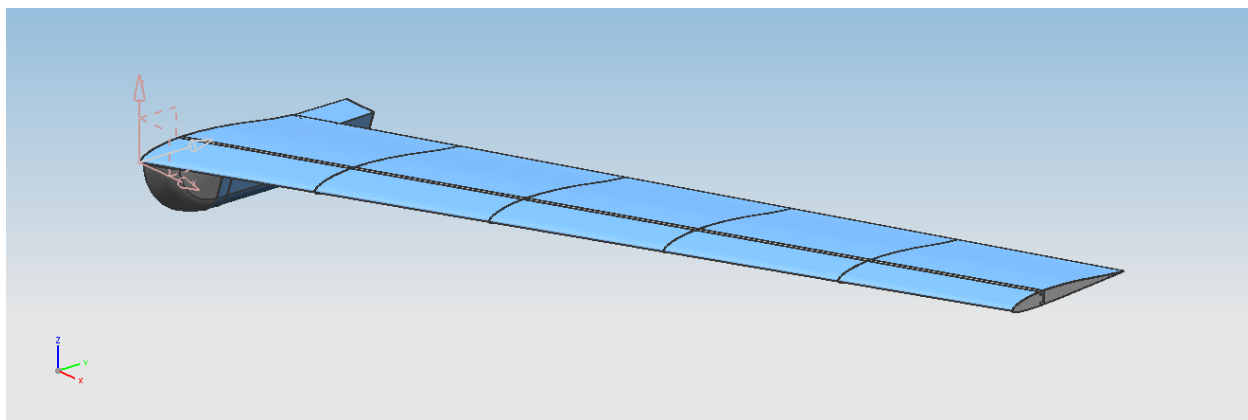


Figure 42- the left half of the aircraft

¹ The ANSYS report in Appendix A

² The ANSYS report in Appendix B

The Preprocessing:

- Solid bodies are generally 3-D or 2-D:
 - 3-D solids are meshed with higher-order tetrahedral or hexahedral solid elements with quadratic shape functions
 - 2-D solids are meshed with higher order triangle or quadrilateral solid elements with quadratic shape function.
- Surface bodies are geometrically 2-D but spatially 3-D:
 - Surface bodies represent structures which are thin in one dimension (through thickness).
 - Thickness is not modeled but supplied as an input value.
 - Surface bodies meshed with linear shell elements having six DOF (UX, UY, UZ, ROTX, ROTY, ROTZ).
- Line bodies are geometrically 1-D but spatially 3-D.

In our analysis we will solve the ribs, spar, and frames as 2-D solid body and Wing skin and fuselage skin as surface bodies.

Material Properties:

To assign material properties to a body highlight it and select from available properties in the Engineering data but we will use carbon fiber then we will input its properties in the engineering data. For surface bodies a thickness needs to be supplied. We get the material properties using Cambridge Engineering Selector (ESC) Program.

Epoxy/HS Carbon Fiber, Woven Fabric Composite, Biaxial Lamina General

Tradenames

Cycom, Fiberdux, Scotchply

Designation

High Strength Carbon Fibre/Epoxy Composite, 0/90° Biaxial Lamina

Density	0.05564	-	0.05816	lb/in ³ =1.6 *10 ⁻⁶ MPa
(N/mm ³)				

Energy Content	*4.836e+004	-	6.898e+004	kcal/lb
----------------	-------------	---	------------	---------

Price	*25.65	-	30.42	USD/lb
-------	--------	---	-------	--------

Recycle Fraction	0.01	-	0.02	
------------------	------	---	------	--

Composition

Composition (Summary)

Epoxy + Carbon fibre reinforcement

Base	Polymer			
C (Carbon)	60	-	65	%
Carbon (fibre)	60	-	65	%
Polymer	35	-	40	%

Mechanical

Bulk Modulus	*1.14	-	1.479	10 ⁶ psi
--------------	-------	---	-------	---------------------

Compressive Strength	95	-	135.9	ksi =655 MPa
----------------------	----	---	-------	--------------

Elongation	0.98	- 1.41	%
Elastic Limit	90.94	- 132	ksi
Endurance Limit	* 50.02	- 85.79	ksi
Fracture Toughness	* 39.48	- 42.6	ksi.in ^{1/2}
Hardness - Vickers	* 10.8	- 21.5	HV
Loss Coefficient	* 1.4e-003	- 3.3e-003	
Modulus of Rupture	90.94	- 132	ksi
Poisson's Ratio	0.058		
Shape Factor	8		
Shear Modulus	0.5076		10 ⁶ psi = 3499.778 MPa
Tensile Strength	90.94	- 132	ksi = 627.0092 MPa
Young's Modulus	9.094	- 9.964	10 ⁶ psi = 62700.92 MPa
Thermal			
Maximum Service Temperature	* 743.4	- 887.4	°R
Minimum Service Temperature	* 414	- 504	°R
Specific Heat	* 0.2266	- 0.2613	BTU/lb.F
Thermal Conductivity	* 0.624	- 1.271	BTU.ft/h.ft ² .F
Thermal Expansion	* 3.061	- 16.27	µstrain/°F
Electrical			
Resistivity	* 1.71e+005	- 5.64e+005	µohm.cm
Optical			
Transparency	Opaque		
Environmental Resistance			
Flammability	Good		
Fresh Water	Very Good		
Organic Solvents	Good		
Oxidation at 500C	Very Poor		
Sea Water	Very Good		
Strong Acid	Average		
Strong Alkalis	Very Good		
UV	Good		
Wear	Average		
Weak Acid	Very Good		
Weak Alkalis	Very Good		

Epoxy/HS Carbon Fibre, Woven Fabric Composite, QI Laminate General

Tradenames

Cycom, Fiberdux, Scotchply

Designation

High Strength Carbon Fibre/BMI Composite, Quasi-isotropic Laminate [0/90,+45/-45]s

Density 0.05564 - 0.05816 lb/in³

Energy Content * 4.836e+004 - 6.898e+004 kcal/lb

Price * 25.65 - 30.42 USD/lb

Recycle Fraction 0.01 - 0.02

Composition

Composition (Summary)

Epoxy + Carbon fibre reinforcement

Base	Polymer		
C (Carbon)	60	- 65	%
Carbon (fibre)	60	- 65	%
Polymer	35	- 40	%
Mechanical			
Bulk Modulus	* 1.14	- 1.479	10 ⁶ psi
Compressive Strength	* 68.12	- 96.89	ksi = 469.6708
Elongation	* 0.84	- 0.93	%
Elastic Limit	* 65.22	- 94.1	ksi
Endurance Limit	* 35.87	- 61.17	ksi
Fracture Toughness	* 5.569	- 79.73	ksi.in ^{1/2}
Hardness - Vickers	* 10.8	- 21.5	HV
Loss Coefficient	* 1.4e-003	- 3.3e-003	
Modulus of Rupture	* 65.22	- 94.1	ksi
Poisson's Ratio	* 0.335	- 0.339	
Shape Factor	7.9		
Shear Modulus	* 2.403	- 2.608	10⁶ psi
Tensile Strength	* 65.22	- 94.1	ksi = 449.676
Young's Modulus	6.416	- 6.986	10⁶ psi = 44236.7609
Thermal			
Maximum Service Temperature	* 743.4	- 887.4	°R
Minimum Service Temperature	* 414	- 504	°R
Specific Heat	* 0.2266	- 0.2613	BTU/lb.F
Thermal Conductivity	* 0.624	- 1.271	BTU.ft/h.ft ² .F
Thermal Expansion	* 3.061	- 16.27	µstrain/°F
Electrical			
Resistivity	* 2.31e+005	- 7.2e+005	µohm.cm
Optical			
Transparency	Opaque		
Environmental Resistance			
Flammability	Good		
Fresh Water	Very Good		
Organic Solvents	Good		
Oxidation at 500C	Very Poor		
Sea Water	Very Good		
Strong Acid	Average		
Strong Alkalies	Very Good		
UV	Good		
Wear	Average		
Weak Acid	Very Good		
Weak Alkalies	Very Good		

Contact regions:

Contact regions define how parts interact with each other, without contact parts will not interact with each other. Contact regions prevent parts from penetrating through each other and provide a mean of load transfer between parts. When an assembly is import contact surfaces are automatically detected and created and it must be checked. In our project we have 22 contact regions.

Model 1:

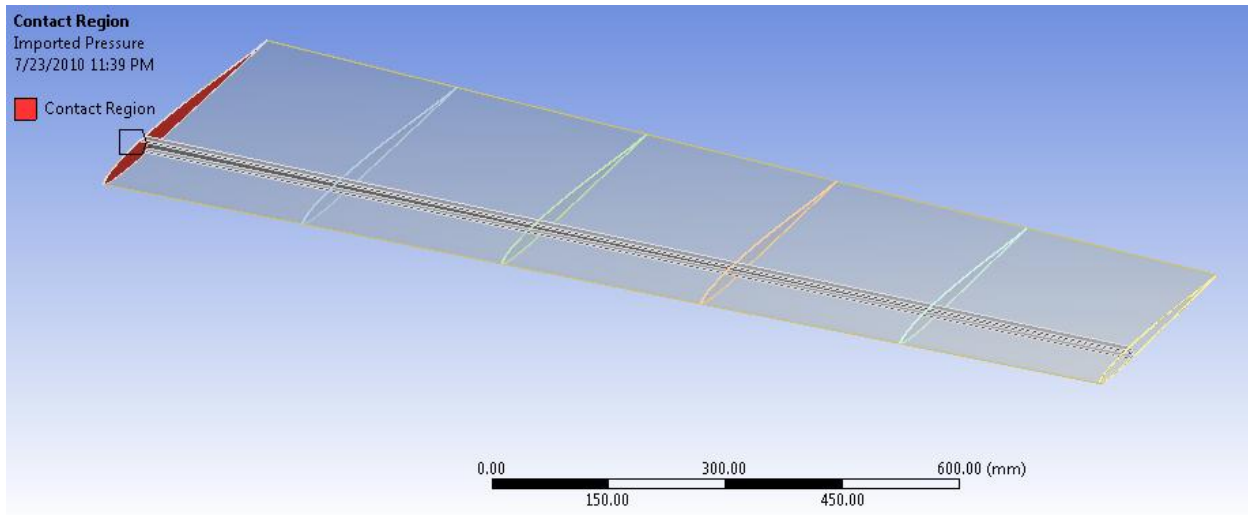


Figure 43 -The contact regions

Model 2:

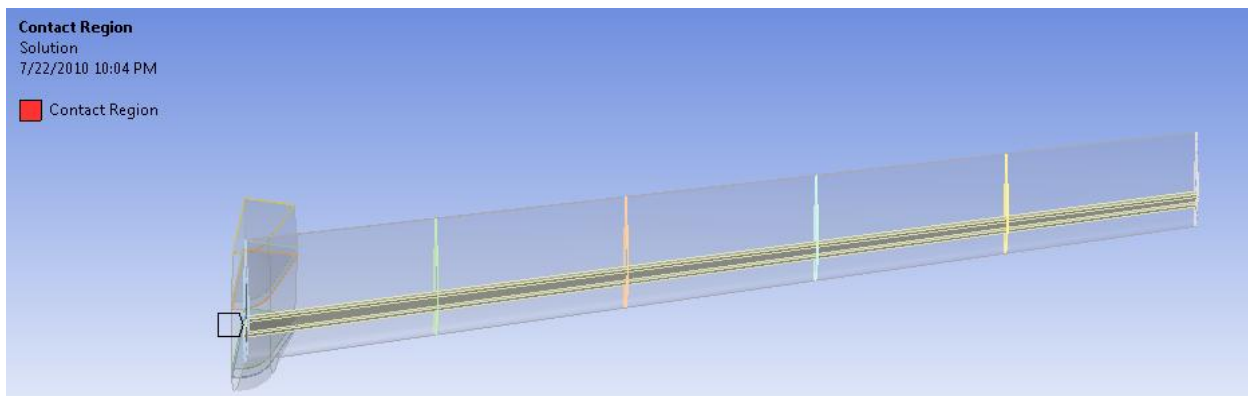


Figure 44-The contact regions

Meshing:

A finer mesh produces more precise answer but also increase CPU time and memory requirements.

Model 1:

A fine meshes With 27289 nodes and 13791 elements and using triangle elements.

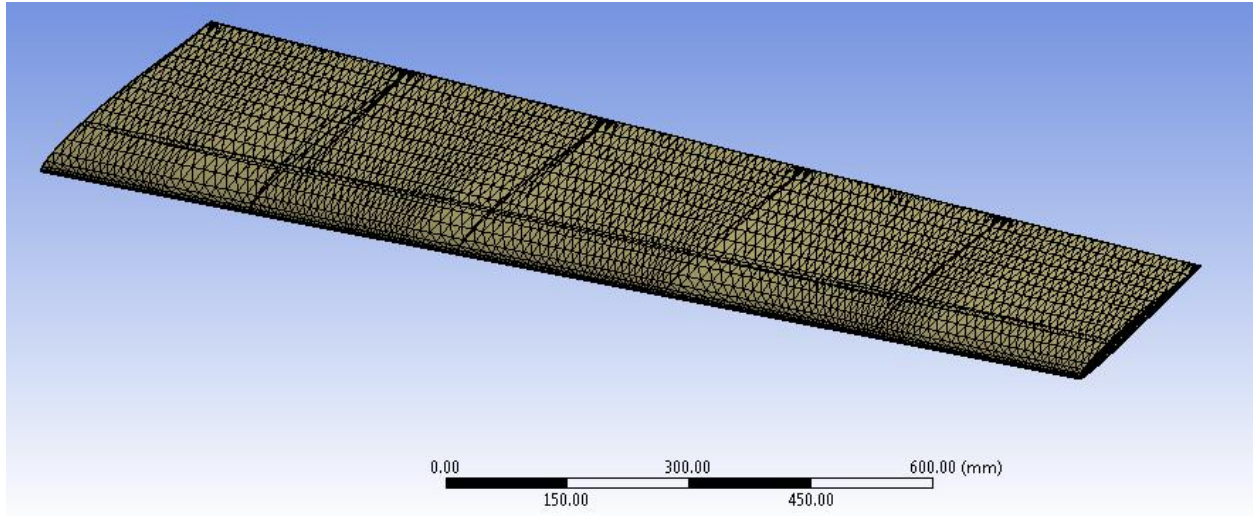


Figure 45-Generating mesh (model 1)

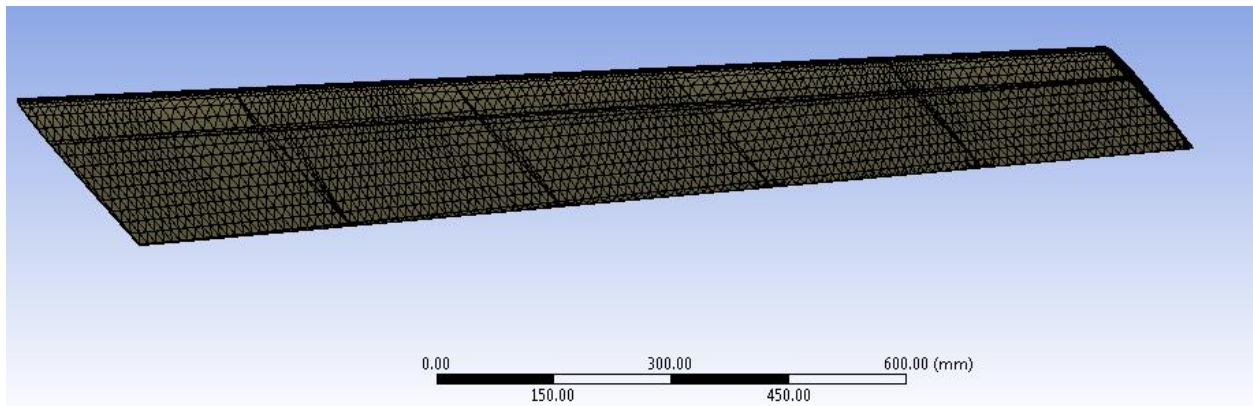


Figure 46-Generating mesh (Model 1)

Model 2:

A fine meshes with 91115 nodes and 27276 elements and using triangle elements.

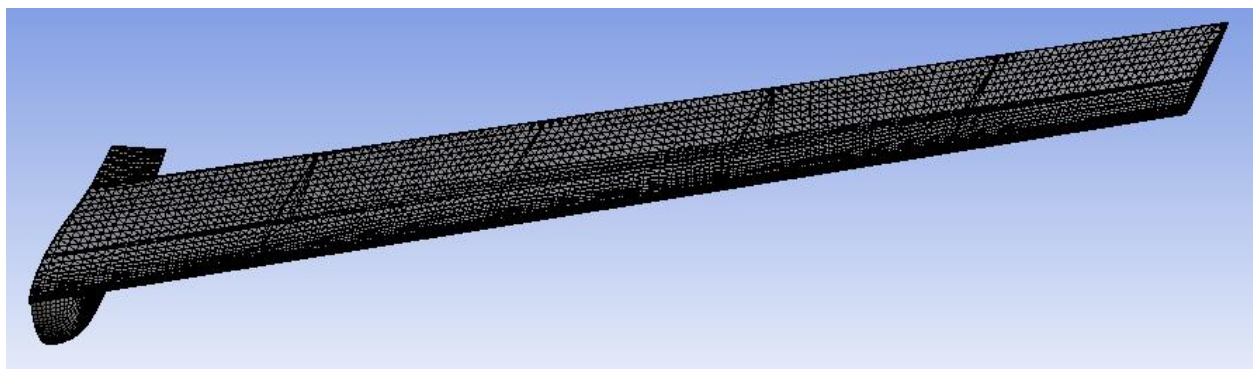


Figure 47-Generating mesh (Model 2)

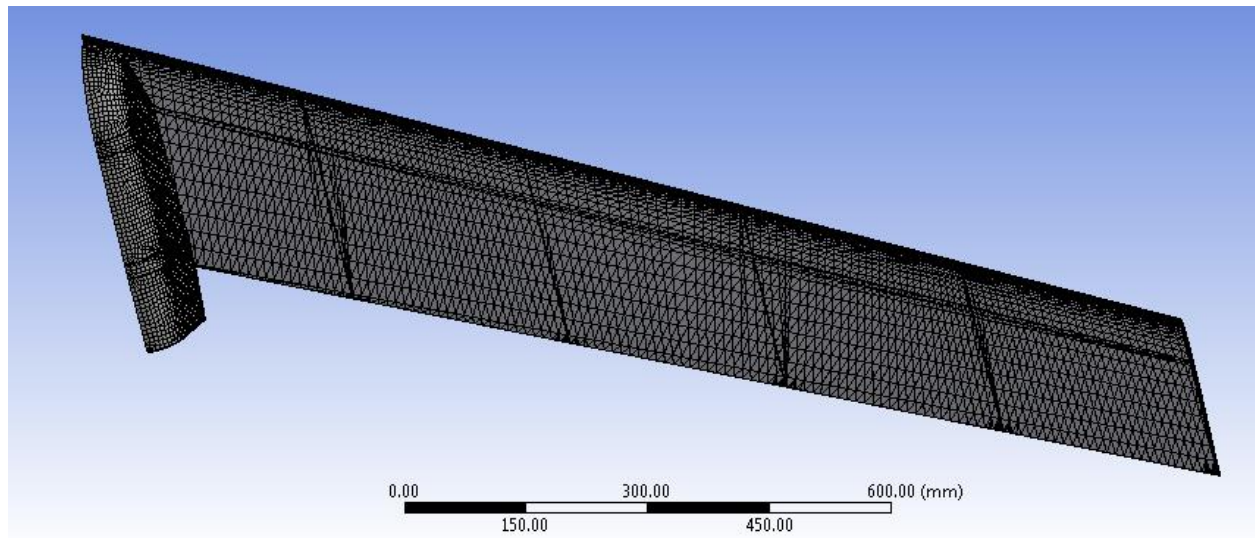


Figure 48-Generating mesh (Model 2)

Aircraft loads:

Load types:

- Inertia loads:
 - These loads act on the entire system
 - Density is required for mass calculations.
 - These are only loads which act on defined point masses.
- Structural loads:
 - Pressure, Forces and moments acting on parts of the system.
- Thermal Loads:
 - Thermal load results in temperature field causing thermal expansion/contraction in the model.

To import the aircraft load we solve the flow around the aircraft using CFD ANSYS program and then translate this data to static structure analysis

Model 1:

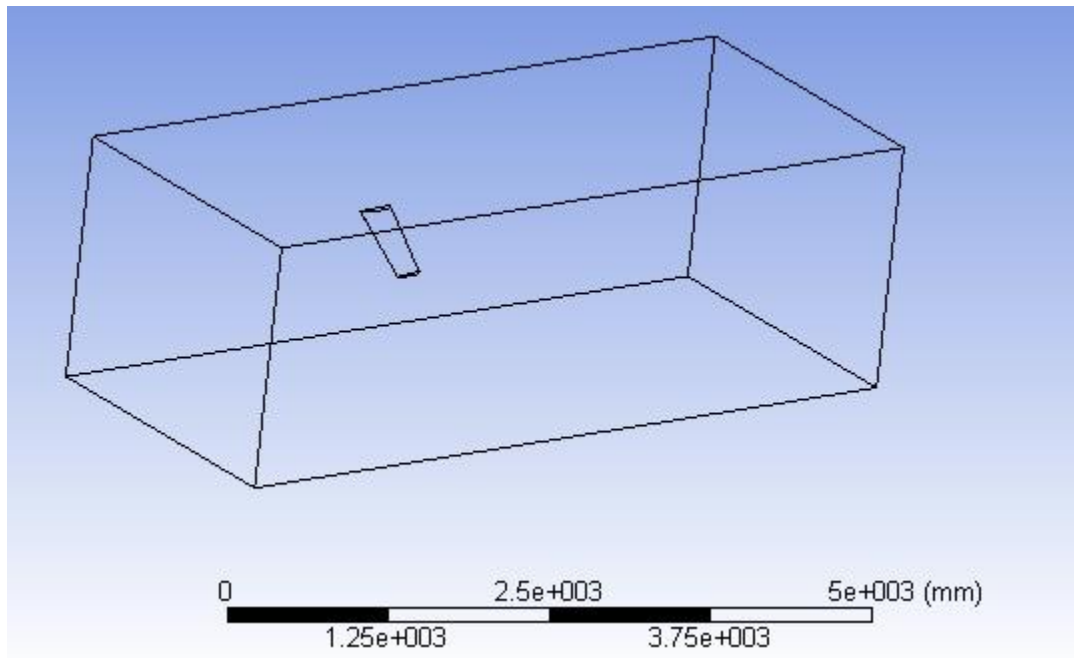


Figure 49-The geometric model 1 for aerodynamic analysis

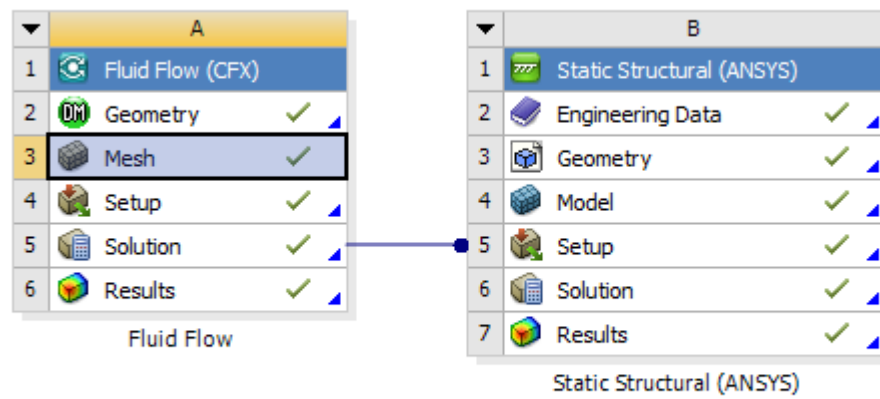


Figure 50-Import the aerodynamic load to structural analysis

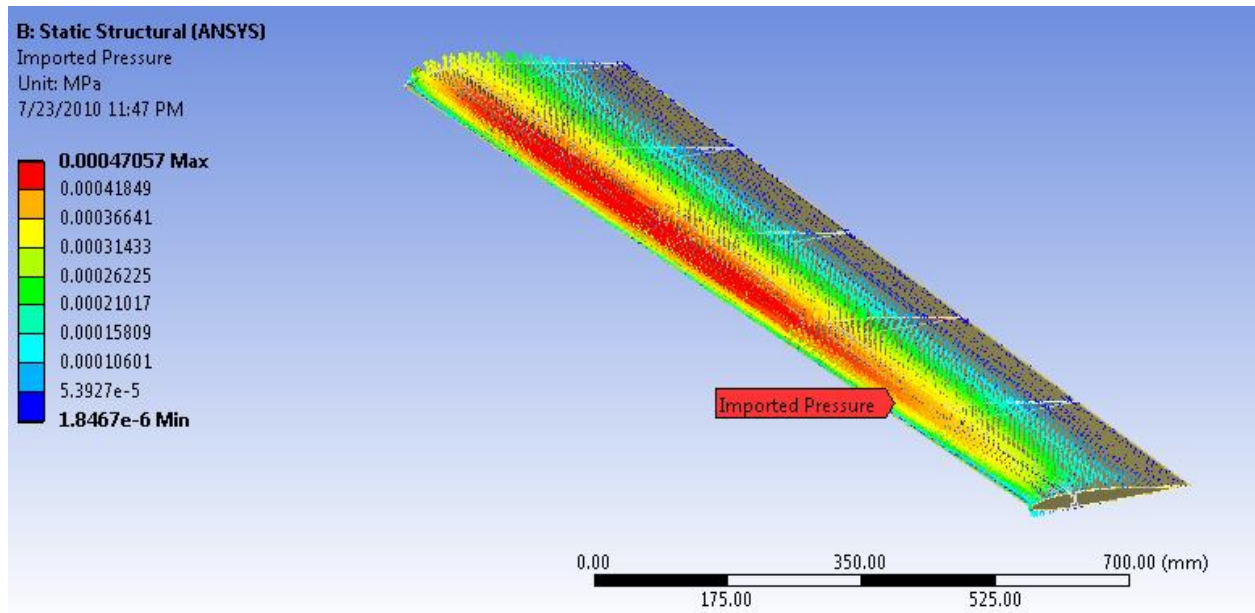


Figure 51-the aerodynamic load (Model 1)

Model 2:

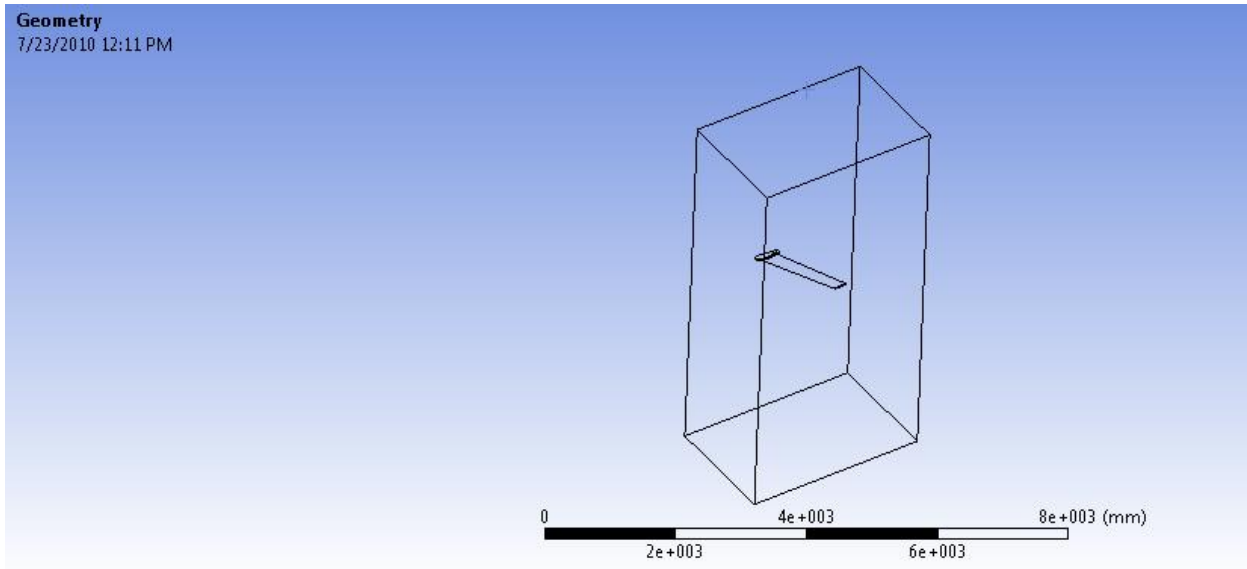


Figure 52-geometric model 2 for aerodynamic analysis

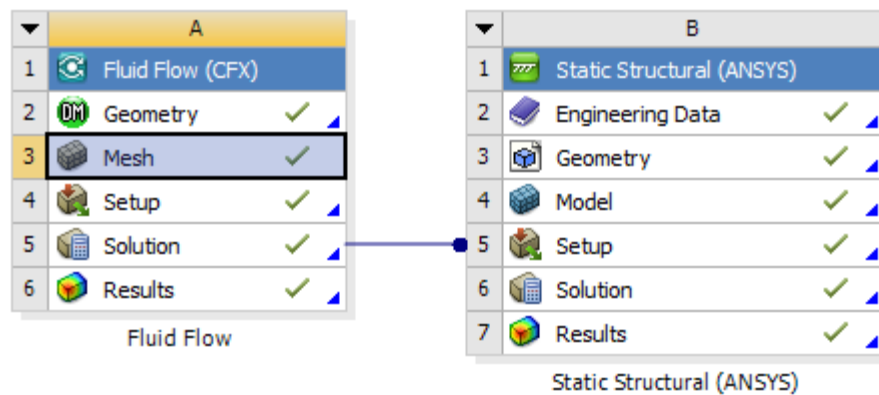


Figure 53-Import the aerodynamic load to structural analysis

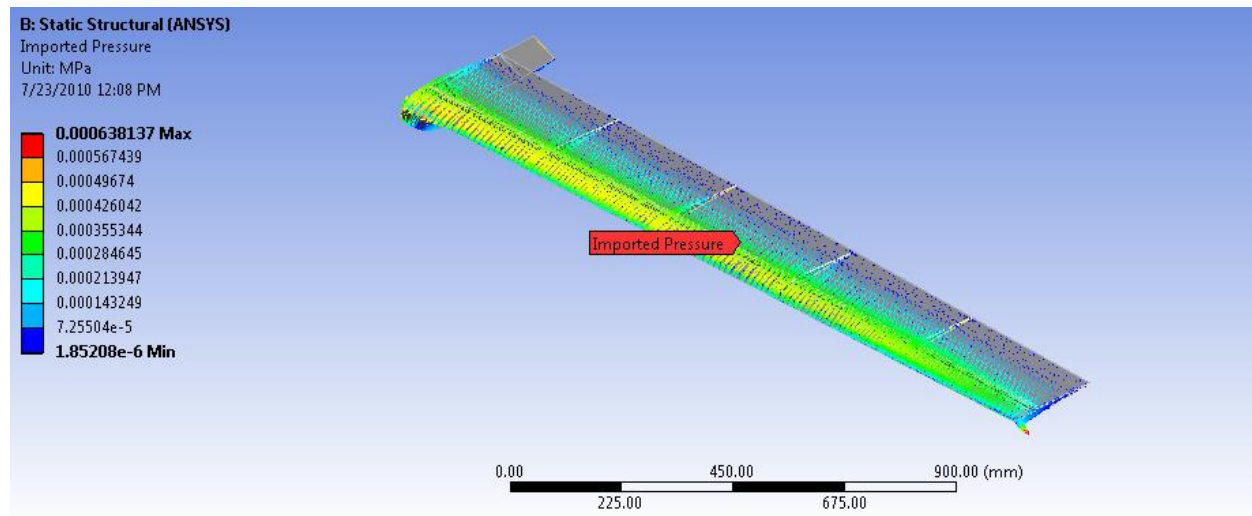


Figure 54-The aerodynamic load (Model 2)

The thrust force:

$$F_{max} = 52 \text{ N}$$

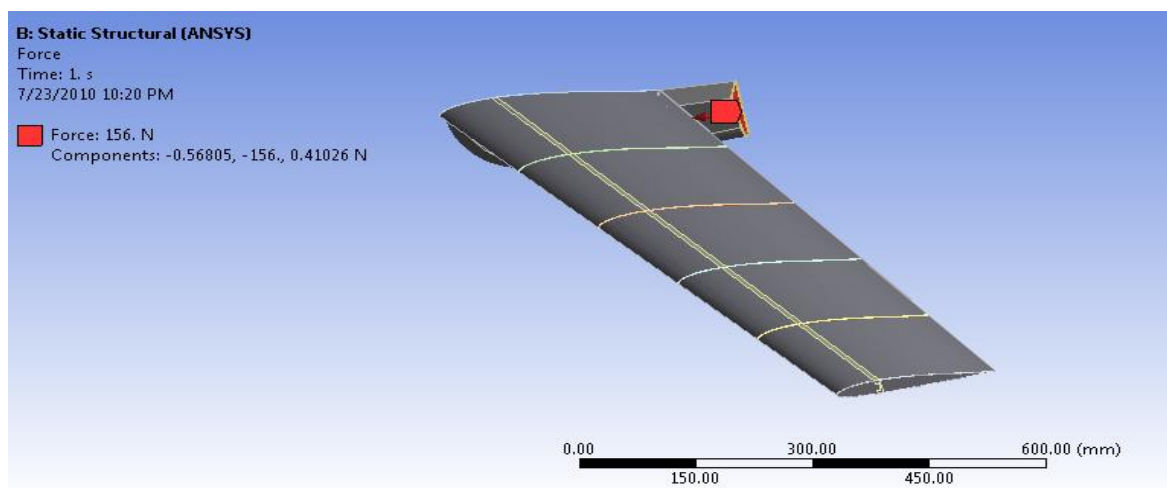


Figure 55-The engine thrust force

For our aircraft category the maximum load factor for it is 3, after we import the pressure distribution to the structural model we multiply this load by the load factor.

Structural Supports:

Constraints prevent movement on certain regions.

Model 1:

We desire to make the wing supported to the fuselage with simply support.

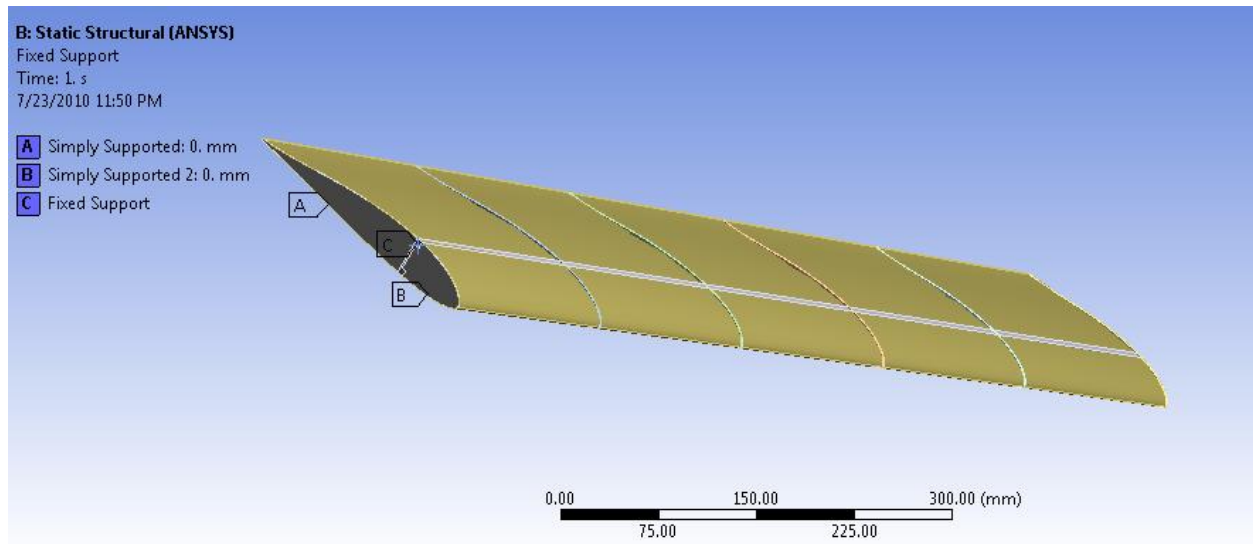


Figure 56-Structure supports (Model 1)

Model 2:

We desire to make the complete aircraft fixed at the axis of symmetry

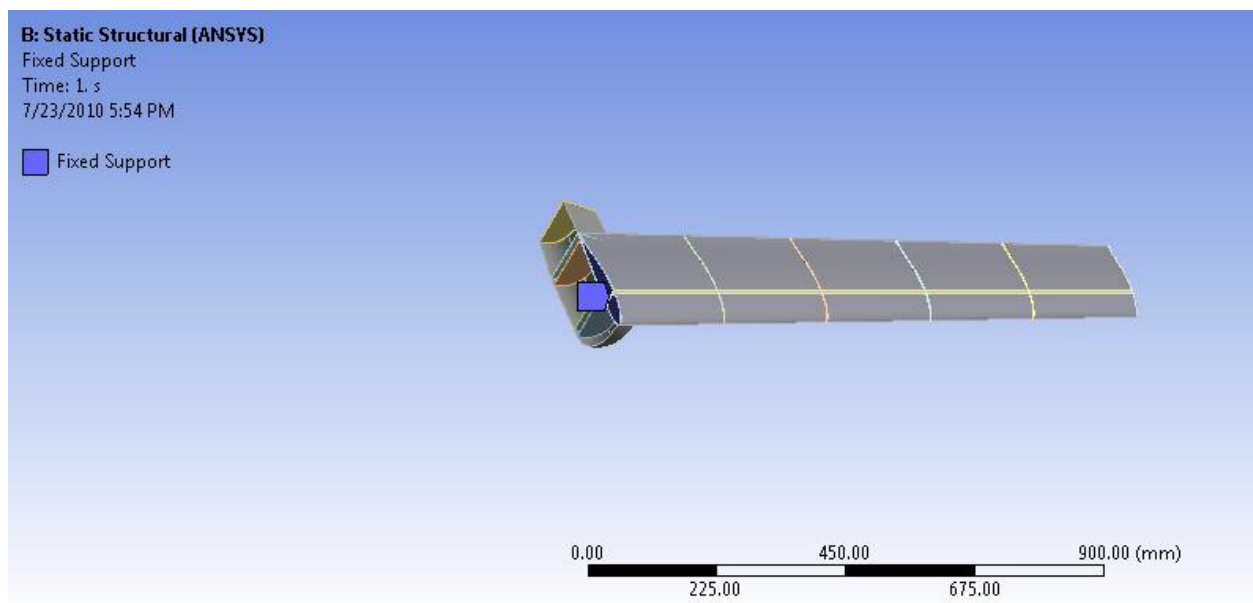


Figure 57-Structure supports (Model 2)

Then we solve the model

The post processing:

Include

- Review results.
- Check the validity of the solution.

Model 1:

The equivalent Von-Mises stress:

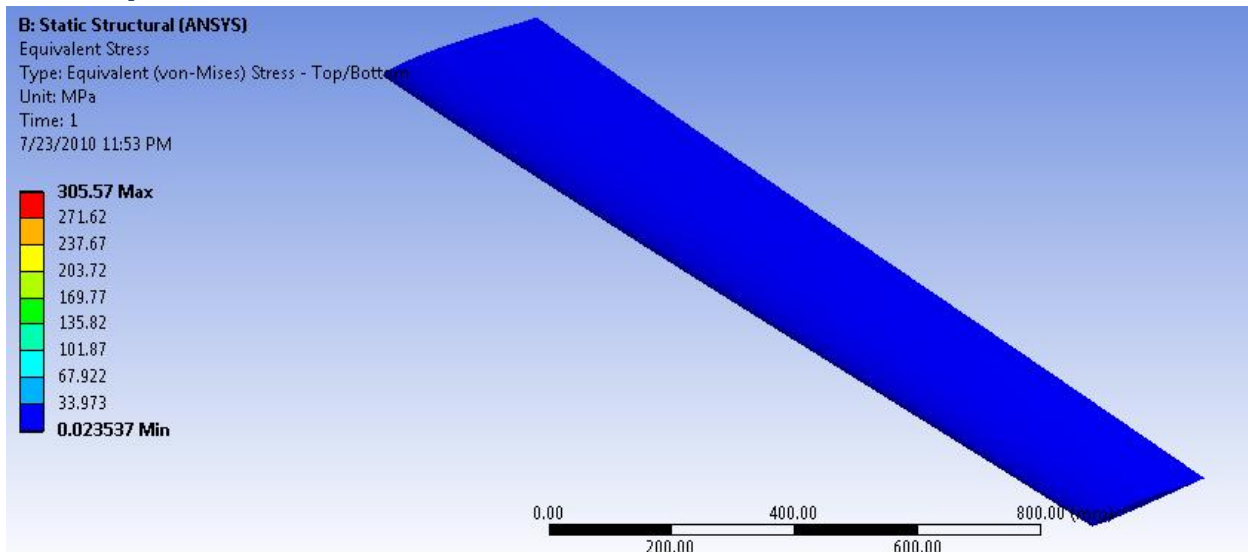


Figure 58-The equivalent Von-Mises stress (Model 1)

The total deformation:

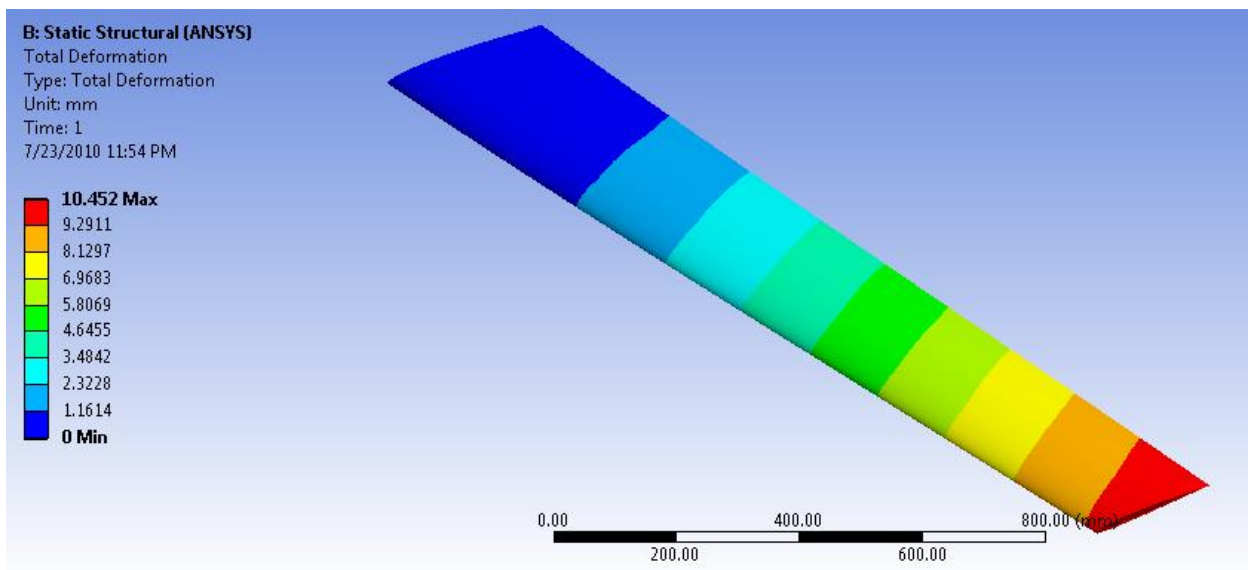


Figure 59-The total deformation (Model 1)

The equivalent Von-Mises elastic strain:

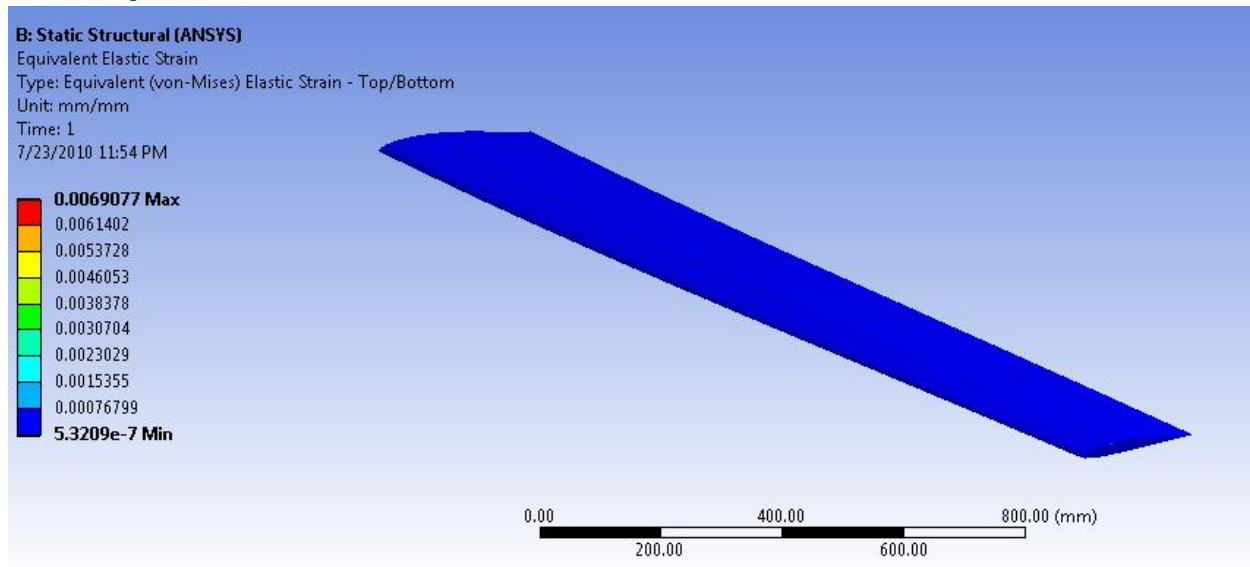


Figure 60-The equivalent Von-Mises elastic strain (Model 1)

The factor of safety:

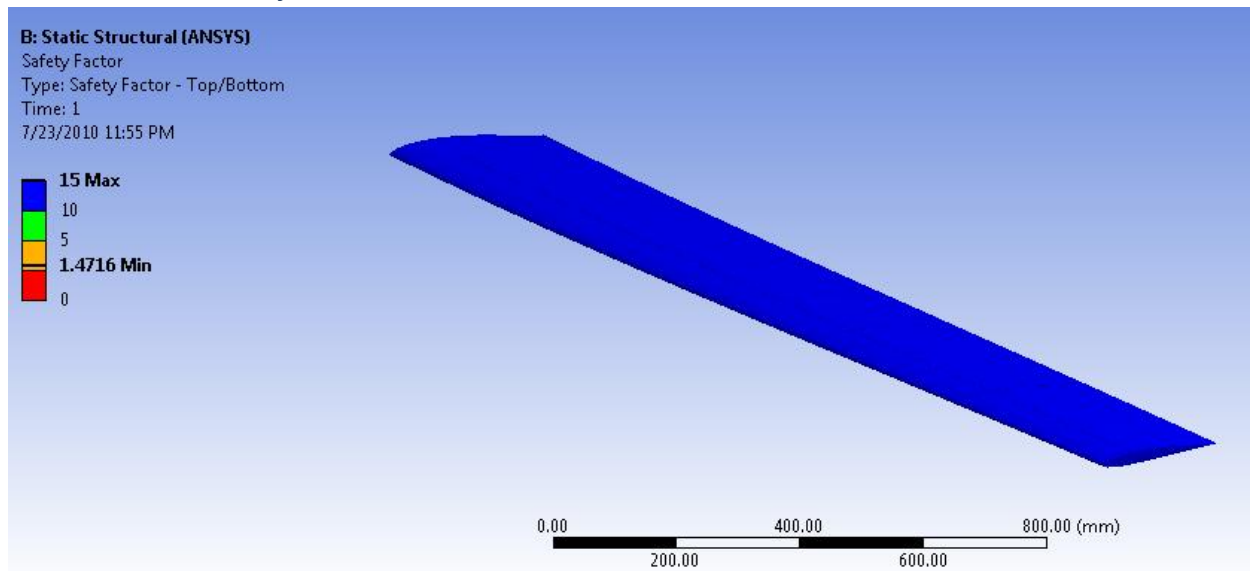


Figure 61-The factor of safety (Model 1)

Model 2:

The equivalent Von-Mises stress:

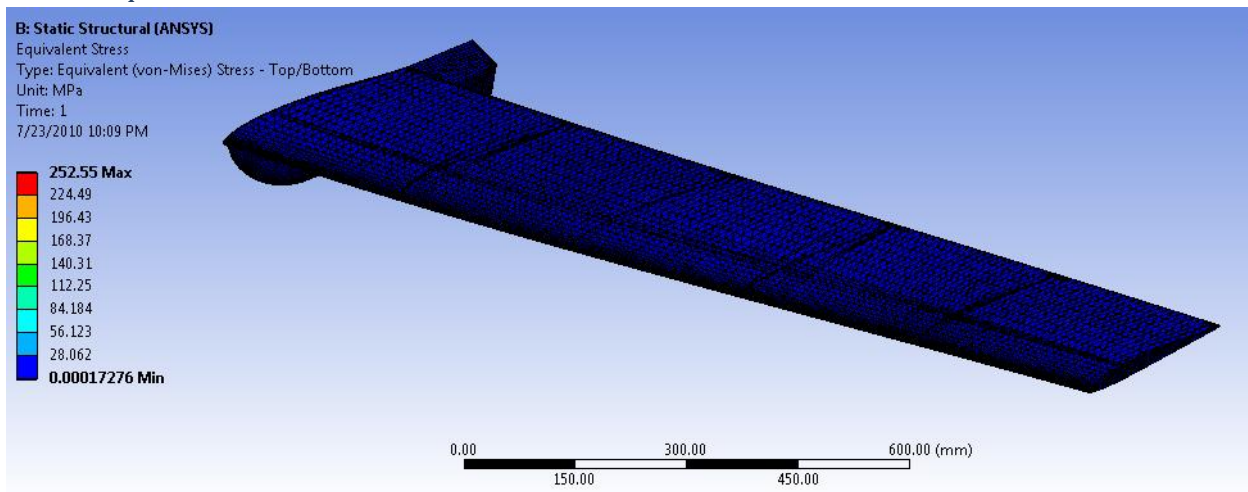


Figure 62-The equivalent Von-Mises stress (Model 2)

The total deformation:

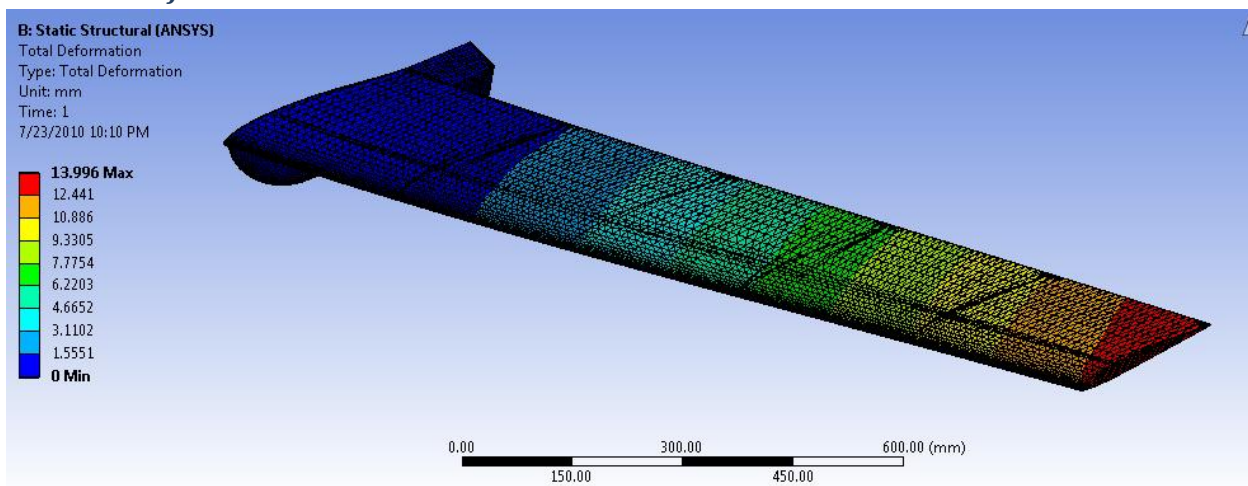


Figure 63-The total deformation (Model 2)

The equivalent Von-Mises elastic strain:

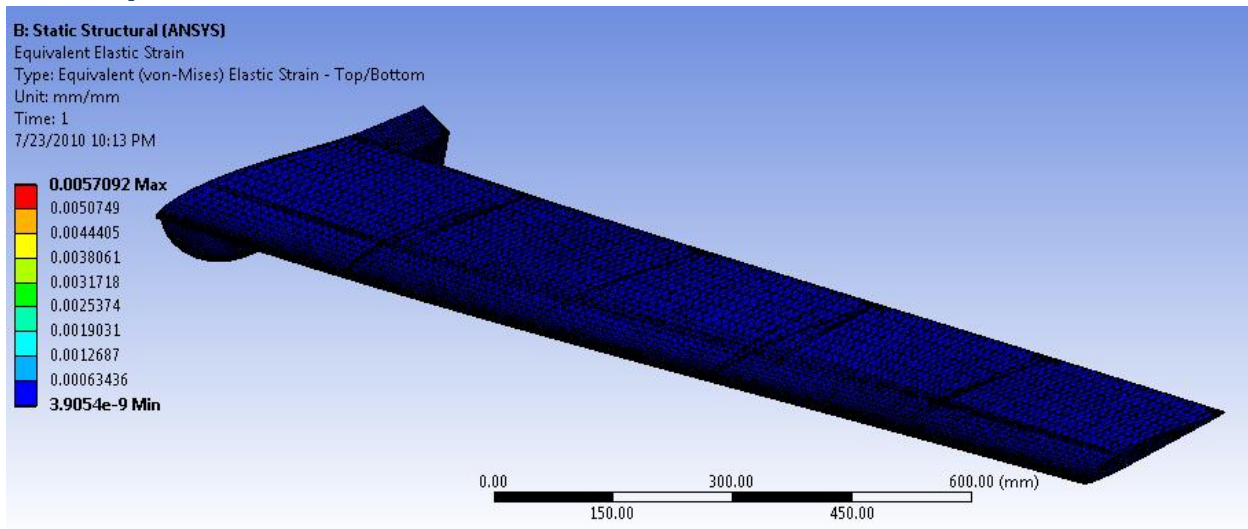


Figure 64-The equivalent Von-Mises elastic strain (Model 2)

The factor of safety:

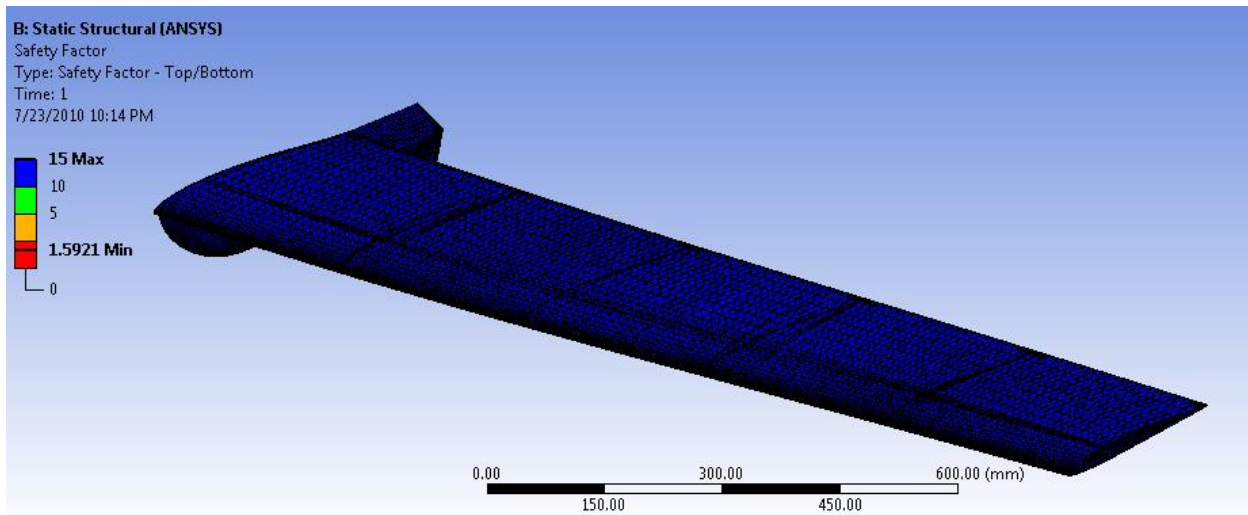


Figure 65-The factor of safety (Model 20)

Conclusion:

These results differ from the results for our actual aircraft this for two reasons;

1. The material properties are not accurate because I didn't get it from the company that we bought the carbon fiber from it or by test it in the laboratories.
2. Our actual aircraft structure differ from the design one because some difficulty in the manufacturing process and there wasn't enough time.

Chapter 6 Aircraft Geometric model

The Purpose of this chapter is to make a geometric model for the complete aircraft using the UG-NX5 Program and based on the geometric model we can make the aircraft Mass model.

The Solid model:

The wing solid model:

Configuration:

- Swept back tapered wing with geometric twist
- Span = 2500 mm
- Root chord = 290 mm
- Tip chord = 210 mm
- Sweep back angle = 26°
- Wash out angle = -2.5°

The root Section:

MH 60 with $C_r = 290 \text{ mm}$

Using spline » through points » points from file and by made uniform scale

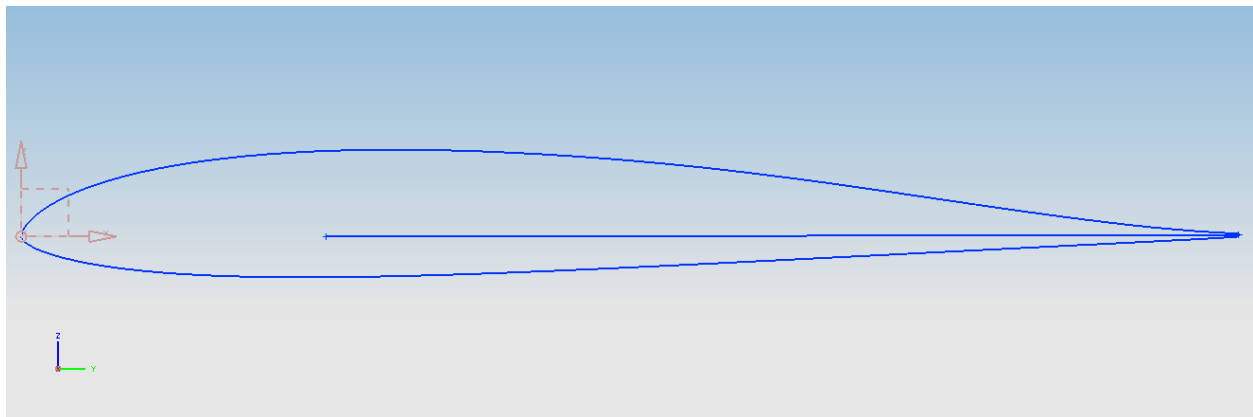


Figure 66-Airfoil MH60

The tip Section:

MH 60 with $C_t = 210 \text{ mm}$, $\alpha_w = -2.5^\circ$ and $\phi = 26^\circ$

We made the washout and sweep back angle by right click on the tip chord and choose Edit Positioning

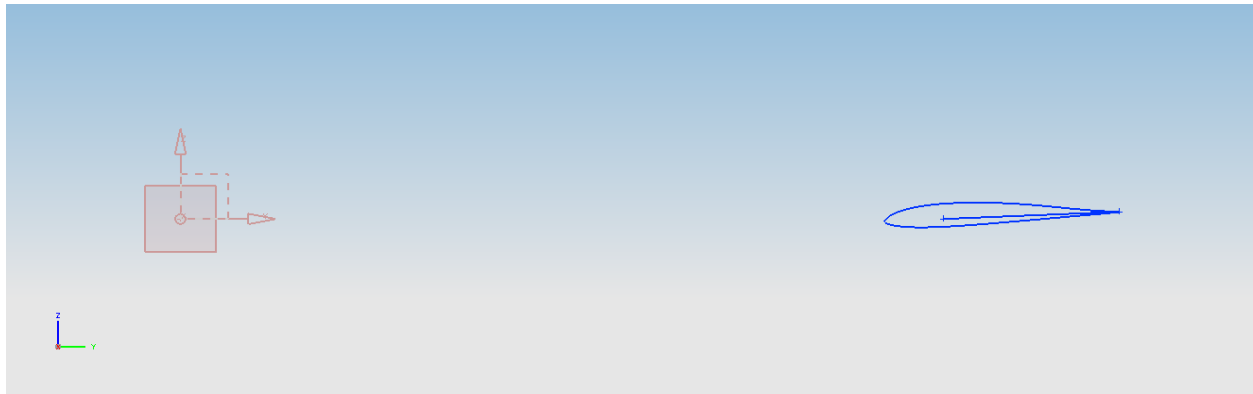


Figure 67-the tip airfoil section

Generate the left wing:

Using insert » Mesh surface » Ruled and select the tip chord then the root chord

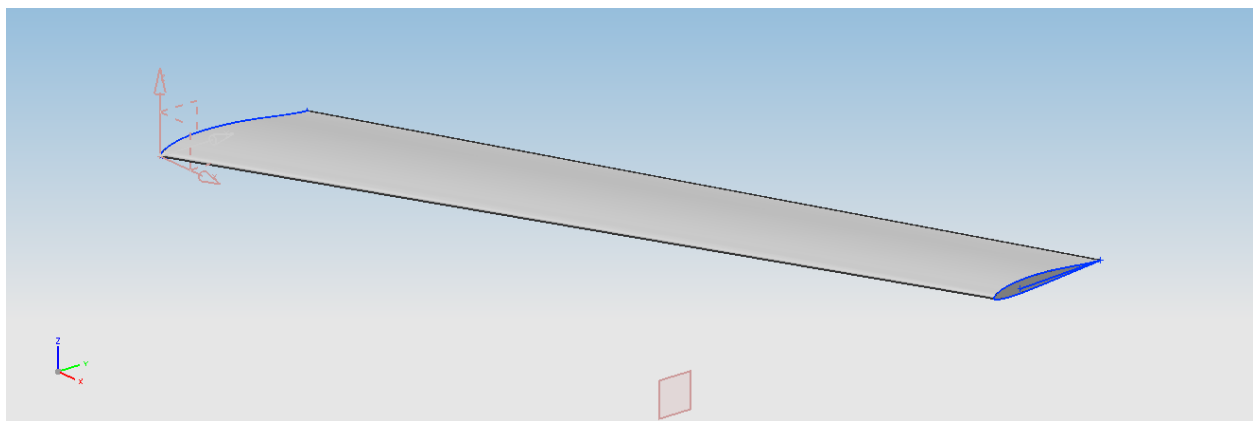


Figure 68-Left wing solid model

And we made the other part of the wing using Mirror Feature.

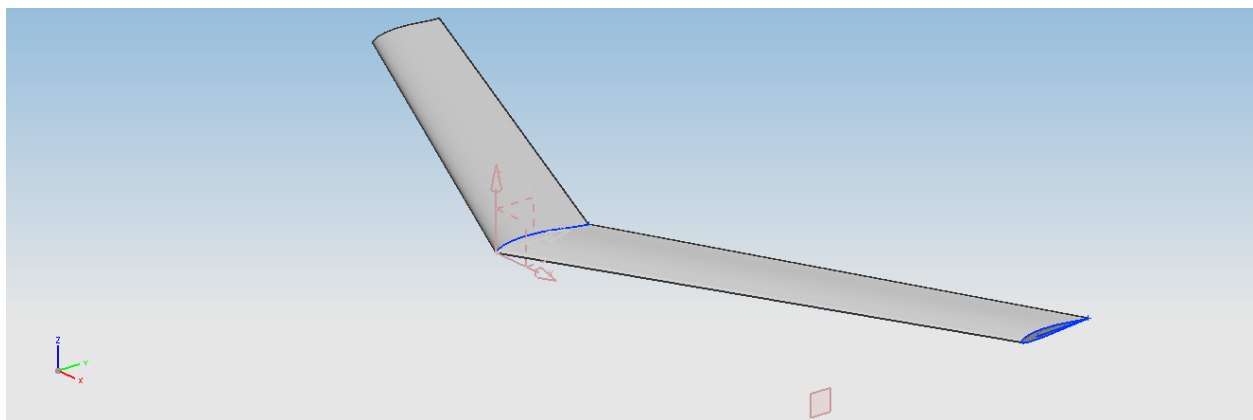


Figure 69-Wing solid model

The Fuselage solid model:**Configuration:**

Length = 390 mm

Max height = 100 mm

The fuselage is consists of three parts

Cylindrical part:

Length = 182 mm

Height = 100 mm

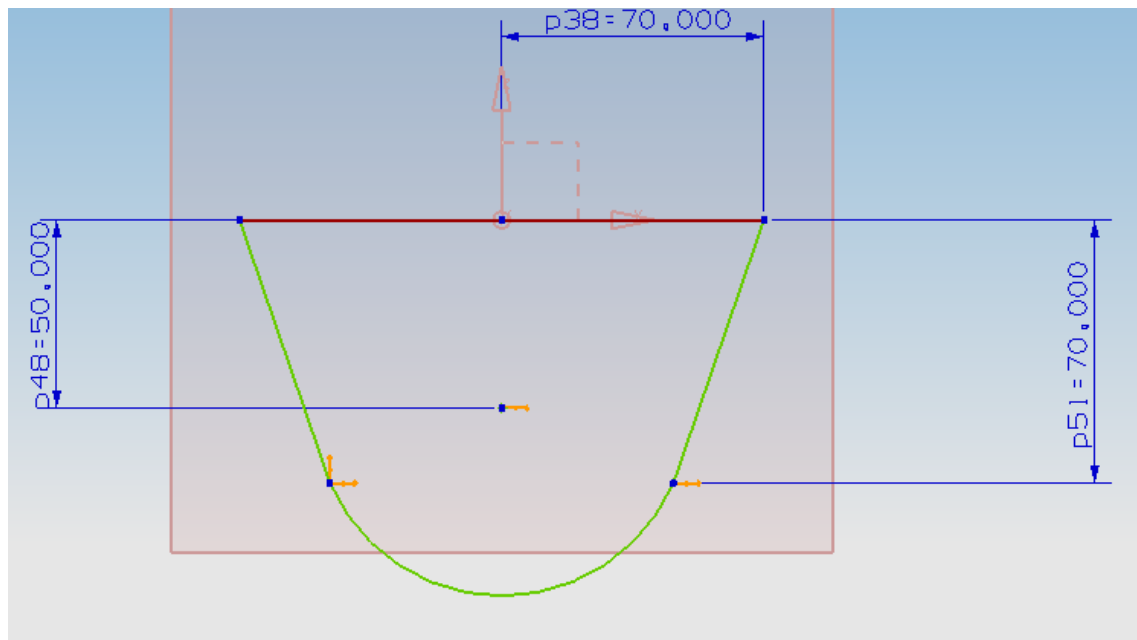
The Part cross section

Figure 70-Cylindrical part cross section

And by extrude it

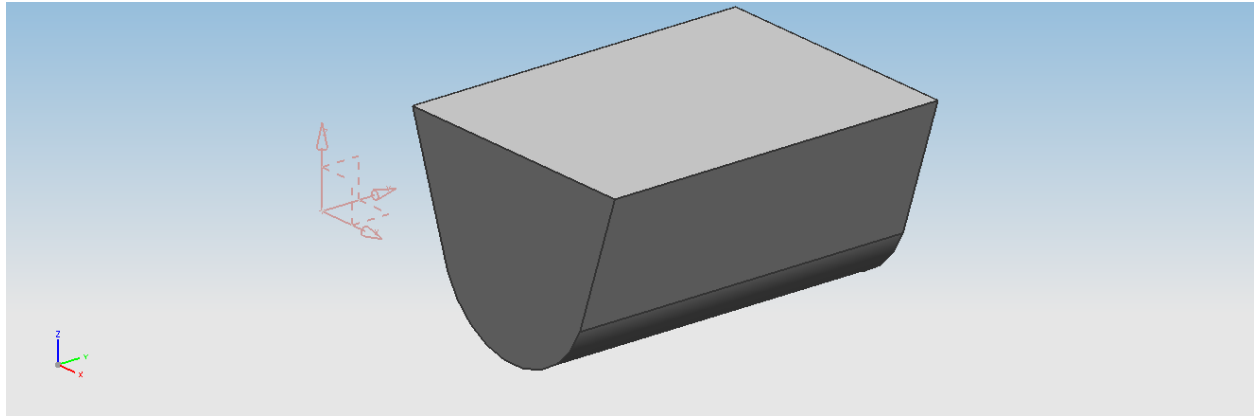


Figure 71-The part solid model

Nose part:

We get the nose part by revolve the cylindrical part cross section around axis in x-direction

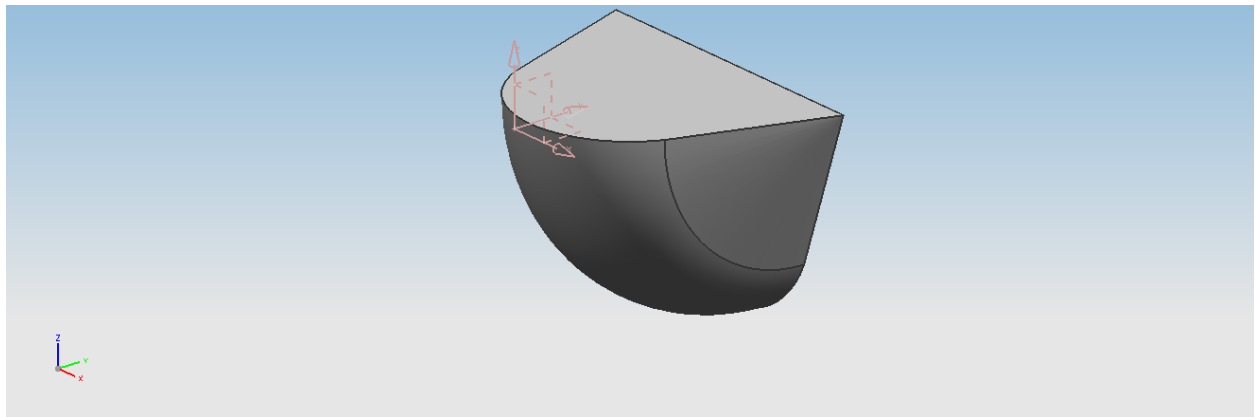


Figure 72-The nose part solid model

Tail part:

We can make the tail part by sweep a body between the cylindrical part cross and another cross section with height 90 mm

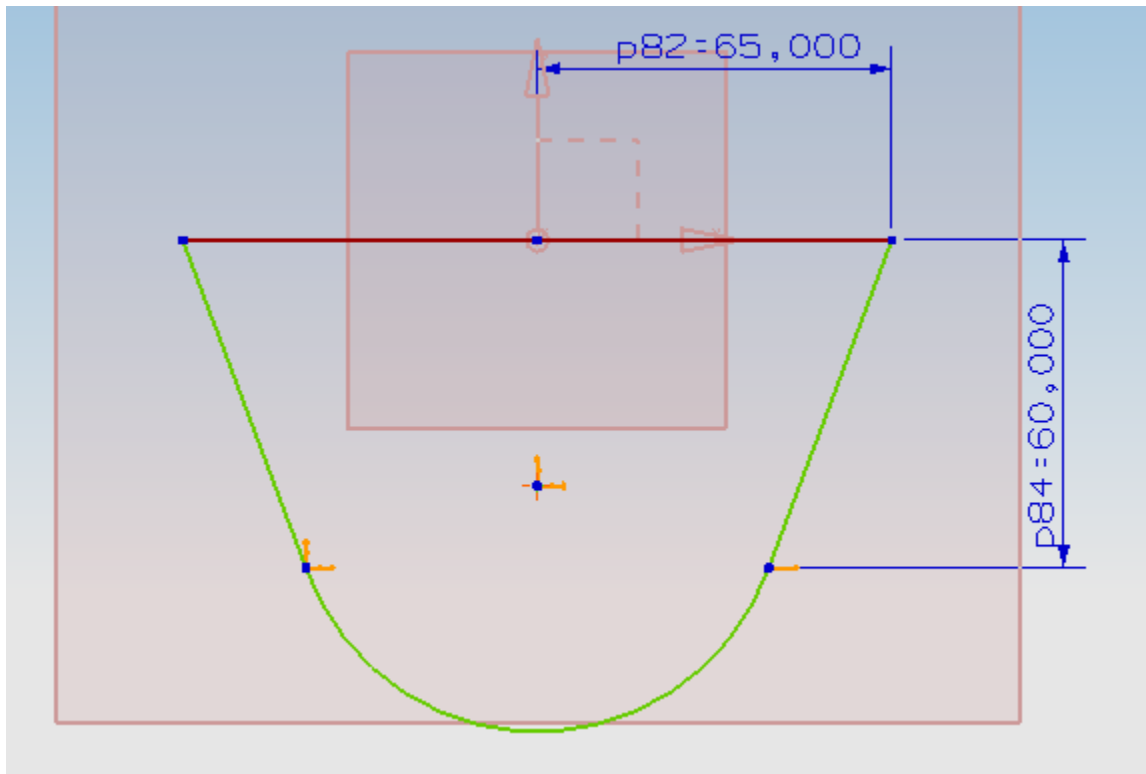


Figure 73-Tail part cross section

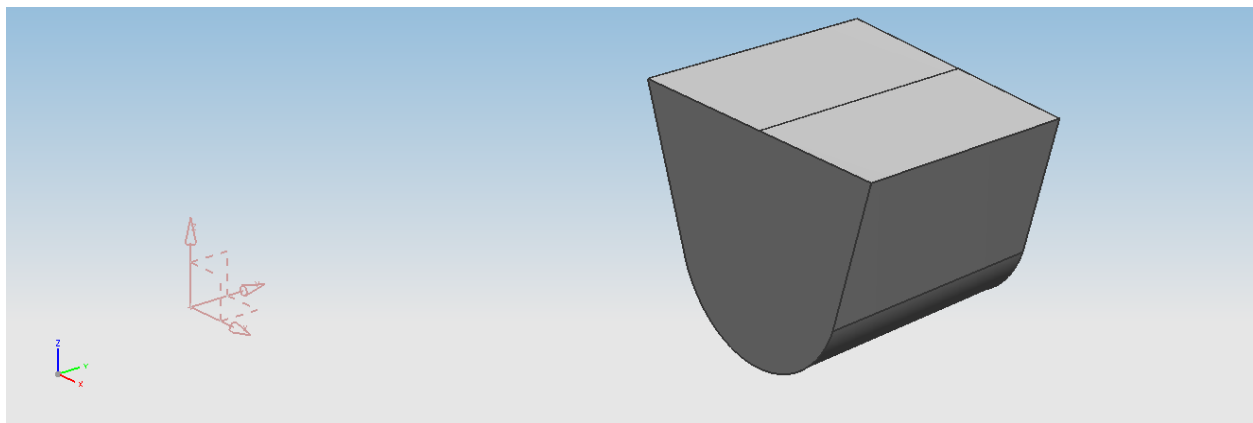


Figure 74-Tail part solid model

By assemble the three parts we get the fuselage solid model

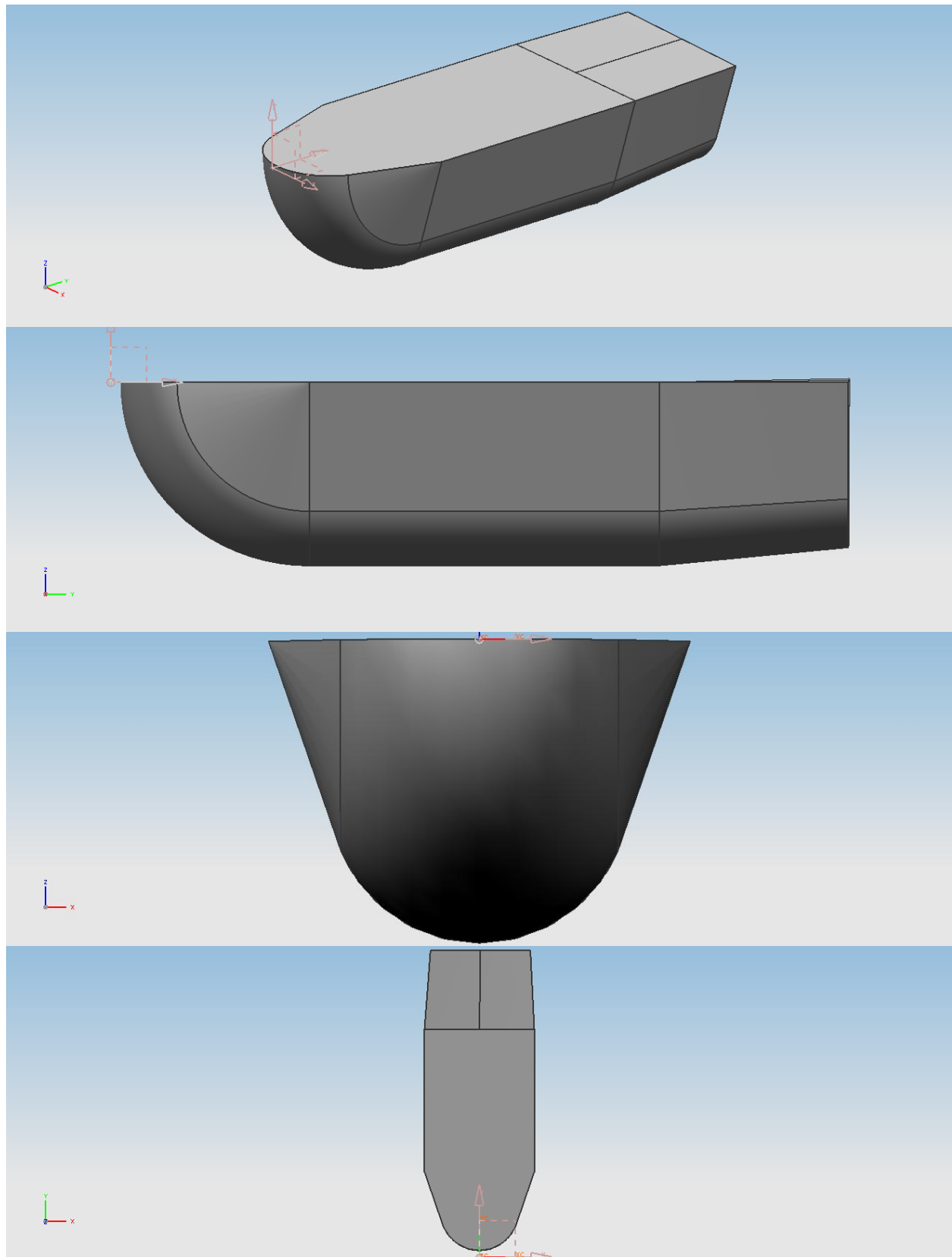


Figure 75-Fuselage solid model

Finally the aircraft solid model assembly

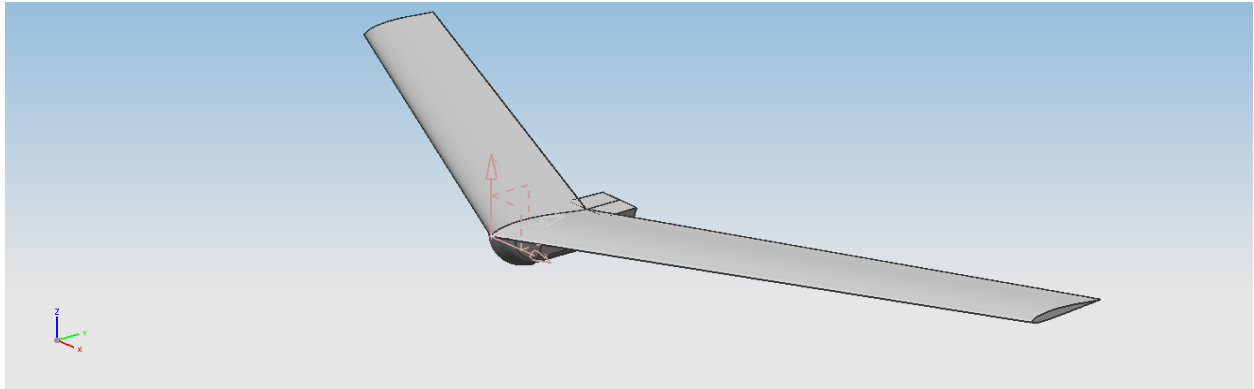


Figure 76-the solid model assembly

The control surfaces:

Wing Flap:

Configuration

$$L_f = 450 \text{ mm} , C_{f1} = 114.5 \text{ mm} , C_{f2} = 103.7 \text{ mm}$$

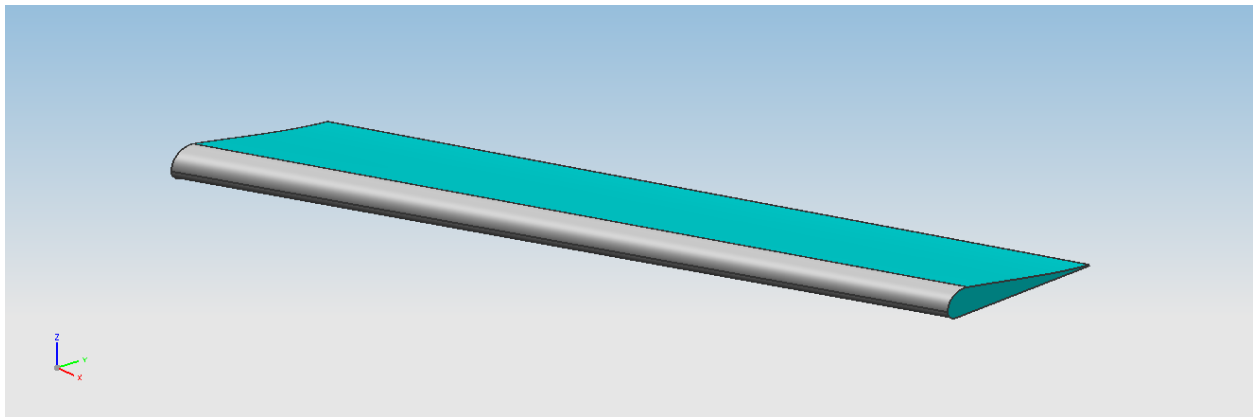


Figure 77-The wing flap

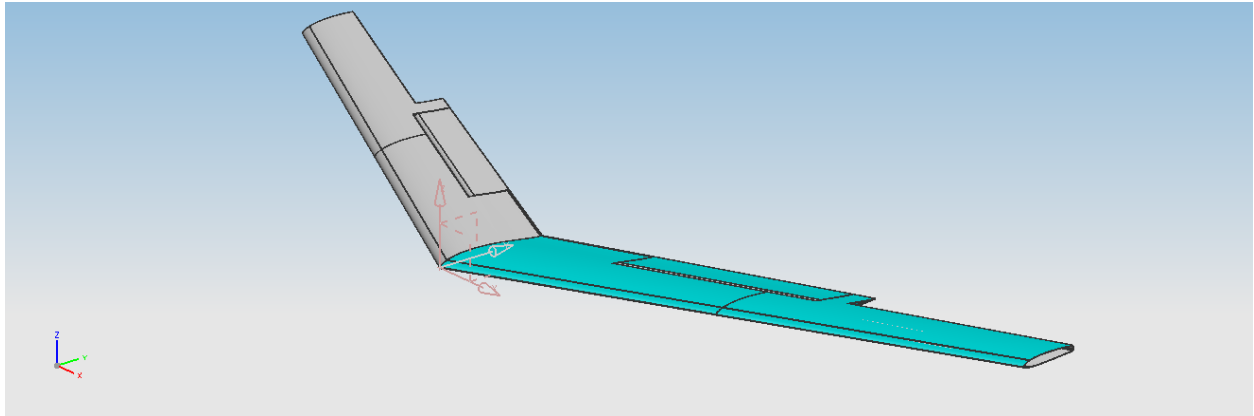
Wing –Flap assembly

Figure 78-the wing flap assembly

Wing Elevon:

Wing elevon is consists of two parts.

Configuration

$$L_e = 500 \text{ mm} , C_{e1} = 77.2 \text{ mm} , C_{e2} = 67.2 \text{ mm}$$

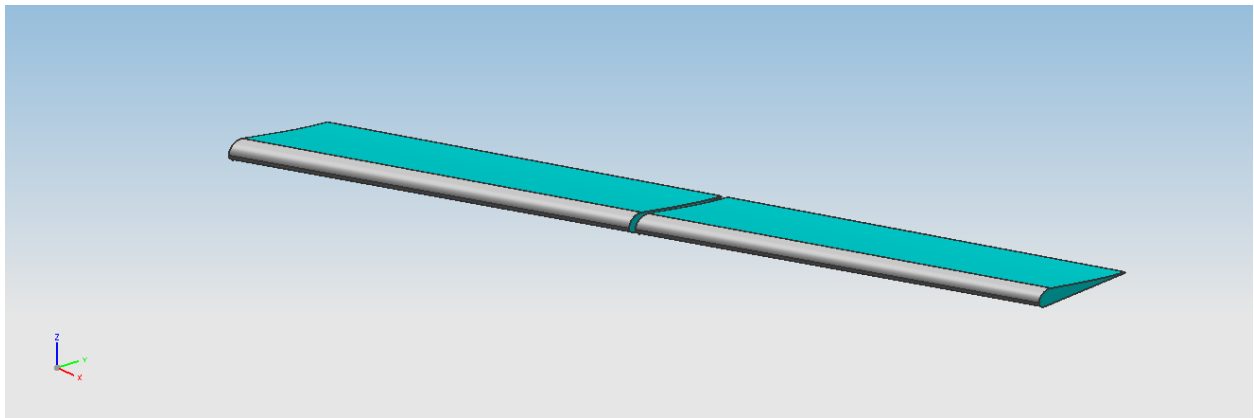


Figure 79-The wing elevon

Wing elevon assembly

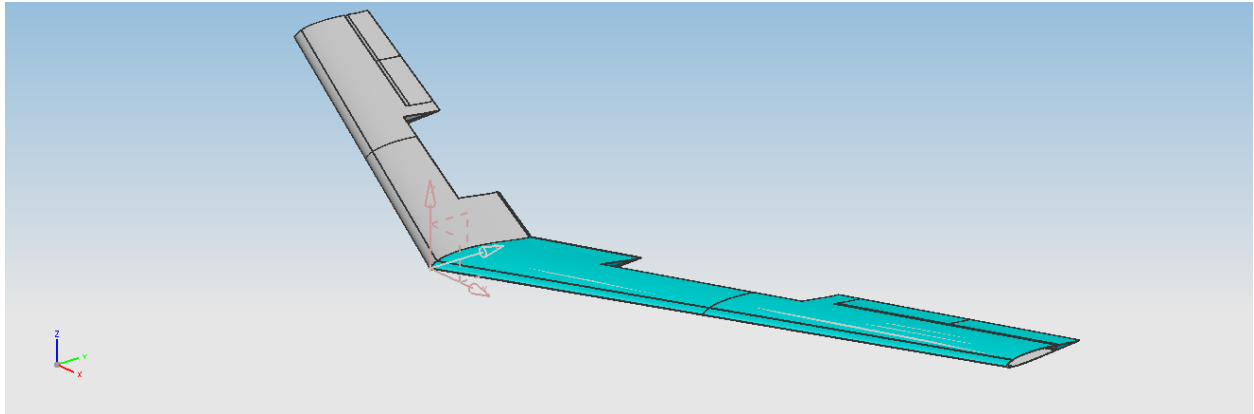


Figure 80-Wing elevon assembly

The control surfaces assembly

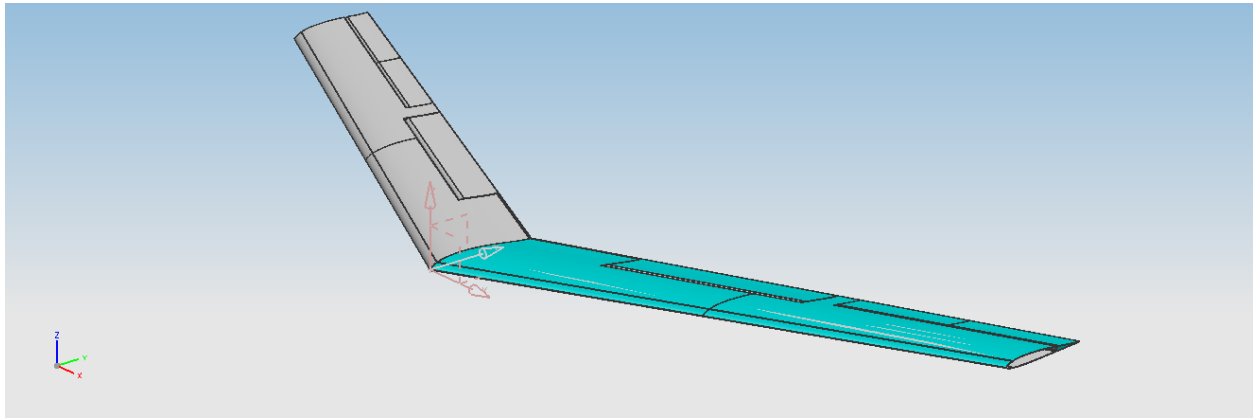


Figure 81-the control surfaces assembly

The wing structure:

The upper skin:

The wing upper skin divides to two parts

The inboard skin with thickness $t = 0.6096 \text{ mm}$

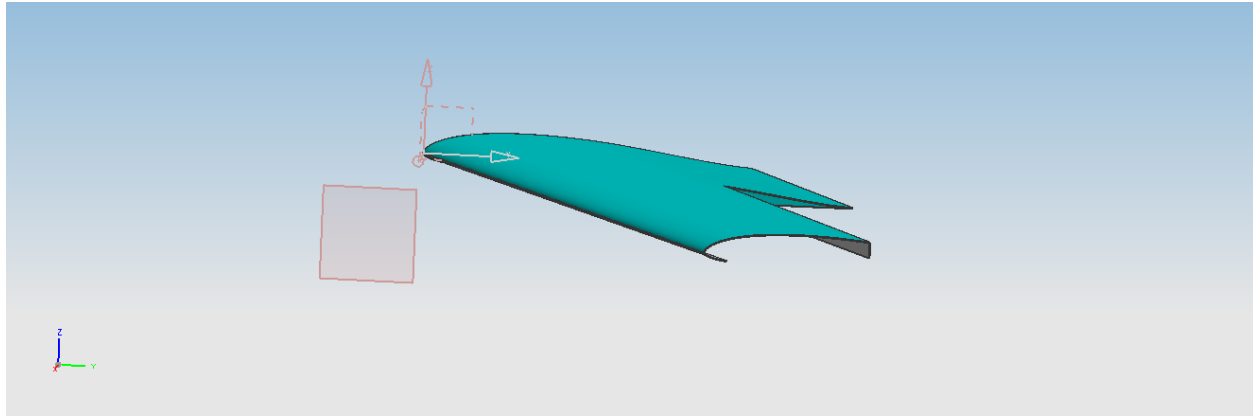


Figure 82-The inboard upper skin

And the outboard skin with thickness $t = 0.3048$ mm

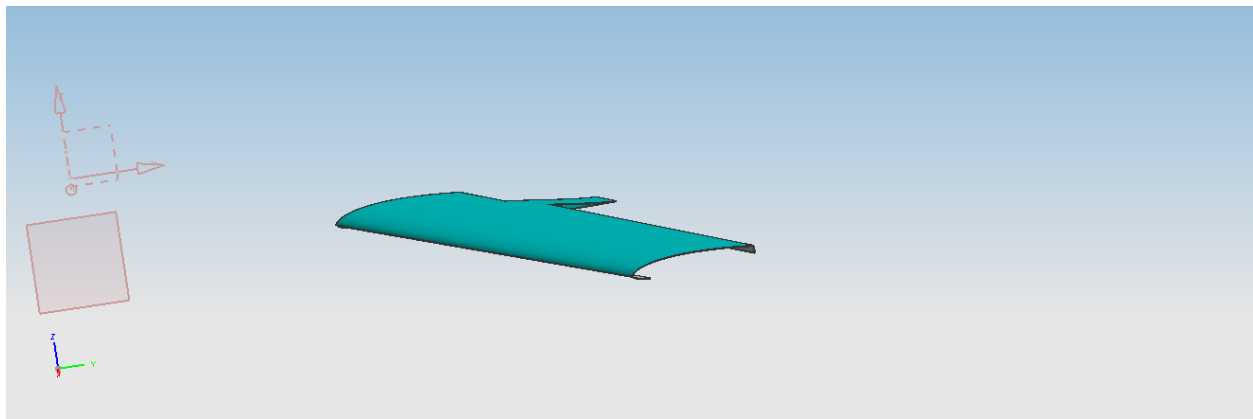


Figure 83-the outboard upper skin

And by assembly the two parts

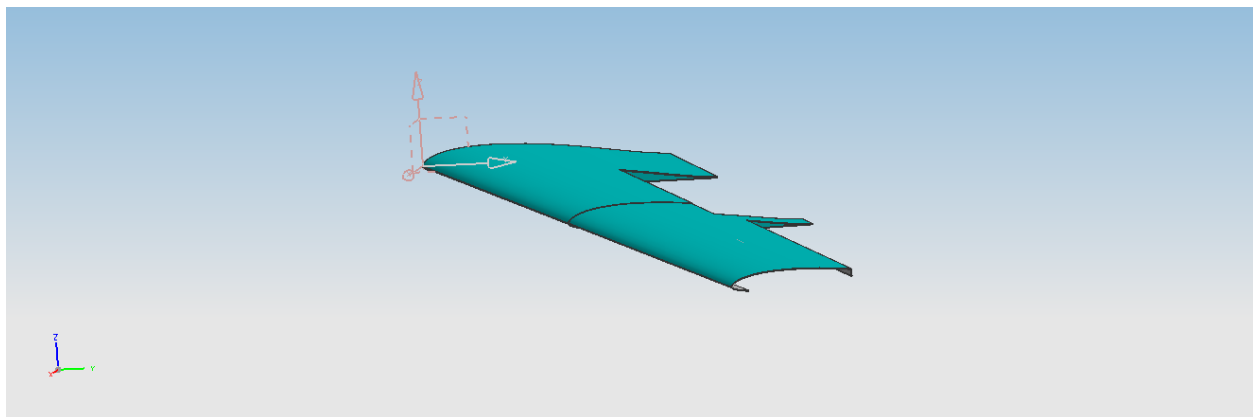


Figure 84-Upper skin assembly

The Lower Skin:

Same as the upper skin

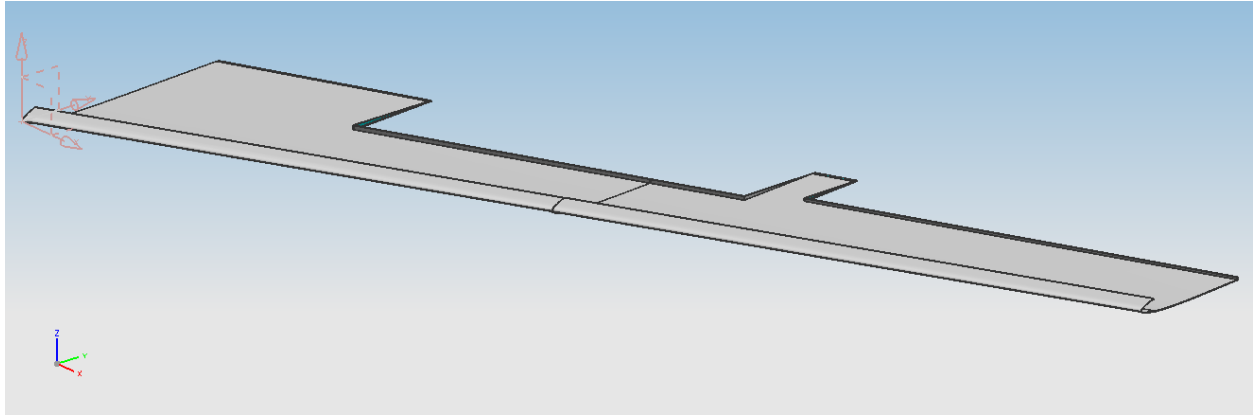


Figure 85-Lower skin assembly

By assembly the upper skin with the lower skin

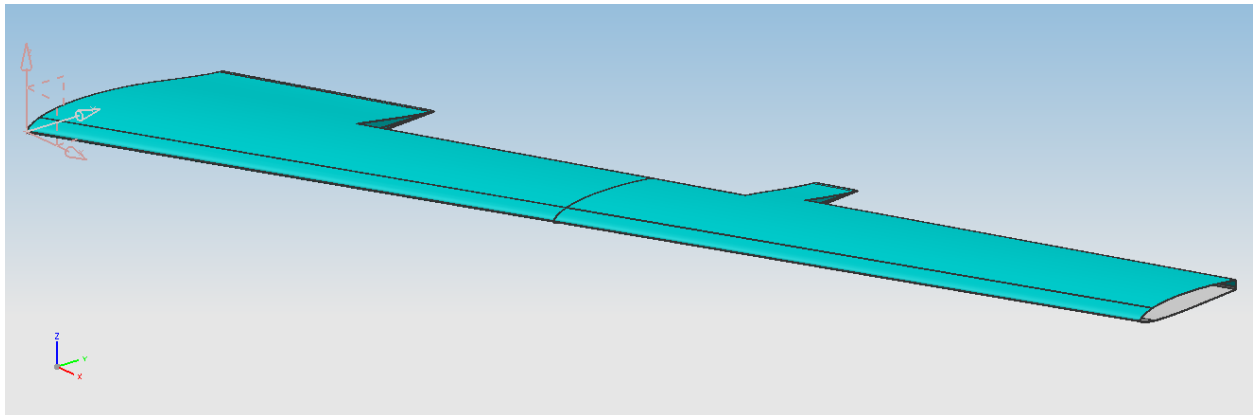


Figure 86-Upper and lower skin assembly

Wing Ribs:

The wing is consisting of six ribs in the half span and we will construct the ribs with thickness $t=1.2192$ mm and rib spacing 250 mm.

The ribs assembly:

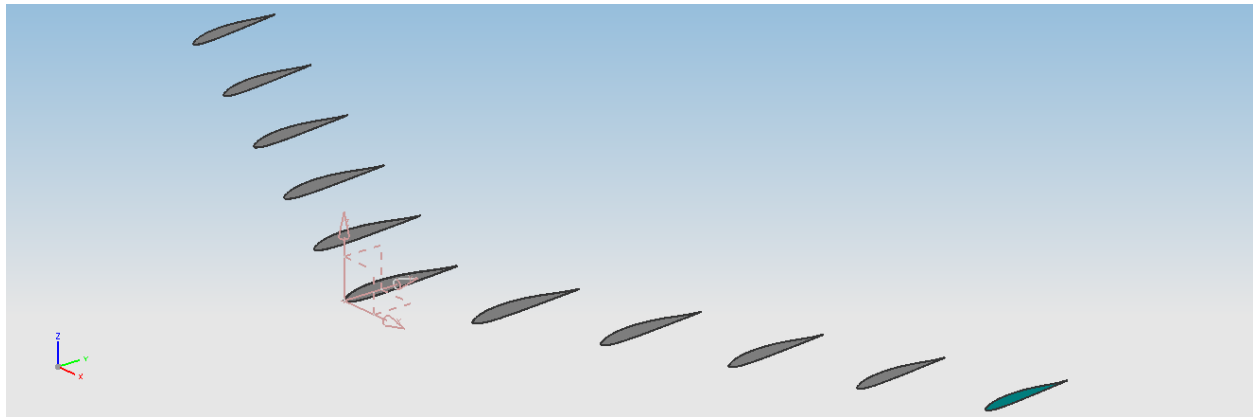


Figure 87-The wing ribs

The Fuselage Structure:

The fuselage Skin:

With thickness $t=0.9144$ mm

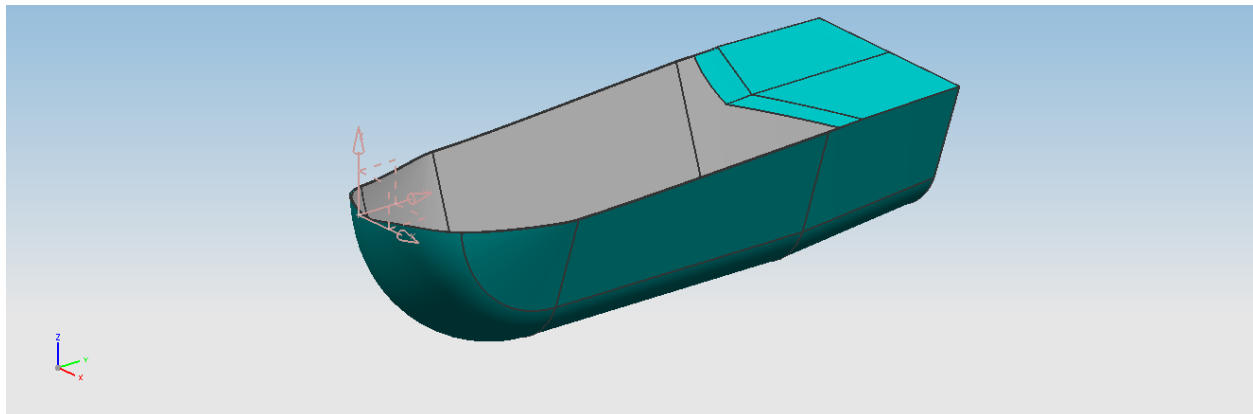


Figure 88-The fuselage skin

The fuselage Frames:

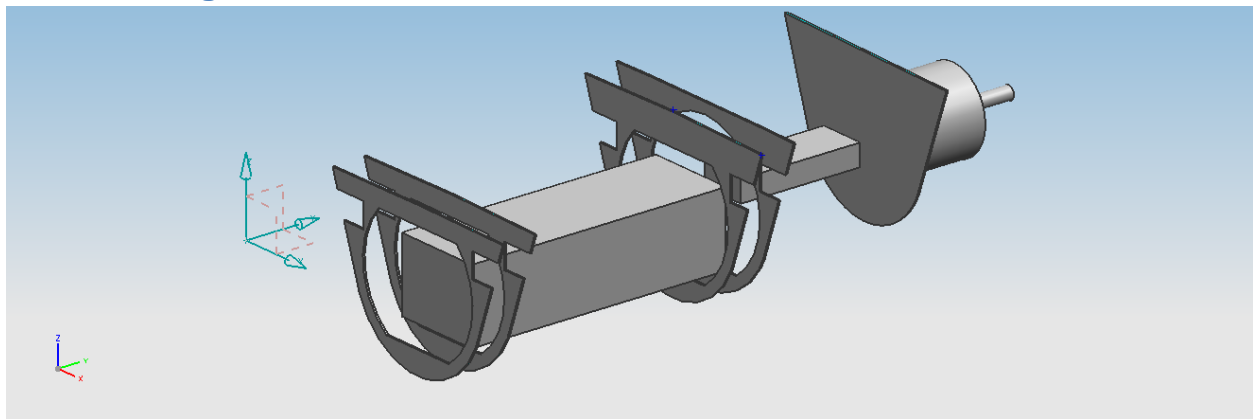


Figure 89-The fuselage frames

Finally the aircraft assembly

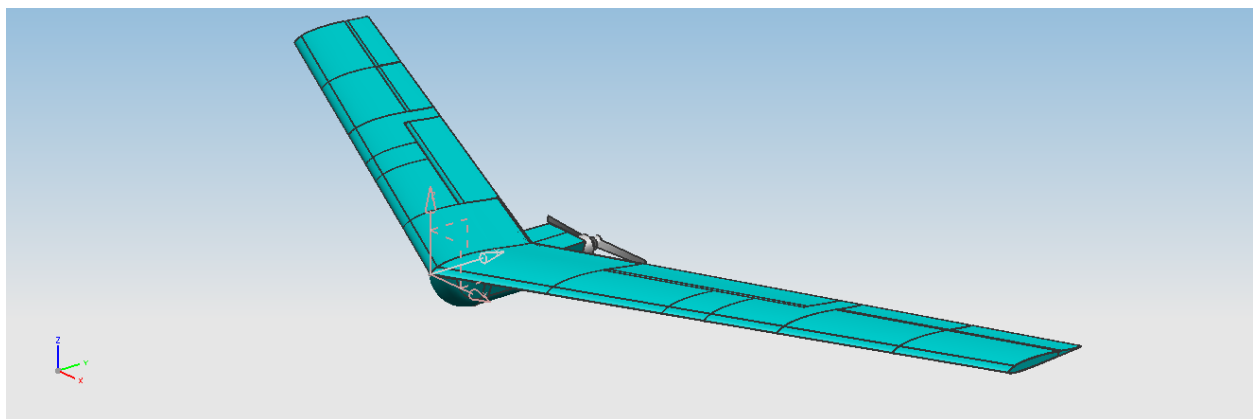
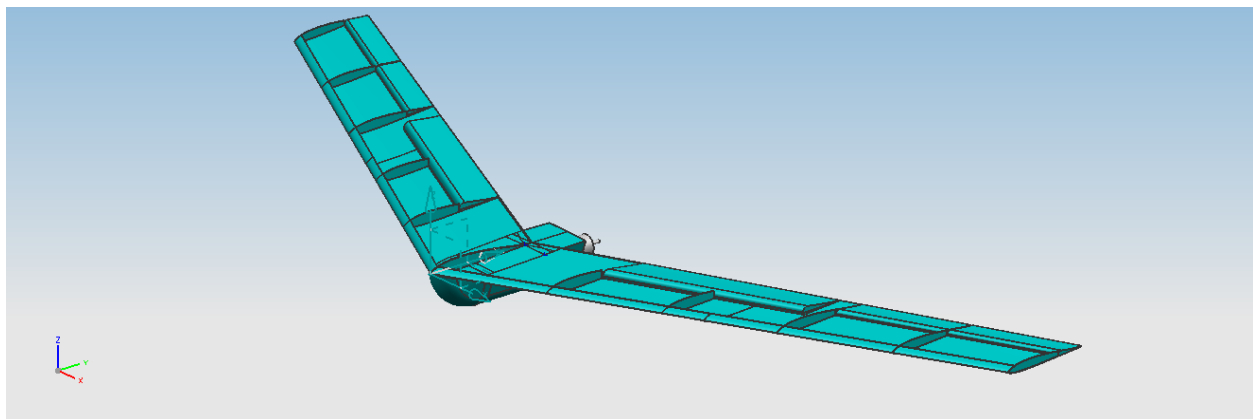


Figure 90-the aircraft assembly

The Flying wing views:

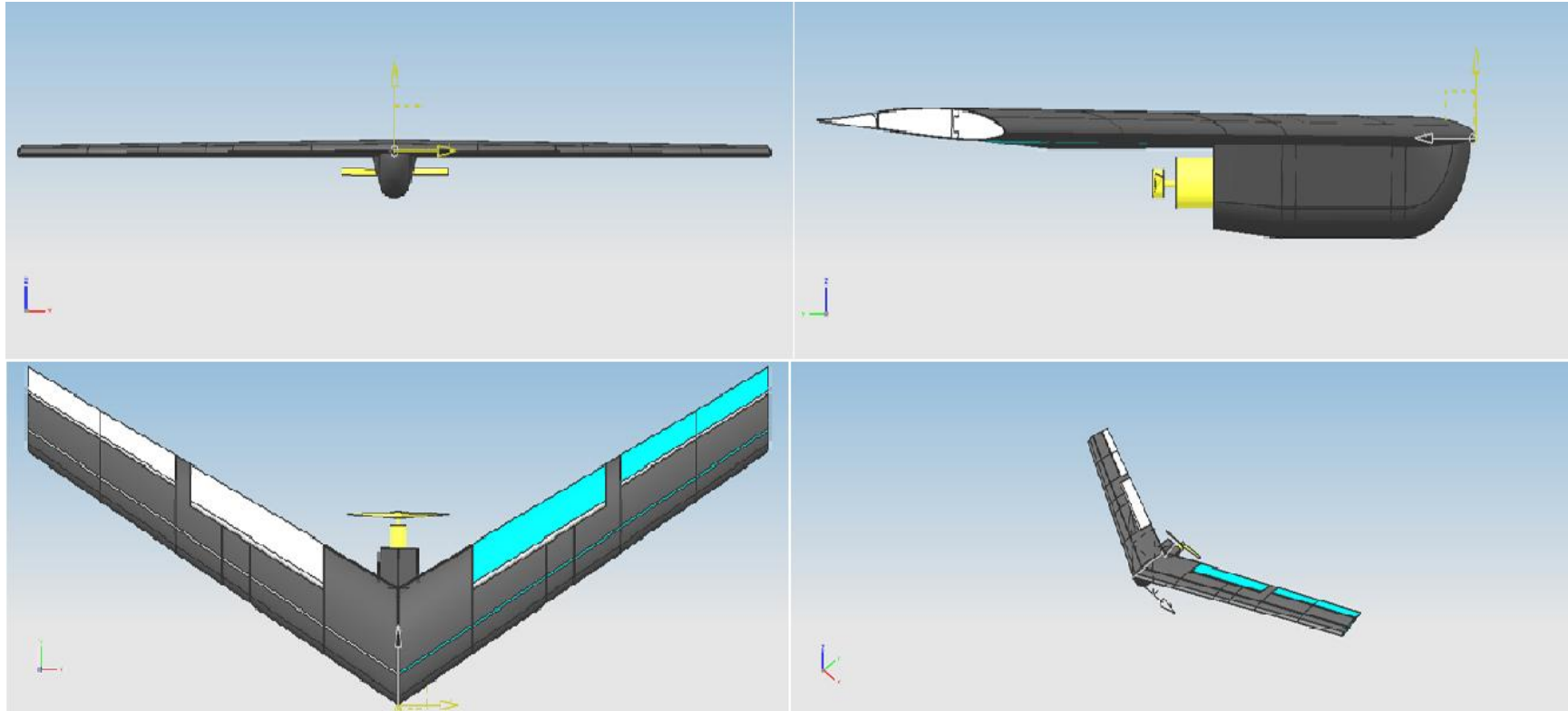


Figure 91-The aircraft views

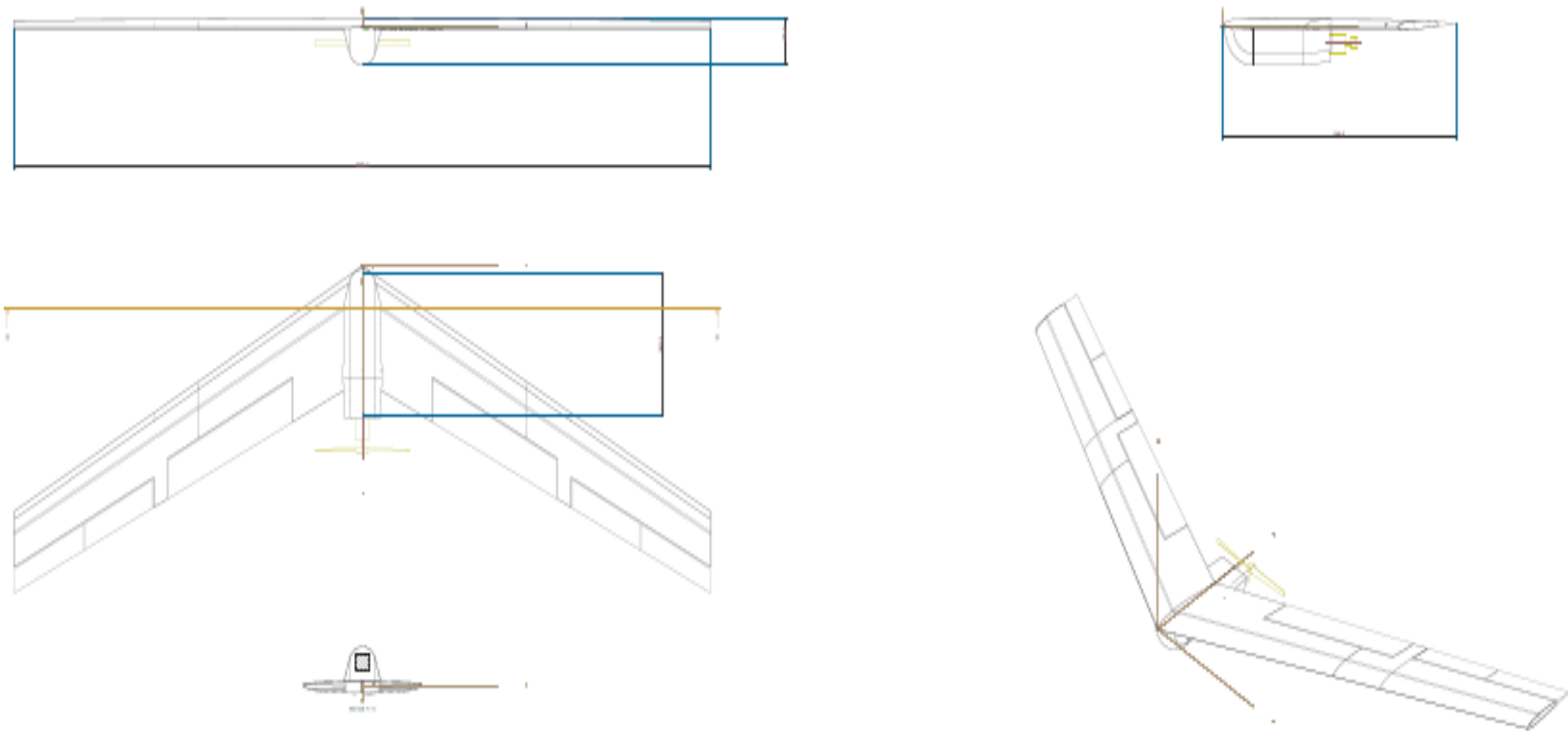


Figure 92-The aircraft views

Chapter 7 The Flying Wing mass model:

The purpose of this chapter is to determine the total aircraft component mass and its CG position and the moment of inertia. We make all this using UG-NX5 Program.

We can divide the aircraft components to

- Structural Components
- Propulsion components
- Control elements

Structural Component:

Consists of

- The wing upper skin
- The wing lower skin
- The wing ribs
- The wing spar
- The fuselage skin
- The fuselage Frames

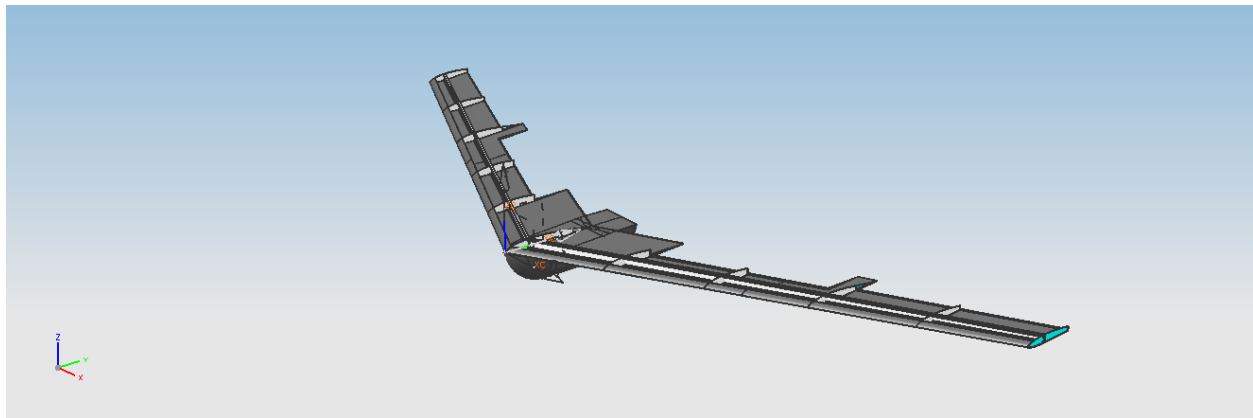


Figure 93-Flying wing components

Component	Weight (Kg)	CG Position (mm)		
		X_{CG}	Y_{CG}	Z_{CG}
The wing upper skin	0.4114	0.2651	327.5861	11.5189
The wing lower skin	0.3929	0.0293	324.5304	-4.4729
The Wing ribs	0.08175	0.001644	358.1565	4.4943
The wing spar	0.42223	0.0003392	372.7217	4.6146
The fuselage Skin	0.1534	0.1781	219.5495	-50.5912
The fuselage Frames	0.04550	-0.5549	276.9984	-38.05907

Propulsion Components:

Consists of

- Battery
- **ELECTRONIC SPEED CONTROL (ESC)**
- **Motor**
- **Propeller**

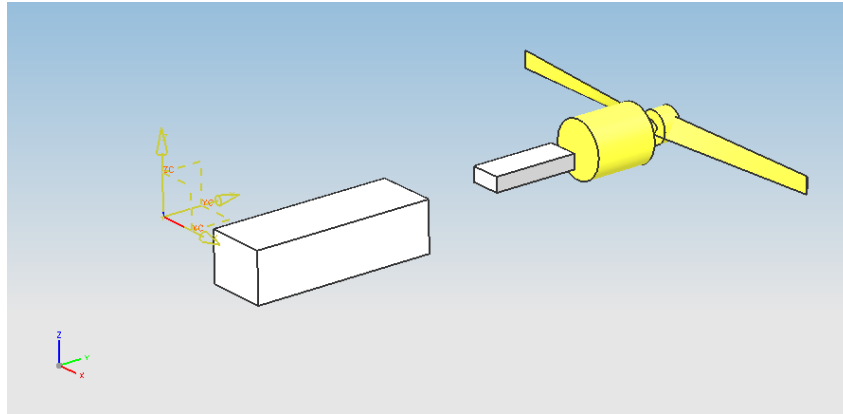


Figure 94-Propulsion components

Components	Weight (Kg)	CG Position (mm)		
		X_{CG}	Y_{CG}	Z_{CG}
Battery	0.792	0	145	-57
ESC	0.054	0	337.5	-46.5
Motor	0.298	0	418.2213	-45
Propeller	0.09699	0	472.4507	-44.5393

Control elements:

Consists of

- Wing Flap
- Wing aileron
- Wing elevator

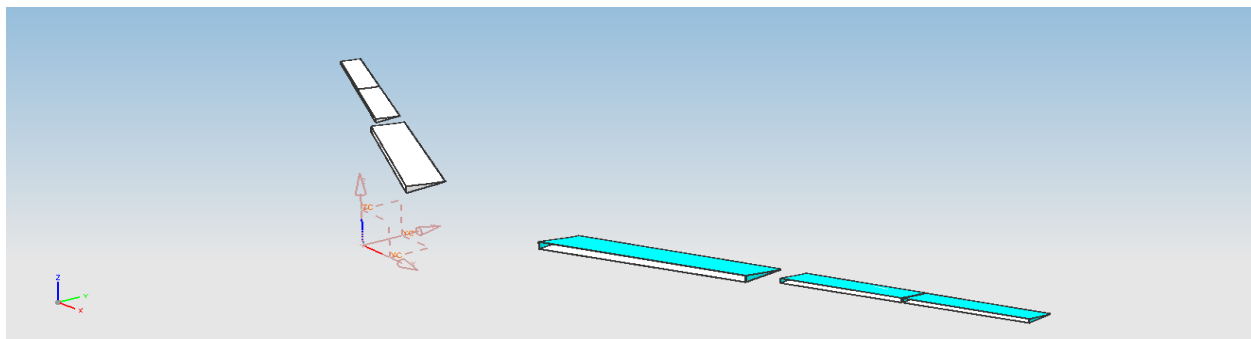


Figure 95-Control surfaces

Component s	Weight (Kg)	CG Position (mm)		
		X_{CG}	Y_{CG}	Z_{CG}
Wing Flap	0.2790	311.07776126 5	444.45672771 6	3.67397309 1
Wing aileron	0.1031	579.4117	638.7158	4.7726
Wing elevator	0.0954 6	742.7231	751.3107	5.7176

The aircraft center of mass:

The total mass = 3.2257 kg

X_{CG}	Y_{CG}	Z_{CG}
67.4369	328.6988	-20.93117

The aircraft moment of inertia (Kg m²):

Moment of inertia, also called **mass moment of inertia**, **rotational inertia**, or the **angular mass**, (SI units kg·m²) is a measure of an object's resistance to changes to its rotation. It is the inertia of a rotating body with respect to its rotation. The moment of inertia plays much the same role in rotational dynamics as mass does in linear dynamics, describing the relationship between angular momentum and angular velocity, torque and angular acceleration, and several other quantities. The symbol I and sometimes J are usually used to refer to the moment of inertia or polar moment of inertia.

I_{xx}	0.072519
I_{yy}	0.76103
I_{zz}	0.83189
I_{yz}	0.0014264

Chapter 8 Aircraft Simulation:

Introduction:

Aircraft nonlinear simulation means giving the initial conditions of the aircraft variables along with the controlling parameters during a certain period of time, all the flight variables can then be calculated along this period of time. Because of the high cost of building and flight testing a real aircraft, the importance of aircraft mathematical models goes far beyond control system design. The mathematical model is used, in conjunction with computer simulation, to evaluate the performance of the prototype aircraft and hence improve the design. It can also be used to drive training simulators, to reconstruct the flight conditions involved in accidents, and to study the effects of modifications to the design. Furthermore, other mathematical models are used in all aspects of the aircraft design (e.g., structural models for studying stress distribution and predicting fatigue life).

The Equation of motion for the rigid aircraft:

The term rigid aircraft used earlier implies that all points in the aircraft structure maintain fixed relative positions in space at all time. The equation of motion of a rigid body can be separated into rotational equations and translational equations if the coordinate origin is chosen to be at the center of mass. The rotational motion of the aircraft will then be equivalent to yawing, pitching, and rolling motions about the center of mass as if it were a fixed point in space. The remaining components of the motion will be three components of translation of the cg. Therefore, the aircraft model derived here will be a six-degrees-of-freedom (6-DOF) model and we have 12-equation of motion.

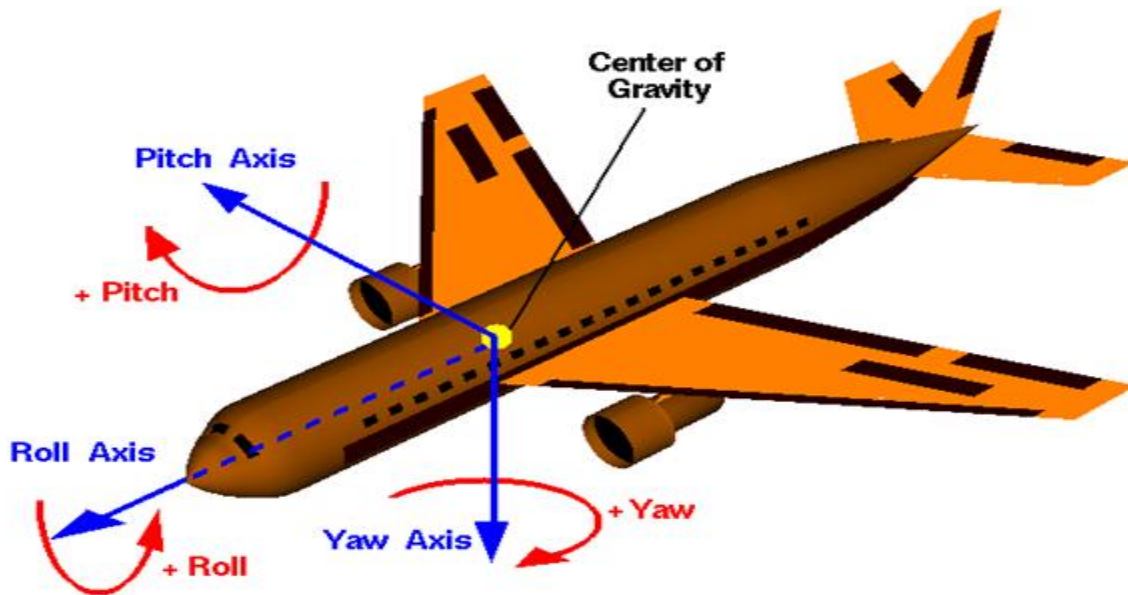


Figure 96 the 6-DOF of the aircraft

The force equations from the linear momentum:

$$F_x = m(u + qw - rv) + mg \sin\theta$$

$$F_y = m(v + ru - pw) - mg \cos\theta \sin\varphi$$

$$F_z = m(w + pv - qu) - mg \cos\theta \cos\varphi$$

The moment equations from the angular momentum:

$$L = I_x \dot{p} - I_{xz} \dot{r} - I_{xz} pq + qr(I_z - I_y)$$

$$M = I_y \dot{q} + I_{xz}(p^2 - r^2) + pr(I_x - I_z)$$

$$N = I_z \dot{r} - I_{xz} \dot{p} + I_{xz} rq + pq(I_y - I_x)$$

The Euler angles:

$$\dot{\varphi} = p + q \sin\varphi \tan\theta + r \cos\varphi \tan\theta$$

$$\dot{\theta} = q \cos\varphi - r \sin\varphi$$

$$\dot{\Psi} = q \sin\varphi \sec\theta + r \cos\varphi \sec\theta$$

The Aircraft position X, Y, Z:

$$\dot{X} = u \cos\Psi \cos\theta + v(\cos\Psi \sin\varphi \sin\theta - \sin\Psi \cos\varphi) + w(\sin\Psi \sin\varphi + \cos\Psi \cos\varphi \sin\theta)$$

$$\dot{Y} = u \sin\Psi \cos\theta + v(\sin\Psi \sin\varphi \sin\theta - \cos\Psi \cos\varphi) + w(-\cos\Psi \sin\varphi + \sin\Psi \cos\varphi \sin\theta)$$

$$\dot{Z} = -u \sin\theta + v \sin\varphi \cos\theta + w \cos\varphi \cos\theta$$

Which together 12-equation in 12-unknown

Position: **X, Y, Z**

Velocity: **u, v, w**

Angular acceleration: **p, q, r**

Orientation: **φ, θ, Ψ**

And the controlling parameters (inputs) are: **$\delta_a, \delta_e, \delta_r, \delta_T$**

MATLAB simulink:

We solve this system of equations using **MATLAB** simulink and to make this we required to relate the forces F_x, F_y, F_z and the moments L, M, N to the controllers where:

Force Equations:

$$F_x = \frac{1}{2} \rho V^2 S C_x + T - mg \sin \theta$$

$$F_y = \frac{1}{2} \rho V^2 S C_y + mg \sin \varphi \cos \theta$$

$$F_z = \frac{1}{2} \rho V^2 S C_z + mg \cos \varphi \cos \theta$$

$$C_x = -C_D \cos \alpha \cos \beta - C_c \cos \alpha \sin \beta + C_l \sin \alpha$$

$$C_y = -C_D \sin \beta + C_c \cos \beta$$

$$C_z = -C_D \sin \alpha \cos \beta - C_c \sin \alpha \sin \beta - C_l \cos \alpha$$

$$C_l = C_{l0} + C_{l\alpha} \alpha + C_{l\dot{\alpha}} \dot{\alpha} \frac{c}{V} + C_{lq} q \frac{c}{V} + C_{l\delta e} \delta e$$

$$C_D = C_{D0} + K_1 C_l + K_2 C_l^2$$

$$C_c = C_{c\beta} \beta + C_{cr} r \frac{b}{V} + C_{cp} p \frac{b}{V}$$

Moment equations:

$$L = \frac{1}{2} \rho V^2 S C_L b$$

$$M = \frac{1}{2} \rho V^2 S C_m c$$

$$N = \frac{1}{2} \rho V^2 S C_n b$$

$$C_L = C_{L\beta} \beta + C_{Lp} p \frac{b}{V} + C_{Lr} r \frac{b}{V} + C_{L\delta a} \delta a + C_{L\delta r} \delta r$$

$$C_m = C_{m0} + C_{m\alpha} \alpha + C_{m\dot{\alpha}} \dot{\alpha} \frac{c}{V} + C_{mq} q \frac{c}{V} + C_{m\delta e} \delta e$$

$$C_n = C_{n\beta} \beta + C_{np} p \frac{b}{V} + C_{nr} r \frac{b}{V} + C_{n\delta a} \delta a + C_{n\delta r} \delta r$$

Euler angle representation of six-degrees-of-freedom equations of motion:

The 6DoF (Euler Angles) block considers the rotation of a body-fixed coordinate frame (X_b , Y_b , Z_b) about a flat Earth reference frame (X_e , Y_e , Z_e). The origin of the body-fixed coordinate frame is the center of gravity of the body, and the body is assumed to be rigid, an assumption that eliminates the need to consider the forces acting between individual elements of mass. The flat Earth reference frame is considered inertial, an excellent approximation that allows the forces due to the Earth's motion relative to the "fixed stars" to be neglected.

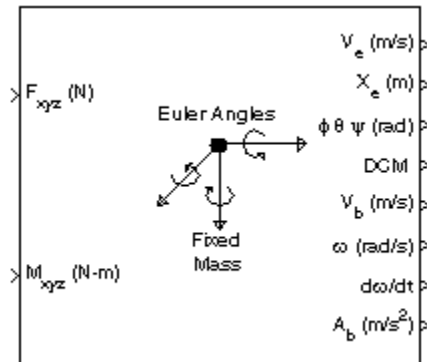


Figure 97-DOF Euler angle MATLAB block

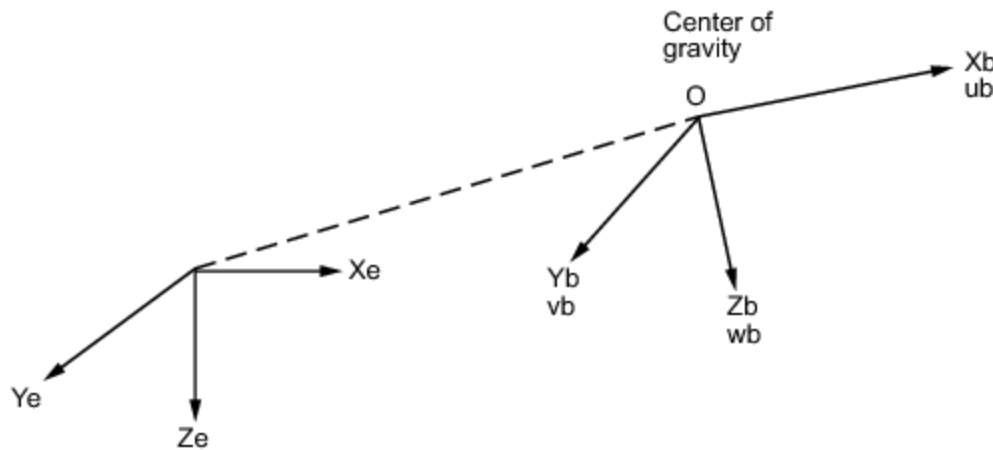


Figure 98-The relation between inertial and body axis

The translational motion of the body-fixed coordinate frame is given below, where the applied forces $[F_x F_y F_z]^T$ are in the body-fixed frame, and the mass of the body m is assumed constant.

$$F_b = \begin{bmatrix} F_x \\ F_y \\ F_z \end{bmatrix} = m(V_b + \omega \times V_b), V_b = \begin{bmatrix} u_b \\ v_b \\ w_b \end{bmatrix}, \omega = \begin{bmatrix} p \\ q \\ r \end{bmatrix}$$

The rotational dynamics of the body-fixed frame are given below, where the applied moments are $[L M N]^T$, and the inertia tensor I is with respect to the origin O .

$$M_B = \begin{bmatrix} L \\ M \\ N \end{bmatrix} = I\omega + \omega \times (I\omega), \quad I = \begin{bmatrix} I_{xx} & -I_{xy} & -I_{xz} \\ -I_{yx} & I_{yy} & -I_{yz} \\ -I_{zx} & -I_{zy} & I_{zz} \end{bmatrix}$$

The relationship between the body-fixed angular velocity vector, $[P \ q \ r]^T$, and the rate of change of the Euler angles, $\dot{\phi}, \dot{\theta}, \dot{\psi}$, can be determined by resolving the Euler rates into the body-fixed coordinate frame.

$$\begin{bmatrix} p \\ q \\ r \end{bmatrix} = \begin{bmatrix} \dot{\phi} \\ 0 \\ 0 \end{bmatrix} + \begin{bmatrix} 1 & 0 & 0 \\ 0 & \cos \phi & \sin \phi \\ 0 & -\sin \phi & \cos \phi \end{bmatrix} \begin{bmatrix} \dot{\theta} \\ 0 \\ 0 \end{bmatrix} + \begin{bmatrix} 1 & 0 & 0 \\ 0 & \cos \phi & \sin \phi \\ 0 & -\sin \phi & \cos \phi \end{bmatrix} \begin{bmatrix} \cos \theta & 0 & -\sin \theta \\ 0 & 1 & 0 \\ \sin \theta & 0 & \cos \theta \end{bmatrix} \begin{bmatrix} 0 \\ 0 \\ \dot{\psi} \end{bmatrix} \equiv J^{-1} \begin{bmatrix} \dot{\phi} \\ \dot{\theta} \\ \dot{\psi} \end{bmatrix}$$

Inverting J then gives the required relationship to determine the Euler rate vector.

$$\begin{bmatrix} \dot{\phi} \\ \dot{\theta} \\ \dot{\psi} \end{bmatrix} = J \begin{bmatrix} p \\ q \\ r \end{bmatrix} = \begin{bmatrix} 1 & (\sin \phi \tan \theta) & (\cos \phi \tan \theta) \\ 0 & \cos \phi & -\sin \phi \\ 0 & \frac{\sin \phi}{\cos \theta} & \frac{\cos \phi}{\cos \theta} \end{bmatrix} \begin{bmatrix} p \\ q \\ r \end{bmatrix}$$

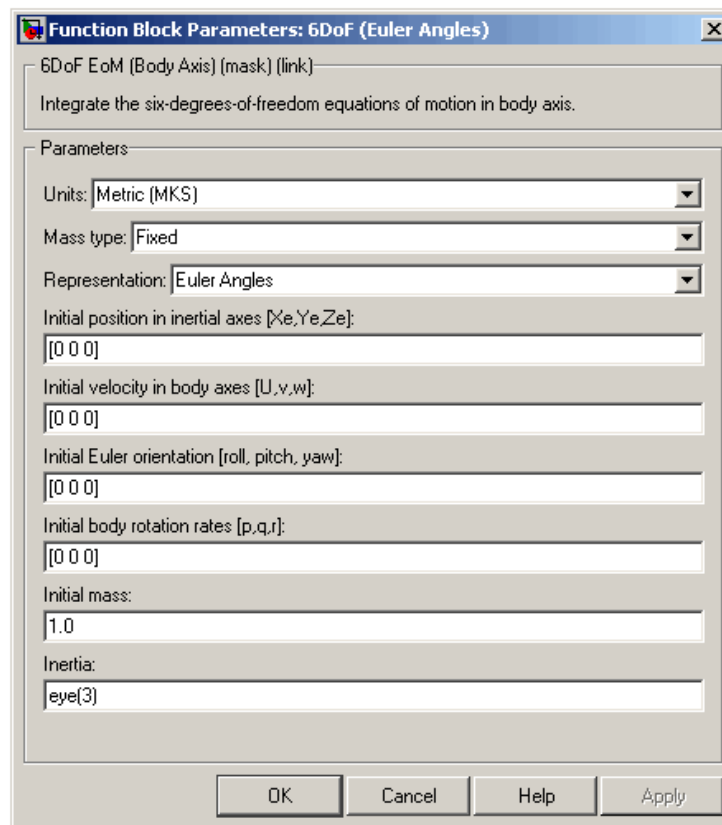


Figure 99-MATLAB block function



The input variables:

Atmospheric Parameter

$\rho=1.185;$

Flight conditions

$g=9.81;$

$m=4;$ % Weight [Kg]

$T=0;$

$\alpha_0=4.88 \cdot \pi/180;$

$U=17.53;$

The Aircraft Geometry

$b=1.42;$ % Span

$S=0.35;$ % Area

$C_t=.25;$

$C_r=.35;$

$M=0.06;$ % Mach number

$\text{Chord}=(C_t+C_r)/2;$ % mean chord

Lift Coefficient

$CL_0=0.0103;$

$CL_{\alpha}=4.5318;$

$CL_{\alpha \dot{}}=0;$

$CL_q=1.8707;$

$CL_{de}=0.3208;$

Drag Coefficient

$CD_0=.0046;$

$K=.032;$

1.1.1 Coefficient of the Y-D force

$C_yB=0;$

1.1.2 Rolling moment coefficient

$CL_B=0;$

$CL_p=-1.0495;$



CLda=.1812;

CLdr=0;

Pitching moments coefficient

Cm0=0.0385;

Cm_alpha=-0.5998;

Cm_alpha_dot=0;

Cmq=-4.3586;

Cmde=-0.8524;

Yawing moment coefficient

CnB=0;

Cnp=-0.7047;

Cnr=0;

Cnda=0;

Cndr=0;

Moment of inertia

Ix=0.76103;

Iy=0.072519;

Iz=0.83189;

Ixz=0.0014264;

Function Block Parameters: 6DoF (Euler Angles)

6DoF EoM (Body Axis) (mask) (link)

Integrate the six-degrees-of-freedom equations of motion in body axis.

Parameters

Units: Metric (MKS)

Mass type: Fixed

Representation: Euler Angles

Initial position in inertial axes [Xe,Ye,Ze]:

[0 0 -100]

Initial velocity in body axes [U,v,w]:

[U*cos(alpha0) U*sin(alpha0) 0]

Initial Euler orientation [roll, pitch, yaw]:

[0 alpha0 0]

Initial body rotation rates [p,q,r]:

[0 0 0]

Initial mass:

m

Inertia:

[Ix 0 -Ixz; 0 Iy 0; -Ixz 0 Iz]

OK Cancel Help Apply

Figure 101-MATLAB Simulink input

And after we make input δ_e with 2°

The final results:

The angle of attack:

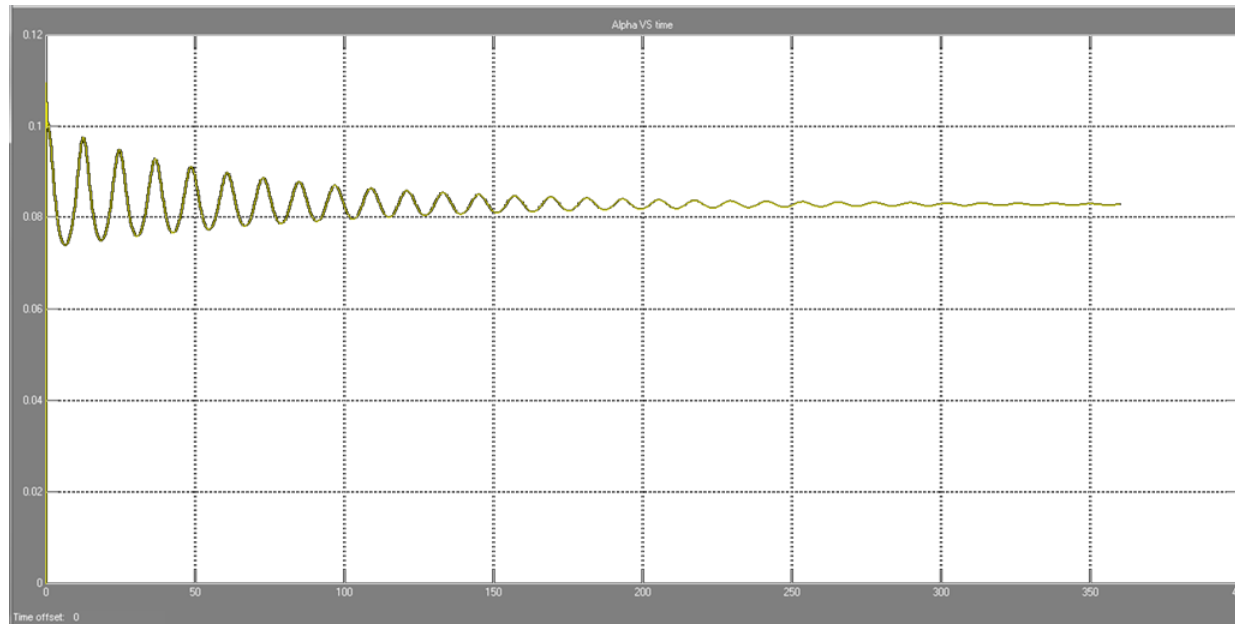


Figure 102-AOA VS Time

The Aircraft velocity:

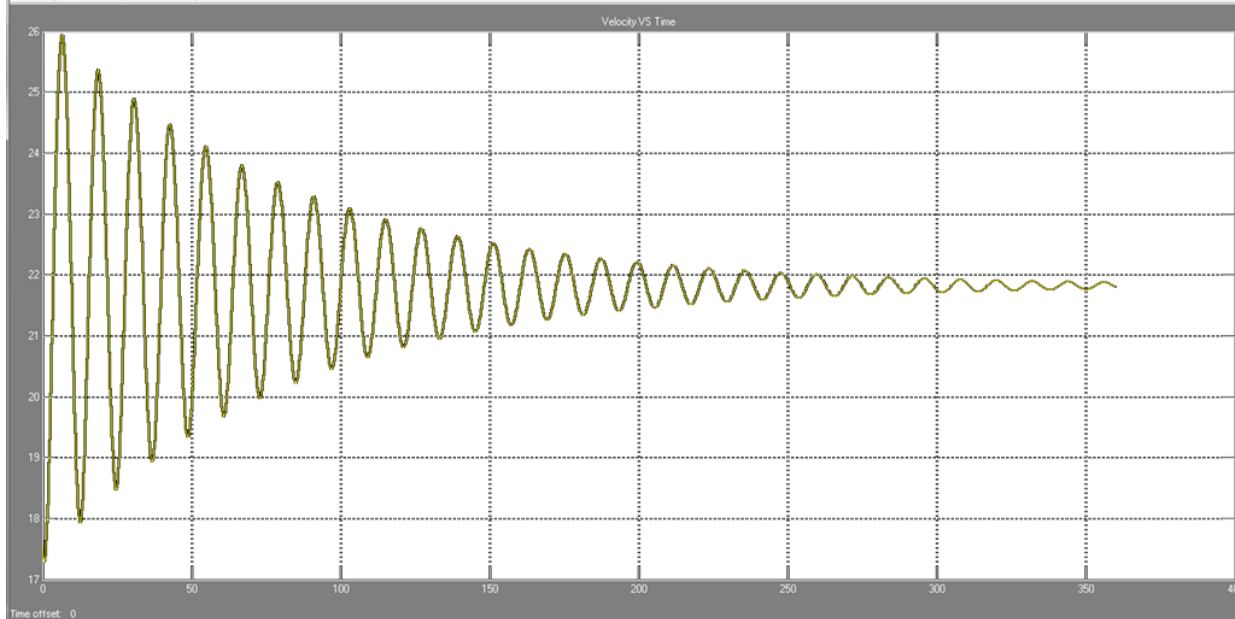


Figure 103-Velocity VS Time

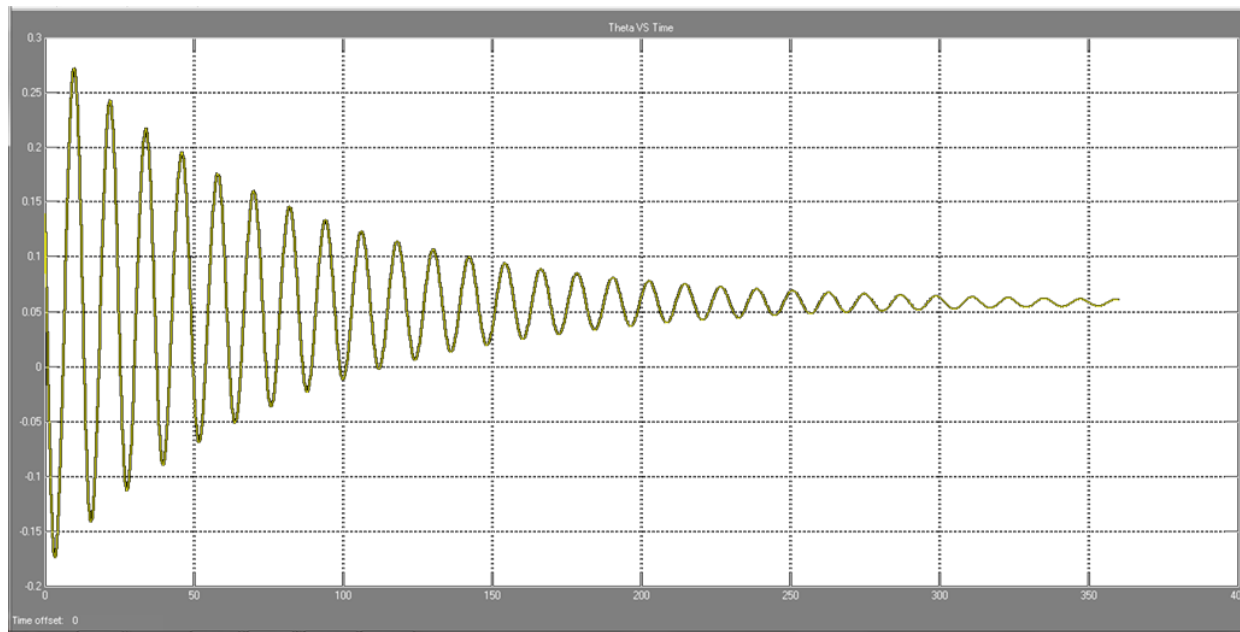
Theta VS Time:

Figure 104-Theta VS Time

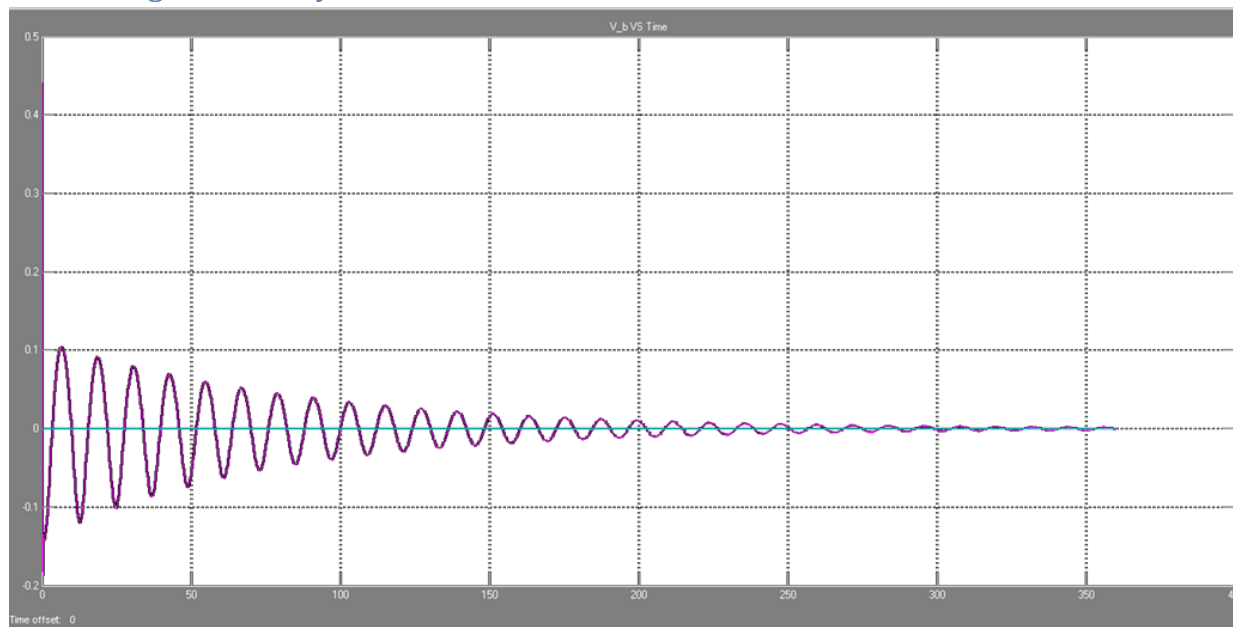
The angular velocity:

Figure 105-angular velocities VS Time

Chapter 9 Performance Analysis:

The inputs to the performance analysis are:

- Wing configuration
- Aircraft weight
- Drag polar for the aircraft
- Propulsion system available power

The outputs of the performance analysis are:

Steady flight performance

- C_L - C_D curves as function of velocity
- Flight envelope
 - Maximum speed
 - Minimum speed
 - Stall speed
 - Speeds corresponding to maximum range and maximum endurance
- Thrust required and thrust available curves
- Power required and power available curves
- Range
- Endurance
- Rate of climb
- Time to climb

Accelerated flight performance

- Level turn
 - Minimum turn radius
 - Maximum turn rate
- Takeoff performance
 - Ground roll
- Landing performance
 - Approach distance
 - Ground roll

Steady flight performance

The analysis procedure:

Given the wing loading (weight and area) , the aircraft drag polar(C_{D0},K), and the free stream density:

1. Choose a value for V_{inf}
2. For the chosen V_{inf} , calculate C_L from the relation

$$L = W = \frac{1}{2}\rho V^2 S C_L$$

Or

$$C_L = \frac{2W}{\rho V^2 S}$$

3. Calculate C_D from

$$C_D = C_{D,o} + K C_L^2$$

4. Calculate C_L/C_D & $C_L^{3/2}/C_D$
5. Calculate drag, hence T_R , from

$$T_R = D = \frac{1}{2}\rho V^2 S C_D$$

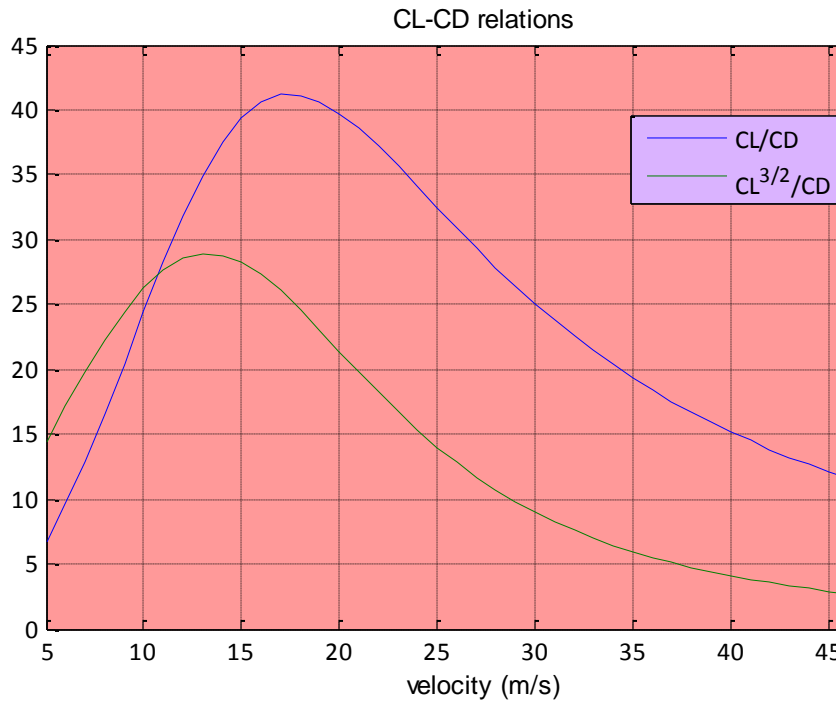
This value of T_R corresponding to the velocity chosen in step 1. This combination (T_R , V_{inf}) is one point on the thrust required curve.

6. Calculate P_R from

$$P_R = T_R V$$

7. Repeat steps 1 to 6 for a large number different values of velocity .Thus generating enough points to plot C_L/C_D & $C_L^{3/2}/C_D$, thrust required and power required curves.

C_L - C_D curves:



From the curve or analytically from equations we get:

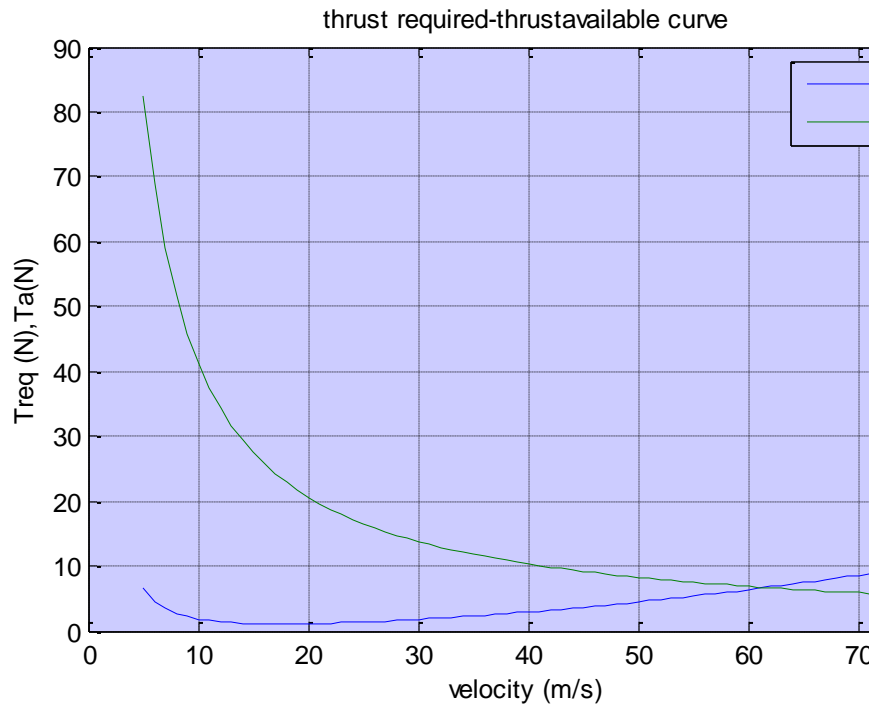
$$\left(\frac{C_L}{C_D}\right)_{max} = \frac{1}{\sqrt{4C_{D,o}K}} = 41.2$$

$$\left(\frac{C_L^{3/2}}{C_D}\right)_{max} = \frac{1}{4} \left(\frac{3}{KC_{D,o}^{1/3}}\right)^{3/4} = 28.9$$

$$V_{\left(\frac{C_L}{C_D}\right)_{max}} = \left(\frac{2}{\rho_{inf}} \sqrt{\frac{K}{C_{D,o}}} \frac{W}{S}\right)^{1/2} = 17.5 \text{ m/s}$$

$$V_{\left(\frac{C_L^{3/2}}{C_D}\right)_{max}} = 0.76 V_{\left(\frac{C_L}{C_D}\right)_{max}} = 13.3 \text{ m/s}$$

Thrust required-thrust available curve:

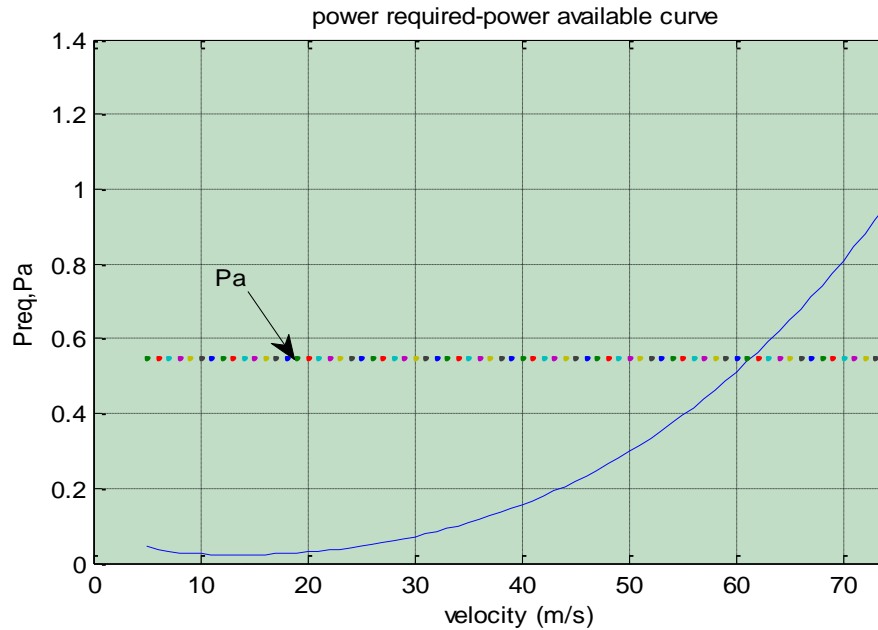


The minimum point of the thrust required curve represents the point where $\frac{C_L}{C_D}$ is maximum and the velocity at this point ‘ $V_{\left(\frac{C_L}{C_D}\right)_{max}}$ ’ is the velocity corresponding to maximum range.

The available power = $\eta \cdot \text{max power} \cdot \text{cruise throttle position} = 0.5 \cdot 1.74 \cdot 0.6 = 0.55 \text{ hp}$

Therefore, the available thrust T_A curve can be drawn using $T_A = P_A / V$

Power required-power available curve:



The minimum point of the power required curve represents the point where $\frac{C_L^{3/2}}{C_D}$ is maximum and the velocity at this point “ $V_{\left(\frac{C_L^{3/2}}{C_D}\right)_{max}}$ ” is the velocity corresponding to maximum endurance.

Flight envelope:

The flight envelope represents the range of velocities the within which the UAV can fly. It is determined by three important speeds, namely, maximum speed, minimum speed and stall speed

- Maximum speed:

From the power required and power available curve the point at which the available power equals the required power gives the maximum speed.

$$V_{max} = 62 \text{ m/s}$$

- Stall speed:

From the aerodynamic model of the aircraft it is known that $C_{Lmax}=0.94$

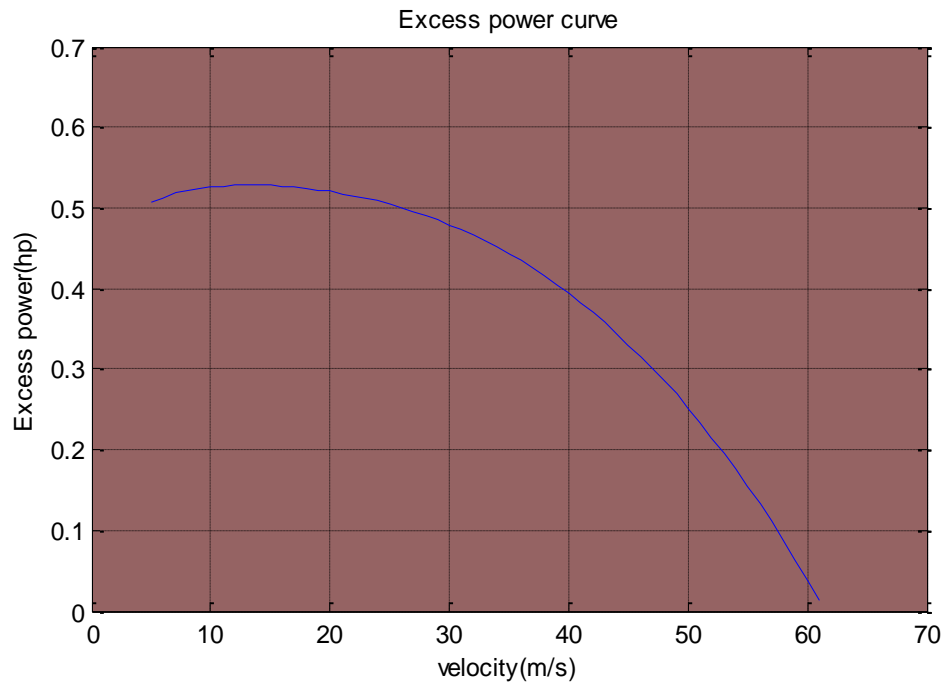
$$V_{stall} = \sqrt{\frac{2W}{\rho S} \frac{1}{C_{Lmax}}} = 11 \text{ m/s}$$

The stall speed is not constant; it increases with increasing altitude because the density decreases.

- Minimum speed:

$$V_{min} = 1.1V_{stall} = 12.1 \text{ m/s}$$

Excess power curve:



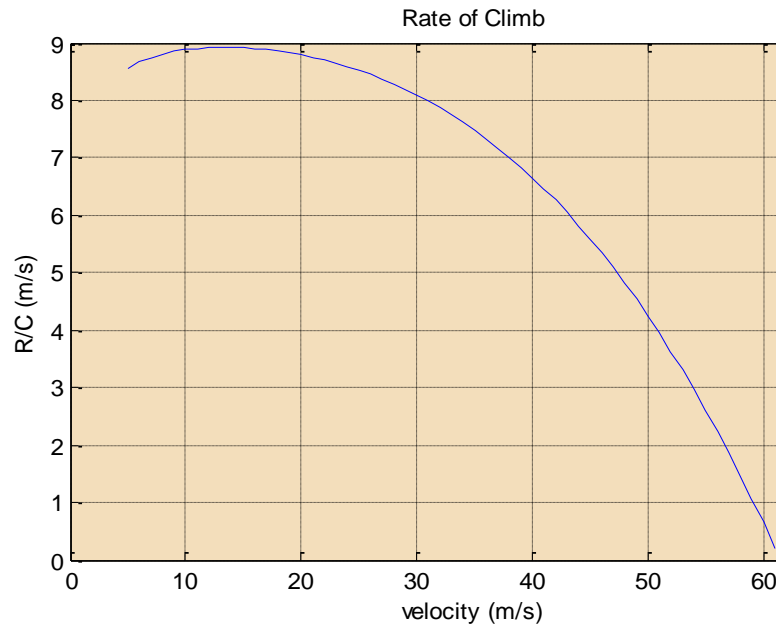
The excess power curve is obtained because it is used to calculate the rate for climb.

Climb characteristics: (steady unaccelerated climb)

1. Rate of climb:

The rate of climb is defined as the vertical component of the airplane's velocity, it depends on the UAV weight and excess power.

$$R/C = \frac{\text{Excess power}}{W}$$



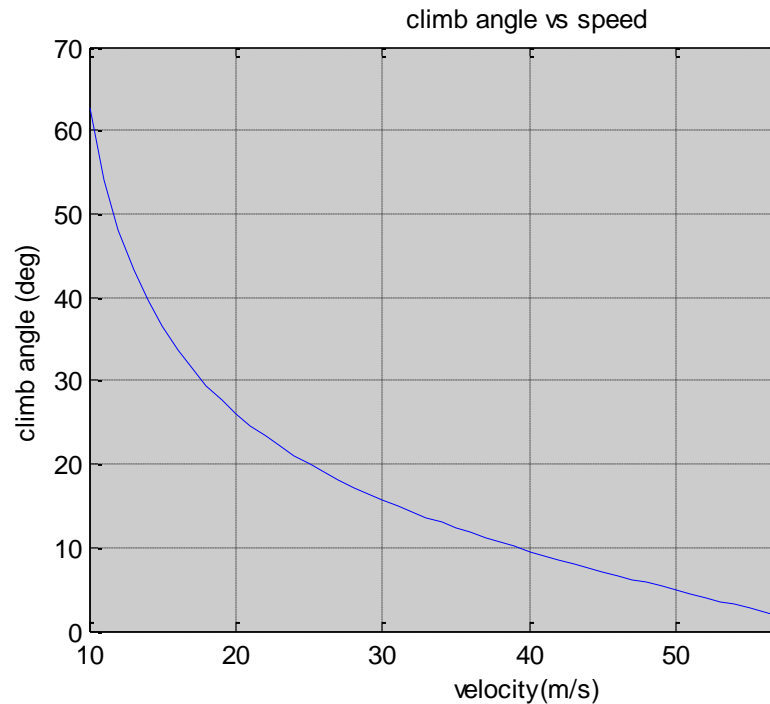
From the figure: $R/C_{\max} = 9 \text{ m/s}$

It occurs at the velocity $V_{\left(\frac{C_L^{3/2}}{C_D}\right)_{\max}}$ (minimum power required).

2. Climb angle:

The climb angle is defined as

$$\sin \theta = \frac{R/C}{V_{\text{inf}}}$$



3. Time to climb:

Since the rate of climb is the vertical component of the aircraft's velocity, then it is simply the time rate of change of altitude. Hence

$$R/C = \frac{dh}{dt}$$

Then the time to climb is given by

$$t = \int_0^h \frac{dh}{R/C}$$

Therefore the minimum time to climb to the cruise altitude (300 m) occurs at maximum rate of climb

$$t_{min} = \frac{1}{R/C_{max}} \int_0^{300} dh = 33 \text{ sec}$$

Range:

By definition, range is the total distance (measured with respect to the ground) traversed by an airplane on one load of fuel (one load of battery cells).

$$-dC = I dt \longrightarrow (1)$$

$$dS = V_{\infty} dt \longrightarrow (2)$$

where:

C= battery charge (mAh)

I=battery current (Amp.)

S=range (m)

$$\text{From 1 \& 2: } ds = - \frac{V_{\infty}}{I} dC \longrightarrow (3)$$

and by multiplying (3) *battery volt V and arranging the equation as shown:

$$dS = -\eta V \frac{C_L}{C_D} \frac{dC}{W}, \text{ where: } W = \text{UAV weight in N.}$$

so by integrating the last equation we get the following equation which is called Breguet Range equation for propeller driven aircraft using electric battery as a power source:

$$R = \eta V \frac{C_L}{C_D} \frac{C_i - C_f}{W}$$

It is clear that the maximum range is corresponding to $\left(\frac{C_L}{C_D}\right)_{\max}$

Where:

C_i = initial battery charge (joule/volt).

C_f = final battery charge (joule/volt).

For the UAV battery :

$V = 22.2$ (volt).

$C_i = 5000$ (mAh)

$C_f = 0$ (joule/volt)

So: $\text{Range}_{\max} = 185 \text{ km.}$

Endurance:

It is the time of the range that the MAV will cover, to determine the endurance of the MAV we need the relation between the charge and the time:

$$-dC = I dt \longrightarrow (1)$$

$$dS = V_{\infty} dt \longrightarrow (2)$$

and using the results obtained before:

$$dS = \eta V \frac{C_L}{C_D} \frac{dC}{W}, \text{ where: } W = \text{MAV weight in N.}$$

$$\text{So: } dt = \frac{dS}{V_{\infty}} = - \eta \frac{V}{V_{\infty}} \frac{C_L}{C_D} \frac{dC}{W}$$

and we get the so called Breguet Endurance equation for propeller driven aircraft using electric battery as a power source:

$$E = \eta \frac{V}{V_{\infty}} \frac{C_L}{C_D} \frac{C_i - C_f}{W}$$

Or we can put it in a more clear form by eliminating the velocity:

$$E = \eta V \frac{C_L^{\frac{3}{2}}}{C_D} \frac{C_i - C_f}{W^{\frac{3}{2}}} \sqrt{\frac{\rho_{\infty} S}{2}}$$

It clear now that the maximum endurance is corresponding to $\frac{C_L^{\frac{3}{2}}}{C_D})_{\max}$.

So : E = 3.4 hour

Accelerated flight performance

Level turn

In level turn the flight path is curved; by definition a level turn is one in which the curved flight path is in a horizontal plane parallel to the plane of the ground; that is, in a level turn the altitude remains constant.

Let the UAV be banked through the roll angle; then

$$L \cos \phi = W \quad (1)$$

$$L \sin \phi = m \frac{V_{\infty}^2}{R} \quad (2)$$

Eqn(2) is simply a physical statement that the centrifugal force $m \frac{V_{\infty}^2}{R}$ is balanced by the radial force $L \sin \phi$

The two performance characteristics of great importance in turning flight are:

1. The turn radius
2. The turn rate $\equiv d\Psi/dt$; the turn rate is simply the local angular velocity of the airplane along the curved flight path.

An important parameter in turning performance is the load factor n ; $n \equiv \frac{L}{W}$

Therefore eqn (1) becomes: $\phi = \cos^{-1} \frac{1}{n}$

Now the turn radius R will be

$$R = \frac{V_{\infty}^2}{g\sqrt{n^2 - 1}}$$

And the turn rate ω will be

$$\omega = \frac{g\sqrt{n^2 - 1}}{V_{\infty}}$$

To obtain the smallest possible turn radius and the largest possible turn rate, we want:

1. The highest possible load factor
2. The lowest possible velocity

By making use of constraint on n & V_{∞} we get:

$$n_{max} = \frac{1}{2} \rho_{\infty} V_{\infty}^2 \frac{(C_L)_{max}}{W/S}$$

$$V_{stall} = \sqrt{\frac{2}{\rho_{\infty}} \frac{W}{S} \frac{n}{(C_L)_{max}}}$$

Finally we get;

1. for minimum turn radius

$$R_{min} = \frac{4K(W/S)}{g\rho_{\infty} T/W \sqrt{1 - 4KC_{D,o}/(T/W)^2}}$$

$$n_{Rmin} = \sqrt{2 - \frac{4KC_{D,o}}{(T/W)^2}}$$

$$(V_{\infty})_{Rmin} = \sqrt{\frac{4K(W/S)}{\rho_{\infty}(T/W)}}$$

2. for maximum turn rate

$$(V_{\infty})_{\omega max} = \left[2 \frac{W/S}{\rho_{\infty}} \right]^2 \left(\frac{K}{C_{D,o}} \right)^{1/4}$$

$$n_{\omega max} = \left(\frac{T/W}{\sqrt{KC_{D,o}}} - 1 \right)^{1/2}$$

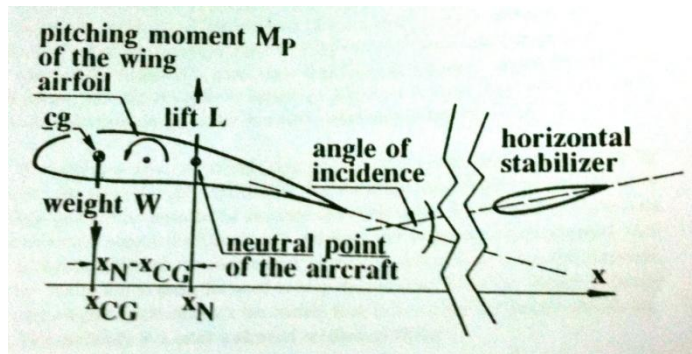
$$\omega_{max} = q \sqrt{\frac{\rho_{\infty}}{W/S} \left[\frac{T/W}{2K} - \left(\frac{C_{D,o}}{K} \right)^2 \right]}$$

Chapter 10 Stability and Control

Longitudinal Stability

The longitudinal stability of aircraft is the stability around the lateral axis.

Large cg forward position only half of the stability problem is solved. The other half is the so-called balance of the pitching moments. ("Trim" or "trimming"). This is done by a combination of sweep and wash –out by a suitable selection of wing sections and by the deflection of the elevator flaps.



For this balance of pitching moments a tailed aircraft needs a positive angle of incidence (angle of Horizontal Tail Setting).

For a Wing to produce the same effect of Horizontal tail a sweep back and wash out is required.

Angle of incidence:

For a tailed aircraft it's the angle between zero-lift direction of wing and zero-lift direction of horizontal tail. For Swept back wing it's the angle between zero-lift direction of Root and zero-lift direction of tip.

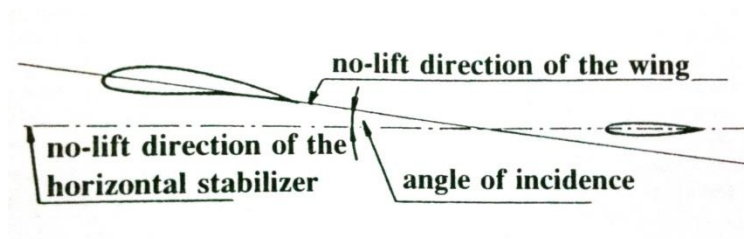


Figure 106 : Angle of incidence

Any inherently stable tailed aircraft needs a positive angle of incidence.

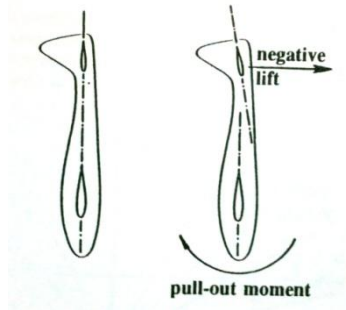


Figure 107 : Pull-out Moment

As we connected two lines between the wing and tail, it looks like the side view of swept back, twisted, wing.

Lateral stability

The lateral stability of aircraft is the stability around the longitudinal axis.

Lateral stability can be produced by several methods:

- Low lying centre of mass
- Dihedral
- Sweep back

Dihedral, sweep back and high wing aircraft has the effect of producing positive skid-roll moment.

Suppose a swept-back wing is skidding as shown in figure. Then the left wing is skidding with large velocity than the right wing, thus the lift on the left wing increase, therefore the whole wing has a positive skid roll moment

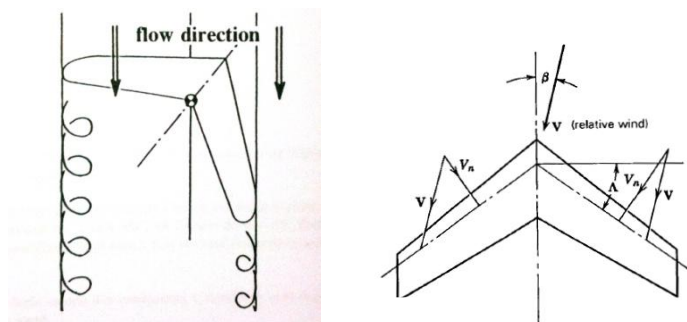
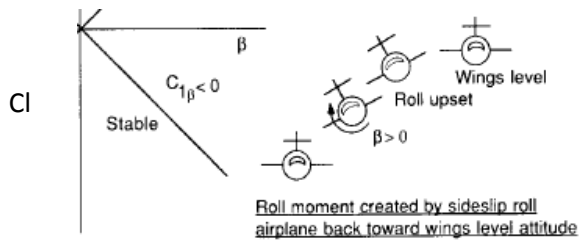


Figure 108 : Dihedral Effect on Sweptwing

Dihedral, sweep back and high wing aircraft has the effect of producing positive skid-roll moment.

Skid-roll moment:

For a high wing aircraft (or wing with dihedral) is side slipping then the leading wing will fly with a larger angle of attack than the trailing one. Therefore it has more lift. This produces a roll moment which raises the front wing tips. This rolling moment induce an acceleration in the opposite direction of the side slip velocity, so it damp it after a period, and the wing returns to its level.



➤ High wing aircraft

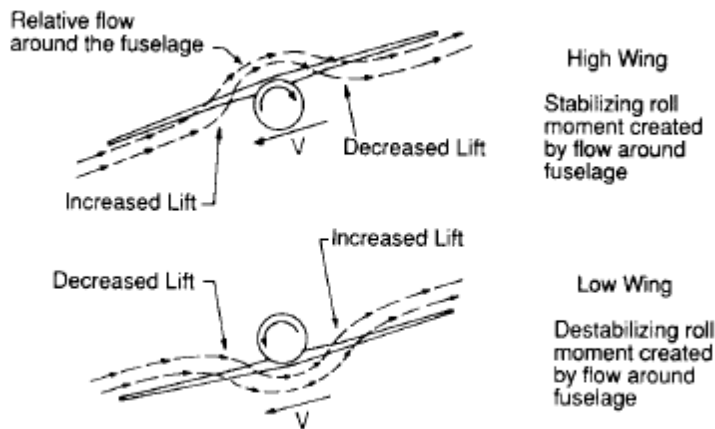


Figure 109 : Fuselage Contributions

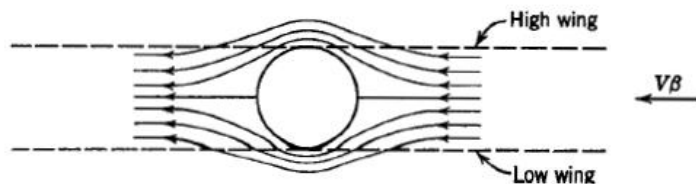


Figure 110 : Influence of body on $C_{l\beta}$

Directional stability

The directional stability of aircraft is the stability around the vertical axis.

The directional stability can be produced by sweep back.

Suppose a swept-back wing is skidding as shown in figure. Then the left wing is skidding with large velocity than the right wing, thus the lift on the left wing increase , also the drag (airfoil and induced) on the left wing increase than the right wing , so the drag wants to pull back the wing to the air flow direction , therefore the whole wing has a positive skid Yaw moment (also positive skid roll moment).

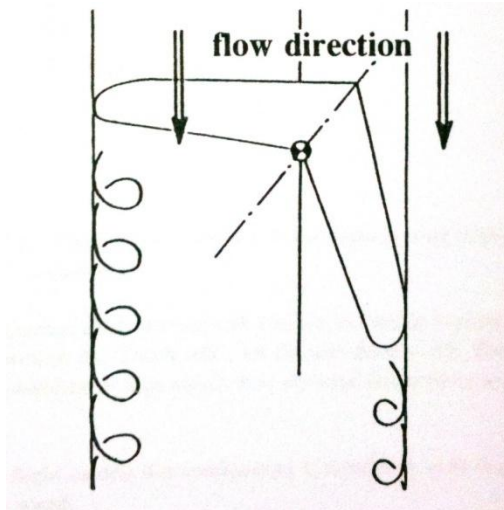


Figure 111 : Skid Roll Moment

The skid roll moment of a sweptback wing is proportional to the lift coefficient and thus to the angle of attack.

The skid yaw moment of a swept back wing is however proportional to the square of lift coefficient (square of angle of attack).

Therefore a swept back wing has poor directional stability at low angle of attack.

Sizing of Control Surfaces

Sizing to Longitudinal Motion (Steady & level Flight) and Take Off

Cruise

$$C_{mcg} = C_{mo} + C_{m\alpha}\alpha + C_{m\delta_e}\delta_e + C_{m\delta_f}\delta_f$$

At cruise $\delta_f = 0$, the most severe case when flying at maximum angle of attack, $\alpha_{max} = 14^\circ$

The Elevator must have enough Control Power to trim the Wing at this Case.

$$C_{mcg} = 0 = C_{mo} + C_{m\alpha}\alpha_{max} + C_{m\delta_e}\delta_e , C_{m\delta_e} \text{ is a function of Geometry}$$

$$\text{Solve to get } \delta_e : \delta_e = -\frac{C_{mo} + C_{m\alpha}\alpha_{max}}{C_{m\delta_e}}$$

Take Off

The Wing has to leave the run way with minimum speed ($V_{min} = 1.1V_{stall}$), so it will generate lift nearly maximum lift coefficient (C_{Lmax})

$$C_{Lreq} = \frac{2W}{\rho_\infty S (1.1V_{stall})^2}$$

$$C_{Lreq} = C_{L0} + C_{L\alpha}\alpha_{sett} + C_{L\delta_e}\delta_e + C_{L\delta_f}\delta_f \rightarrow 1$$

$$C_{mcg} = 0 = C_{mo} + C_{m\alpha}\alpha_{sett} + C_{m\delta_e}\delta_e + C_{m\delta_f}\delta_f \rightarrow 2$$

Choose the setting angle of the wing(at **MAC**) , then solve 1,2 in δ_e, δ_f , this 2 angles will trim the Wing at Take Off , to Pull up the wing from the Ground , increase the δ_e ,in the negative direction , to have more nose up moment.

Calculating Coefficients of Flap, Elevator and Aileron

Flap and elevator is treated as same surface from point of view of analysis.

Elevator & Flap

$$C_{m\delta} = \frac{1}{S\bar{C}} \left[\int_{-\frac{b}{2}}^{\frac{b}{2}} \frac{dc_m}{d\delta}(y) * C^2(y) dy - \int_{-\frac{b}{2}}^{\frac{b}{2}} \frac{dc_l}{d\alpha}(y) * \frac{d\alpha}{d\delta}(y) * h(y) * c(y) dy \right]$$

$$C_{L\delta} = \frac{1}{S} \int_{-\frac{b}{2}}^{\frac{b}{2}} \frac{dc_l}{d\alpha}(y) * \frac{d\alpha}{d\delta}(y) * c(y) dy$$

$$\frac{dc_m}{d\delta}_{2D} = -2\sqrt{X(1-X)^3}$$

$$\frac{dc_m}{d\delta}_{meas} = Factor * \frac{dc_m}{d\delta}_{2D}$$

$$\frac{d\alpha}{d\delta}_{2D} = -\frac{2}{\pi} (\sqrt{X(1-X)} + \sin^{-1}(\sqrt{X}))$$

$$\frac{d\alpha}{d\delta}_{meas} = -X + Factor * \left(\frac{d\alpha}{d\delta}_{2D} + X \right)$$

$$Factor = 1, 0.75, 0.5, X = \frac{C_f}{C}$$

The values of X , is Chosen to get maximum Efficinecy of the control Surface , that means , choosing , X for Falp which gives Maximum Increase in Zero Lift Slope , and Minimum increase on Moment.

$$\frac{C_{L\delta}}{C_{m\delta}} \rightarrow \text{Maximize this Value}$$

Choosing X for Elevator which gives Minimum increase in Zero Lift Slope and Maximum increase in Moment

$$\frac{C_{m\delta}}{C_{L\delta}} \rightarrow \text{Maximize this Value}$$

The Value of this Factor is determined by Lab. Measurements (Ref 2).

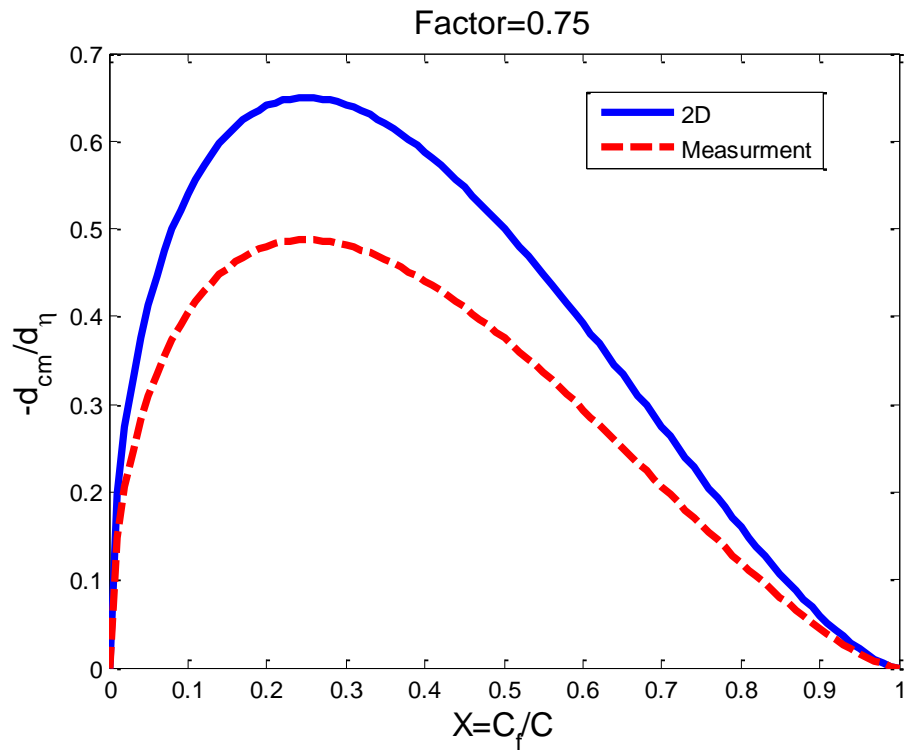


Figure 112 : Comparison between moment calculations and measurement

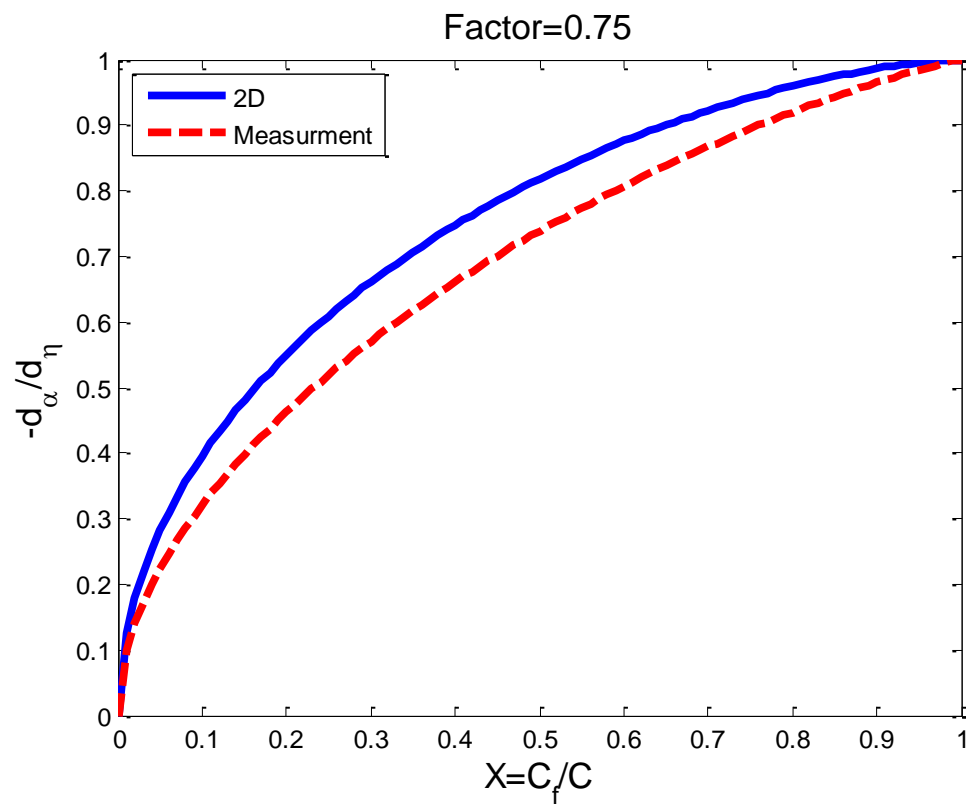


Figure 113 : Comparison between moment calculations and measurement

Aileron

The size of Aileron is chosen equal to the Elevator; As the Idea of Elevon (Elevator + Aileron) is Equally Size to each other.

$$C_{l\delta_a} = \frac{1}{Sb} \int_{-\frac{b}{2}}^{\frac{b}{2}} \frac{dc_l}{d\alpha}(y) * \frac{d\alpha}{d\delta}(y) * y * c(y) dy$$

Control Surface Size & Data

As clearly shown in figure, the size of surfaces based on measurements will be larger than based on 2D-calculations.

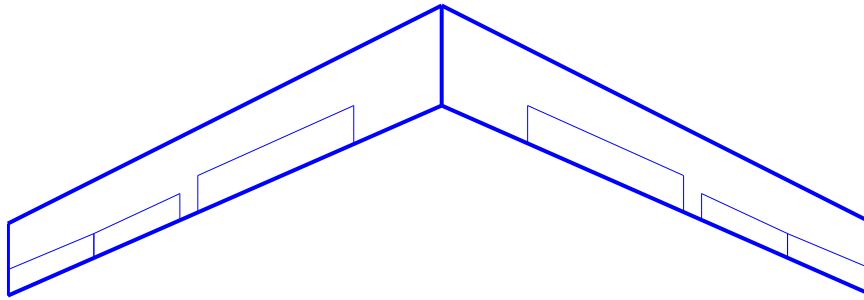


Figure 114 : Wing Planform

$$C_{L\delta_e} = 0.3249/rad$$

$$C_{m\delta_{e.c.g}} = -0.4374/rad$$

$$C_{L\delta_f} = 1.0873/rad$$

$$C_{m\delta_{f_{c.g}}} = -0.0695/\text{rad}$$

$$C_{l\delta_a} = 0.198/\text{rad}$$

1.1.Cruise

$$\alpha_{max} = 14^\circ \quad \delta_{e\alpha_{max}} = -14.11^\circ$$

$$\alpha_{Cruise} = 4^\circ \quad \delta_{e\alpha_{Cruise}} = -0.43^\circ$$

As concluded from results at cruise the wing will fly at neutral elevators.

1.2.Take off

$$C_{Lreq} = 1.024$$

$$\alpha_{Setting_{Root}} = 9.7^\circ$$

$$\delta_{eTake_Off} = -10.3^\circ$$

$$\delta_{fTake_Off} = 20^\circ$$

Stability Study

1. Longitudinal stability study

$$A = \begin{bmatrix} X_u & X_W & 0 & -g * \cos\theta_o \\ Z_u & Z_W & U_o + Z_q - g * \sin\theta_o \\ M_u & M_W & M_q & 0 \\ 0 & 0 & 1 & 0 \end{bmatrix}$$

A =

$$\begin{bmatrix} -1.4032e-002 & 4.1208e-004 & 0 & -9.8000e+000 \\ -2.0134e-002 & 2.7171e-001 & 1.2830e+001 & 0 \\ 0 & -8.4203e+000 & -8.3384e+000 & 0 \\ 0 & 0 & 1.0000e+000 & 0 \end{bmatrix}$$

Eigen Values

$$-4.3057e+000 + 9.5788e+000i$$

$$-4.3057e+000 - 9.5788e+000i$$

$$-6.4288e-003 + 1.2256e-001i$$

$$-6.4288e-003 - 1.2256e-001i$$

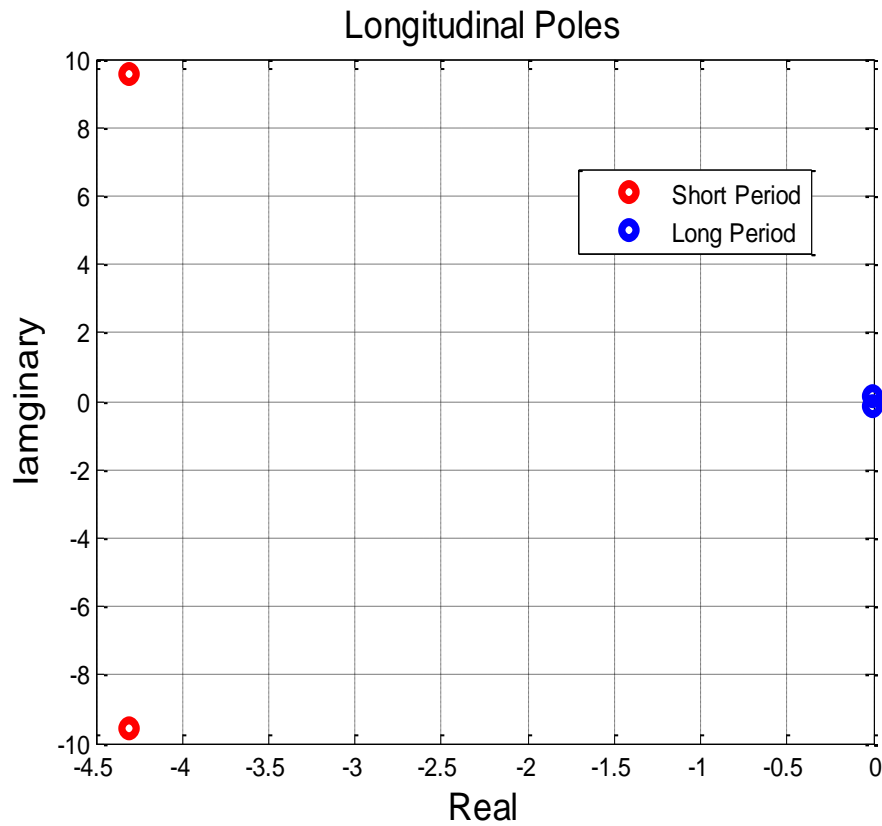


Figure 115 : Longitudinal Poles

Lateral Stability Study

$$A = \begin{bmatrix} \frac{Y_\beta}{U_o} & \frac{Y_p}{U_o} & -(1 - \frac{Y_r}{U_o}) & -\frac{g}{U_o} & 0 \\ L'_\beta & L'_p & L'_r & 0 & 0 \\ N'_\beta & N'_p & N'_r & 0 & 0 \\ 0 & 1 & 0 & 0 & 0 \\ 0 & 0 & 1 & 0 & 0 \end{bmatrix}$$



A =

0	1.8780e-002	-1.0000e+000	7.6383e-001	0
-3.3445e-001	-4.9624e+000	1.8316e+000	0	0
2.4277e-002	-2.3193e-002	1.1790e+000	0	0
0	1.0000e+000	0	0	0
0	0	1.0000e+000	0	0

Eigen Values

0
 -4.9610e+000
 -9.2306e-003 +2.1511e-001i
 -9.2306e-003 -2.1511e-001i
 -1.1619e+000

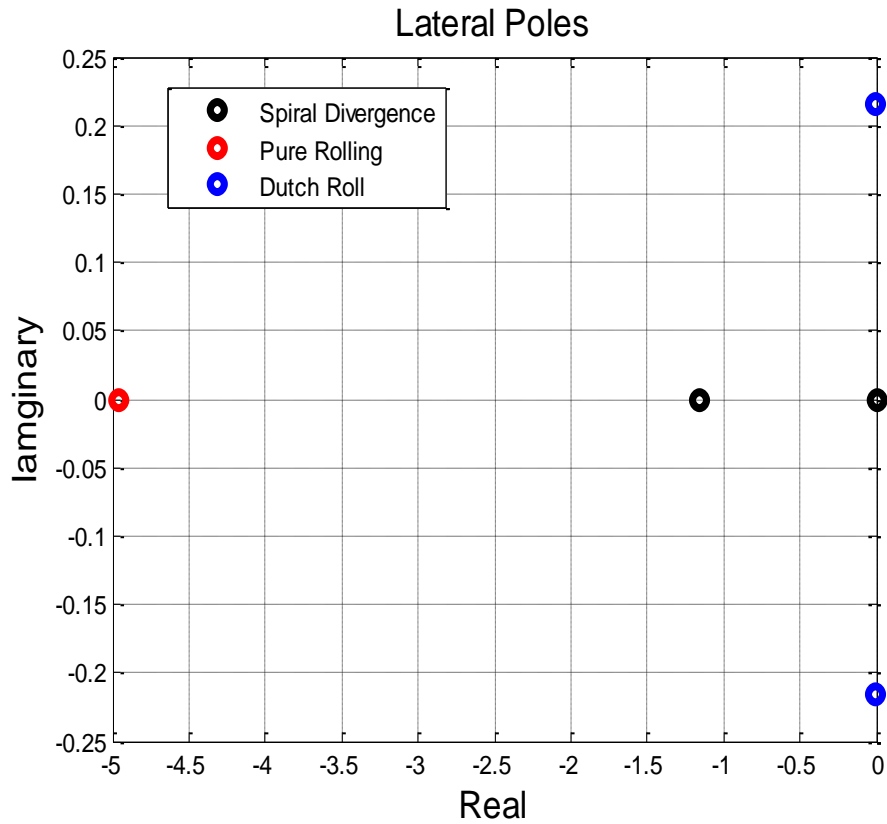


Figure 116 : Lateral Poles

➤ **Comment:** The weak directional stability gives spiral stability.

Chapter 11 Manufacturing

▣ Main Stages:

1. Master Mold.
2. Female Mold.
3. Wing Body.
4. Control Surfaces.
5. Fuselage
6. Installing motor and all other devices.

Master Mold.

Laser cut:

Draw CAD file (*.DWG) for the ribs, each section is attached to its stand with few millimeters to be easily separated later. Each airfoil has an inclination angle on its stand so as to reach the wanted geometric twist of the wing. The file has to be compatible with the laser cutting machine and the wood type has to be a high quality one like Finland ply wood (3 mm.) thickness.



Figure 117: Ribs laser cut

Fix the Jig:

A jig has to be made in the same previous technique with the same sweep back angle of the wing and the holes are to be aligned with the position of the stands of the ribs with same geometry.



Figure 118: Jig

Fix the ribs into the jig:



Figure 119: Ribs fixation

Fix the spars along the ribs:
Ribs dimensions are 6x6mm



Figure 120: Spars fixation

Cover the upper surface of the construction by Balsa wood Sheets:
Balsa wood sheets are of 1.5 mm thickness and it is recommended to be thinner to take the curves shapes easier, and it is to be fixed on the ribs and spars with glue.



Figure 121: balsa covering

Cover the upper skin by Fiber Glass:

To make a strong master mold use woven fiber glass with its matrix which is Polyester and Hardener (peroxide and cobalt) from local market with mass ratio 100:4



Figure 122: Fiberglass Covering-1



Figure 123: Fiberglass Covering-2

7. Break the connection between the ribs and the jig

8. Invert the Body to repeat the previous process to the lower surface.

9. Sanding the Master Mold.



Figure 124: Master mold sanding

10. Fill the Master Mold with Poly-Fiber Putty and Paint it

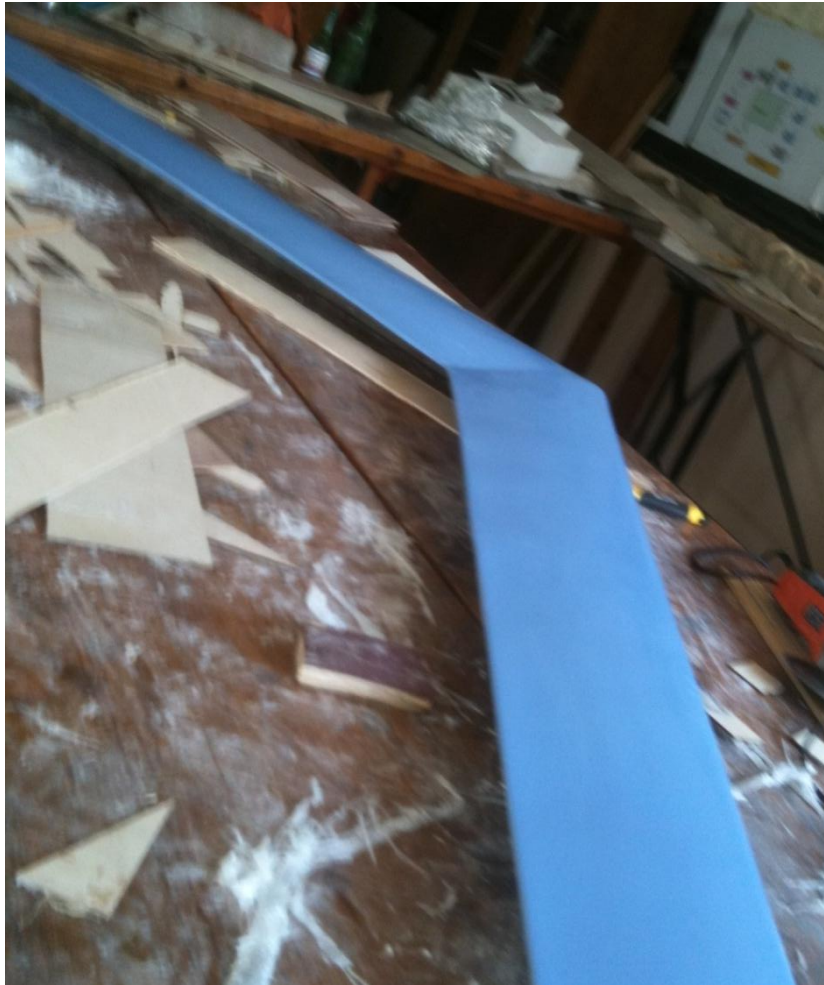


Figure 125: Master mold

Female Mold

Construct a frame around the master mold.



Figure 126: Frame

Fill the empty space between the frame and the mold by Klean Klay.



Figure 127: Klean Klay filling

Isolate the surface by one Gel Coat layer, 3 PVA layers, and 3 Wax layers to ensure complete isolation between the master mold and the female mold which will be preceded later on.



Figure 128: Master mold isolation

Make an AEROSIL Fillet between the frame and the Master Mold. It must be taken in consideration the highly toxic effect of the Aerosil. It has to be mixed with polyester and its hardener to be like dough.



Figure 129: Aerosil fillet

Cover Master Mold with Fiber Glass and proceed in adding its matrix like the previous steps, repeat for 9 layers and leave it many hours to guarantee that it became strong enough and dry.

Separate the frame from the female mold but keep the master mold inside the female mold and get both out from the frame and invert them then repeat the procedure of adding 9 layers of fiber glass to make the female mold of the lower surface. Then use a release wedge to separate the upper from the lower surfaces.



Figure 130: Female mold

Make a check using checking templates that was made using by laser cutting machine.

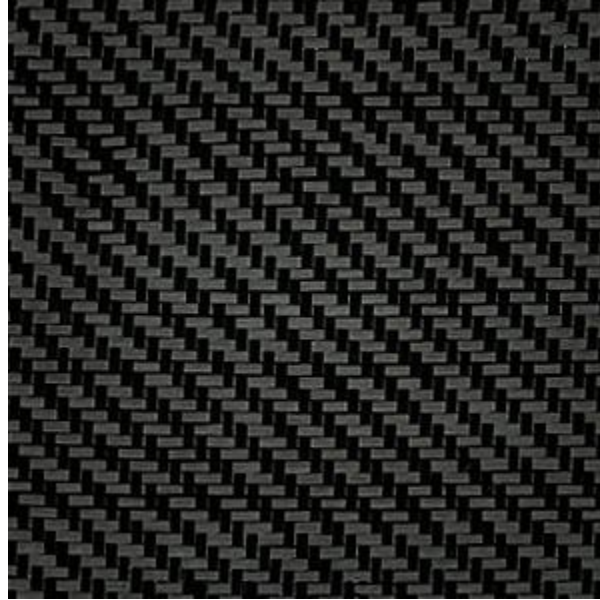


Figure 131: Checking templates

Wing Body:

Put the Carbon Fiber inside the female molds and add its matrix which consists of Epoxy and its hardener (EPOLAM 2001/ EPO 95 S) with a very accurate ratio 100:32, the weight of the matrix should be the same weight of the carbon fiber after trimming the excess parts outside the female mold.

Another carbon fiber Layer is to be put all over the upper female mold while the lower female mold only a layer was put from the root chord to the middle of half spans.



3K, 2 x 2 Twill Weave Carbon Fiber Fabric

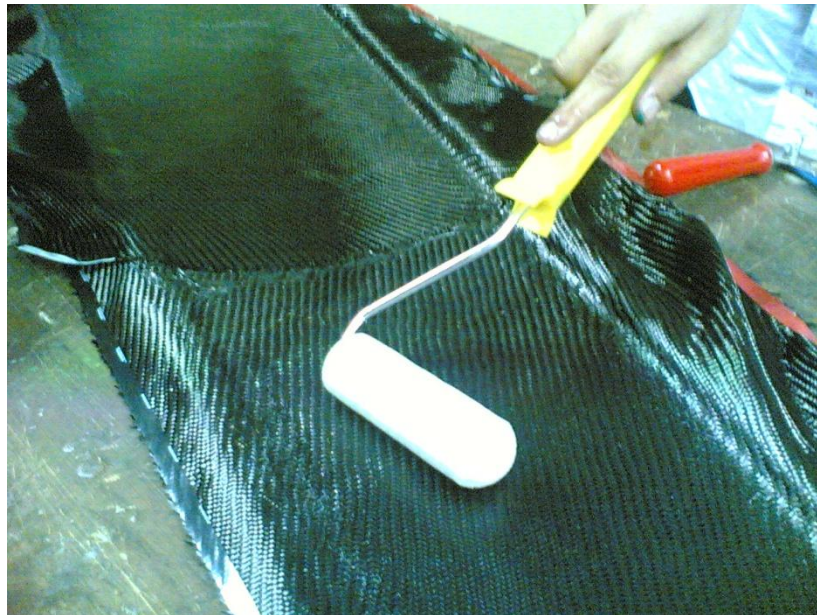


Figure 132: Carbon Fiber skin making

Construct the internal structure whose ribs and shear webs were cut using laser cutting machine and integrate them with the spars using **STRUCTURAL EPOXY ADHESIVE (ADEKIT A140)**.



Figure 133: Structure Fixation-1

Install the structure inside the wing skin using the same structural epoxy adhesive and then close the wing with the other skin.



Figure 134: Structure Fixation-2

Use carbon fiber tape to close the clearance in the leading edge from outside since if it fills the clearance from inside it will lead to flow separation starting from the leading edge point.

Spray paint the wing.

Control Surfaces:

Cut the control surfaces and fill all the empty edges with thick balsa wood using glue to be easily broken later for maintenance issues.



Figure 135: Cutting Control Surfaces



Figure 136: Filling empty edges

Install the servos.

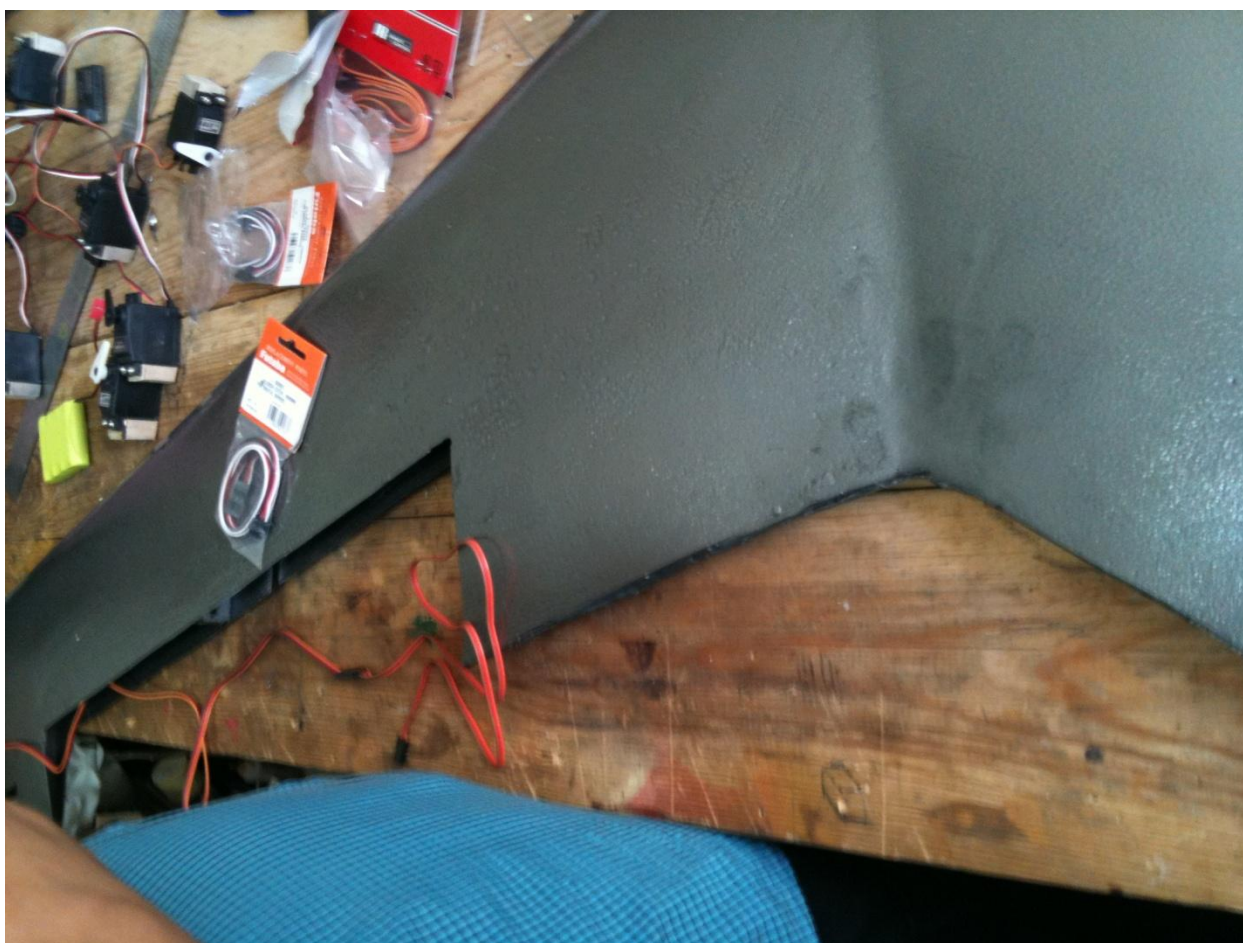


Figure 137: Servos installing-1



Figure 138: Servos installing-2

Install the control surfaces using “easy hinges” by making 2 cuts in the balsa wood in both the control surface and on the wing and fix it in between to hold them together.



Figure 139: Easy hinges

Fuselage:

Make the Master Mold using center lathe machine taking in consideration the airfoil profile of the two contact lines between the fuselage and the lower surface of the wing on which the fuselage is going to be installed.



Figure 140: Fuselage master mold

Make the female mold using 7 layers of Matt Fiberglass using same procedure



of wing female mold.

Figure 141: Female mold making

Make the fuselage body using 3 layers of Carbon Fiber using same procedure of wing skin.



Figure 142: Fuselage body-1



Figure 143: Fuselage body-2 "after trimming"

Spray Paint the fuselage.

Installing motor and all other devices:

Mount the motor at the end of the fuselage from outside to be exposed to air for ventilation.



Figure 144: Mounting the motor

Fix the landing gear under the fuselage.

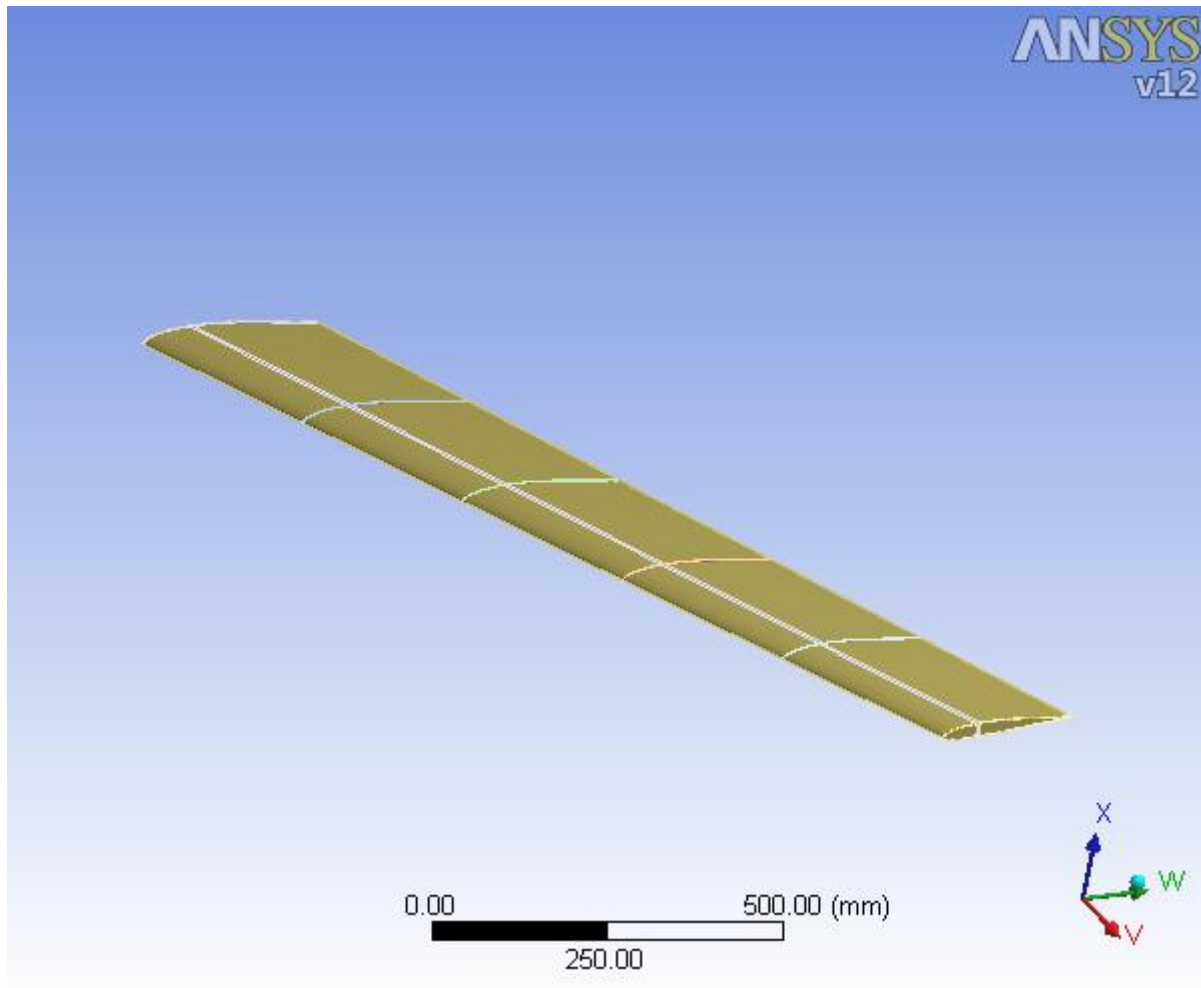
Fix the Instruments (the battery, the speed controller, and the receiver) inside the fuselage.

Fix the Fuselage into the wing.

Make proper preparations for flying test.

Appendices:

Appendix A: The ANSYS Report for model 1:



Units

TABLE 1

Unit System	Metric (mm, t, N, s, mV, mA) Degrees rad/s Celsius
Angle	Degrees
Rotational Velocity	rad/s
Temperature	Celsius

Model (B4)

Geometry

TABLE 2
Model (B4) > Geometry

Object Name	Geometry
State	Fully Defined
Definition	
Source	F:\Data\Ansys\Structural design\The aircraft solid model_2.igs
Type	Iges
Length Unit	Meters
Element Control	Program Controlled
Display Style	Part Color
Bounding Box	
Length X	1250. mm
Length Y	839.54 mm
Length Z	120.65 mm
Properties	
Volume	5.5139e+005 mm ³
Mass	8.8222e-004 t
Scale Factor Value	1.
Statistics	
Bodies	14
Active Bodies	8
Nodes	27289
Elements	13791
Mesh Metric	None

Preferences	
Import Solid Bodies	Yes
Import Surface Bodies	Yes
Import Line Bodies	No
Parameter Processing	Yes
Personal Parameter Key	DS
CAD Attribute Transfer	No
Named Selection Processing	No
Material Properties Transfer	No
CAD Associativity	Yes
Import Coordinate Systems	No
Reader Save Part File	No
Import Using Instances	Yes
Do Smart Update	No
Attach File Via Temp File	Yes
Temporary Directory	C:\Users\Mohamed\AppData\Local\Temp
Analysis Type	3-D
Mixed Import Resolution	None
Enclosure and Symmetry Processing	Yes

TABLE 3
Model (B4) > Geometry > Parts

Object Name	Part 1	Part 2	Part 3	Part 4	Part 5
State	Meshed				
Graphics Properties					
Visible	Yes				
Transparency	1				

Definition					
Suppressed	No				
Stiffness Behavior	Flexible				
Coordinate System	Default Coordinate System				
Reference Temperature	By Environment				
Material					
Assignment	carbon fiber_2				
Nonlinear Effects	Yes				
Thermal Strain Effects	Yes				
Bounding Box					
Length X	1.2192 mm				
Length Y	290.54 mm	274.51 mm	258.49 mm	242.46 mm	226.44 mm
Length Z	30.336 mm	28.824 mm	27.367 mm	25.973 mm	24.652 mm
Properties					
Volume	6846.4 mm³	6111.6 mm³	5418.7 mm³	4767.5 mm³	4158.8 mm³
Mass	1.0954e-005 t	9.7786e-006 t	8.6699e-006 t	7.628e-006 t	6.654e-006 t
Centroid X	0.60954 mm	250.37 mm	500.12 mm	749.88 mm	999.63 mm
Centroid Y	116.98 mm	236.48 mm	355.87 mm	475.17 mm	594.51 mm
Centroid Z	4.5101 mm	4.433 mm	4.394 mm	4.3528 mm	4.3021 mm
Moment of Inertia Ip1	4.7029e-002 t·mm²	3.7493e-002 t·mm²	2.953e-002 t·mm²	2.2832e-002 t·mm²	1.7397e-002 t·mm²
Moment of Inertia Ip2	5.6689e-004 t·mm²	4.4296e-004 t·mm²	3.4806e-004 t·mm²	2.6933e-004 t·mm²	2.0643e-004 t·mm²
Moment of Inertia Ip3	4.6465e-002 t·mm²	3.7053e-002 t·mm²	2.9184e-002 t·mm²	2.2565e-002 t·mm²	1.7192e-002 t·mm²
Statistics					

Nodes	2722	4241	2699	2687	2776
Elements	337	664	333	332	344
Mesh Metric	None				

TABLE 4
Model (B4) > Geometry > Parts

Object Name	Part 6	Part 7	Part 8	Part 9	Part 10
State	Meshed		Suppressed		
Graphics Properties					
Visible	Yes		No		
Transparency	1				
Definition					
Suppressed	No		Yes		
Stiffness Behavior	Flexible				
Coordinate System	Default Coordinate System				
Reference Temperature	By Environment				
Thickness			0. mm		
Thickness Mode			Refresh on Update		
Offset Type			Middle(Membrane)		
Material					
Assignment	carbon fiber_2				
Nonlinear Effects	Yes				
Thermal Strain Effects	Yes				
Bounding Box					
Length X	1.2192 mm	1250. mm	70. mm		
Length Y	210.41 mm	616.98 mm	381.9 mm	1.2192 mm	

Length Z	23.419 mm	30.214 mm	100. mm		
Properties					
Volume	3594.2 mm³	1.3205e+005 mm³	0. mm³	6150.6 mm³	
Mass	5.7507e-006 t	2.1128e-004 t	0. t	9.8409e-006 t	
Centroid X	1249.4 mm	606.43 mm	39.292 mm	27.174 mm	
Centroid Y	713.84 mm	372.43 mm	220.6 mm	108.61 mm	128.61 mm
Centroid Z	4.2787 mm	4.5948 mm	-50.344 mm	-42.267 mm	
Moment of Inertia Ip1	1.2968e-002 t·mm²	2.2518e-002 t·mm²	0. t·mm²	7.5809e-003 t·mm²	7.581e-003 t·mm²
Moment of Inertia Ip2	1.5338e-004 t·mm²	33.449 t·mm²	0. t·mm²	9.9696e-003 t·mm²	
Moment of Inertia Ip3	1.2816e-002 t·mm²	33.437 t·mm²	0. t·mm²	2.3911e-003 t·mm²	
Surface Area(approx.)			53622 mm²		
Statistics					
Nodes	4321	2336	0		
Elements	680	340	0		
Mesh Metric	None				

TABLE 5
Model (B4) > Geometry > Parts

Object Name	Part 11	Part 12	Part 13	Part 14
State	Suppressed			Meshed
Graphics Properties				
Visible	No			Yes
Transparency				1
Definition				

Suppressed	Yes		No	
Stiffness Behavior	Flexible			
Coordinate System	Default Coordinate System			
Reference Temperature	By Environment			
Thickness			0.6096 mm	
Thickness Mode			Manual	
Offset Type			Middle(Membrane)	
Material				
Assignment	carbon fiber_2			
Nonlinear Effects	Yes			
Thermal Strain Effects	Yes			
Bounding Box				
Length X	70. mm		65.061 mm	1250. mm
Length Y	1.2192 mm		1.4891 mm	839.54 mm
Length Z	100. mm		91.094 mm	30.321 mm
Properties				
Volume	6150.6 mm³		5371.8 mm³	3.8844e+005 mm³
Mass	9.8409e-006 t		8.5948e-006 t	6.215e-004 t
Centroid X	27.174 mm	27.173 mm	24.663 mm	591.68 mm
Centroid Y	270.61 mm	289.39 mm	389.41 mm	422.6 mm
Centroid Z	-42.267 mm	-42.222 mm	-36.995 mm	3.9367 mm
Moment of Inertia Ip1	7.5809e-003 t·mm²	7.5613e-003 t·mm²	5.414e-003 t·mm²	2.8201 t·mm²
Moment of Inertia Ip2	9.9695e-003 t·mm²	9.947e-003 t·mm²	7.2346e-003 t·mm²	98.755 t·mm²
Moment of Inertia Ip3	2.391e-003 t·mm²	2.3882e-003 t·mm²	1.8229e-003 t·mm²	101.47 t·mm²
Surface Area(approx.)				6.3721e+005 mm²

Statistics		
Nodes	0	5507
Elements	0	10761
Mesh Metric	None	

Coordinate Systems

TABLE 6
Model (B4) > Coordinate Systems > Coordinate System

Object Name	<i>Global Coordinate System</i>
State	Fully Defined
Definition	
Type	Cartesian
Ansys System Number	0.
Origin	
Origin X	0. mm
Origin Y	0. mm
Origin Z	0. mm
Directional Vectors	
X Axis Data	[1. 0. 0.]
Y Axis Data	[0. 1. 0.]
Z Axis Data	[0. 0. 1.]

Connections

TABLE 7
Model (B4) > Connections

Object Name	<i>Connections</i>
State	Fully Defined
Auto Detection	
Generate Contact On Update	Yes

Tolerance Type	Slider
Tolerance Slider	0.
Tolerance Value	3.7765 mm
Face/Face	Yes
Face/Edge	No
Edge/Edge	No
Priority	Include All
Group By	Bodies
Search Across	Bodies
Revolute Joints	Yes
Fixed Joints	Yes
Transparency	
Enabled	Yes

TABLE 8
Model (B4) > Connections > Contact Regions

Object Name	Contact Region	Contact Region 2	Contact Region 3	Contact Region 4	Contact Region 5
State	Fully Defined	Suppressed			
Scope					
Scoping Method	Geometry Selection				
Contact	1 Face	2 Faces	1 Face		2 Faces
Target	1 Face	No Selection			
Contact Bodies	Part 1				
Target Bodies	Part 7	Part 8	Part 9	Part 10	Part 11
Target Shell Face		Program Controlled			
Definition					

Type	Bonded
Scope Mode	Automatic
Behavior	Symmetric
Suppressed	No
Advanced	
Formulation	Pure Penalty
Normal Stiffness	Program Controlled
Update Stiffness	Never
Pinball Region	Program Controlled

TABLE 9
Model (B4) > Connections > Contact Regions

Model (B4) > Connections > Contact Regions					
Object Name	Contact Region 6	Contact Region 7	Contact Region 8	Contact Region 9	Contact Region 10
State	Suppressed	Fully Defined			
Scope					
Scoping Method	Geometry Selection				
Contact	2 Faces	3 Faces			
Target	No Selection	3 Faces			
Contact Bodies	Part 1		Part 2	Part 3	Part 4
Target Bodies	Part 12	Part 14			
Target Shell Face		Program Controlled			
Definition					
Type	Bonded				
Scope Mode	Automatic				
Behavior	Symmetric				
Suppressed	No				

Advanced	
Formulation	Pure Penalty
Normal Stiffness	Program Controlled
Update Stiffness	Never
Pinball Region	Program Controlled

TABLE 10
Model (B4) > Connections > Contact Regions

Object Name	Contact Region 11	Contact Region 12	Contact Region 13	Contact Region 14	Contact Region 15
State	Fully Defined				Suppressed
Scope					
Scoping Method	Geometry Selection				
Contact	3 Faces	1 Face	3 Faces	2 Faces	No Selection
Target	3 Faces	1 Face	3 Faces	2 Faces	No Selection
Contact Bodies	Part 5	Part 6		Part 7	Part 8
Target Bodies	Part 14	Part 7	Part 14		Part 9
Target Shell Face	Program Controlled		Program Controlled		
Contact Shell Face					Program Controlled
Definition					
Type	Bonded				
Scope Mode	Automatic				
Behavior	Symmetric				
Suppressed	No				
Advanced					
Formulation	Pure Penalty				



Normal Stiffness	Program Controlled
Update Stiffness	Never
Pinball Region	Program Controlled

TABLE 11
Model (B4) > Connections > Contact Regions

Object Name	Contact Region 16	Contact Region 17	Contact Region 18	Contact Region 19	Contact Region 20
State	Suppressed				
Scope					
Scoping Method	Geometry Selection				
Contact	No Selection				
Target	No Selection				2 Faces
Contact Bodies	Part 8				
Target Bodies	Part 10	Part 11	Part 12	Part 13	Part 14
Contact Shell Face	Program Controlled				
Target Shell Face					Program Controlled
Definition					
Type	Bonded				
Scope Mode	Automatic				
Behavior	Symmetric				
Suppressed	No				
Advanced					
Formulation	Pure Penalty				
Normal Stiffness	Program Controlled				
Update Stiffness	Never				

Pinball Region	Program Controlled
----------------	--------------------

TABLE 12
Model (B4) > Connections > Contact Regions

Object Name	Contact Region 21	Contact Region 22
State	Suppressed	
Scope		
Scoping Method	Geometry Selection	
Contact	No Selection	
Target	2 Faces	
Contact Bodies	Part 11	Part 12
Target Bodies	Part 14	
Target Shell Face	Program Controlled	
Definition		
Type	Bonded	
Scope Mode	Automatic	
Behavior	Symmetric	
Suppressed	No	
Advanced		
Formulation	Pure Penalty	
Normal Stiffness	Program Controlled	
Update Stiffness	Never	
Pinball Region	Program Controlled	

Mesh

TABLE 13
Model (B4) > Mesh

Object Name	<i>Mesh</i>
State	Solved

Defaults	
Physics Preference	Mechanical
Relevance	0
Sizing	
Use Advanced Size Function	On: Curvature
Relevance Center	Fine
Initial Size Seed	Active Assembly
Smoothing	Medium
Transition	Fast
Span Angle Center	Fine
Curvature Normal Angle	Default (18.0 °)
Min Size	Default (0.219860 mm)
Max Face Size	Default (21.9860 mm)
Max Tet Size	Default (43.9730 mm)
Growth Rate	Default (1.850)
Minimum Edge Length	2.3089e-003 mm
Inflation	
Use Automatic Tet Inflation	None
Inflation Option	Smooth Transition
Transition Ratio	0.272
Maximum Layers	5
Growth Rate	1.2
Inflation Algorithm	Pre
View Advanced Options	No
Advanced	

Shape Checking	Standard Mechanical
Element Midside Nodes	Program Controlled
Straight Sided Elements	No
Number of Retries	0
Rigid Body Behavior	Dimensionally Reduced
Mesh Morphing	Disabled
Pinch	
Pinch Tolerance	Default (0.197880 mm)
Generate on Refresh	No
Statistics	
Nodes	27289
Elements	13791
Mesh Metric	None

TABLE 14
Model (B4) > Mesh > Mesh Controls

Object Name	<i>Mapped Face Meshing</i>
State	Ignored
Scope	
Scoping Method	Geometry Selection
Geometry	2 Faces
Definition	
Suppressed	No
Method	Triangles: Best Split
Constrain Boundary	No
Advanced	
Specified Sides	None

Specified Corners	None
Specified Ends	None

Static Structural (B5)

TABLE 15
Model (B4) > Analysis

Object Name	<i>Static Structural (B5)</i>
State	Solved
Definition	
Physics Type	Structural
Analysis Type	Static Structural
Solver Target	ANSYS Mechanical
Options	
Environment Temperature	22. °C
Generate Input Only	No

TABLE 16
Model (B4) > Static Structural (B5) > Analysis Settings

Object Name	<i>Analysis Settings</i>
State	Fully Defined
Step Controls	
Number Of Steps	1.
Current Step Number	1.
Step End Time	1. s
Auto Time Stepping	Program Controlled
Solver Controls	
Solver Type	Program Controlled
Weak Springs	Program Controlled
Large Deflection	Off



Inertia Relief	Off
Nonlinear Controls	
Force Convergence	Program Controlled
Moment Convergence	Program Controlled
Displacement Convergence	Program Controlled
Rotation Convergence	Program Controlled
Line Search	Program Controlled
Output Controls	
Calculate Stress	Yes
Calculate Strain	Yes
Calculate Results At	All Time Points
Analysis Data Management	
Solver Files Directory	F:\Data\Ansys\structural design2\Wing structure_files\dp0\SYS\MECH\
Future Analysis	None
Scratch Solver Files Directory	
Save ANSYS db	No
Delete Unneeded Files	Yes
Nonlinear Solution	No
Solver Units	Active System
Solver Unit System	nmm

TABLE 17
Model (B4) > Static Structural (B5) > Imported Load (Solution)

Object Name	<i>Imported Load (Solution)</i>
State	Fully Defined
Definition	
Type	Imported Data

Interpolation Type	CFD Results Interpolator
Suppressed	No

TABLE 18
Model (B4) > Static Structural (B5) > Imported Load (Solution) > Imported Pressure

Object Name	<i>Imported Pressure</i>
State	Solved
Scope	
Scoping Method	Geometry Selection
Geometry	3 Faces
Definition	
Type	Imported Pressure
Suppressed	No
Transfer Definition	
CFD Surface	ing
CFD Data	
CFD Results File	F:\Data\Ansys\structural design2\Wing structure_files\dp0\SYS\MECH\Solution\Fluid Flow_001.res

Model (B4) > Static Structural (B5) > Imported Load (Solution) > Imported Pressure > Imported Load Transfer Summary

CFD Load Transfer Summary

CFD Computed Forces from CFD Results File **F:\Data\Ansys\structural design2\Wing structure_files\dp0\SYS\MECH\Solution\Fluid Flow_001.res**

X-component = 0.84054 N

Y-component = -0.74477 N

Z-component = 23.557 N

Mechanical Mapped Forces for Mechanical Surface File **F:\Data\Ansys\structural design2\Wing structure_files\dp0\SYS\MECH\Import_ANSYS_131.cdb**

X-component = 0.77517 N

Y-component = -0.71702 N

Z-component = 23.532 N

98% of Mechanical nodes were mapped to the CFD surface, remaining nodes mapped to closest edge or node.

TABLE 19
Model (B4) > Static Structural (B5) > Loads

Object Name	<i>Simply Supported</i>	<i>Simply Supported 2</i>	<i>Fixed Support</i>
State	Fully Defined		
Scope			
Scoping Method	Geometry Selection		
Geometry	1 Edge	1 Face	
Definition			
Type	Simply Supported		Fixed Support
Suppressed	No		

Solution (B6)

TABLE 20
Model (B4) > Static Structural (B5) > Solution

Object Name	<i>Solution (B6)</i>
State	Solved
Adaptive Mesh Refinement	
Max Refinement Loops	1.
Refinement Depth	2.

TABLE 21
Model (B4) > Static Structural (B5) > Solution (B6) > Solution Information

Object Name	<i>Solution Information</i>
State	Solved
Solution Information	
Solution Output	Solver Output
Newton-Raphson Residuals	0

Update Interval	2.5 s
Display Points	All

TABLE 22
Model (B4) > Static Structural (B5) > Solution (B6) > Results

Object Name	Total Deformation	Equivalent Elastic Strain
State	Solved	
Scope		
Scoping Method	Geometry Selection	
Geometry	All Bodies	
Shell		Top/Bottom
Definition		
Type	Total Deformation	Equivalent (von-Mises) Elastic Strain
By	Time	
Display Time	Last	
Calculate Time History	Yes	
Identifier		
Use Average		Yes
Results		
Minimum	0. mm	5.3209e-007 mm/mm
Maximum	10.452 mm	6.9077e-003 mm/mm
Minimum Occurs On	Part 7	Part 6
Maximum Occurs On	Part 14	Part 6
Information		
Time	1. s	
Load Step	1	
Substep	1	

Iteration Number	1
------------------	---

TABLE 23
Model (B4) > Static Structural (B5) > Solution (B6) > Stress Safety Tools

Object Name	<i>Stress Tool</i>
State	Solved
Definition	
Theory	Max Equivalent Stress
Stress Limit Type	Tensile Yield Per Material

TABLE 24
Model (B4) > Static Structural (B5) > Solution (B6) > Stress Tool > Results

Object Name	<i>Safety Factor</i>
State	Solved
Scope	
Scoping Method	Geometry Selection
Geometry	All Bodies
Definition	
Type	Safety Factor
By	Time
Display Time	Last
Calculate Time History	Yes
Use Average	Yes
Identifier	
Results	
Minimum	1.4716
Minimum Occurs On	Part 6
Information	

Time	1. s
Load Step	1
Substep	1
Iteration Number	1

TABLE 25
Model (B4) > Static Structural (B5) > Solution (B6) > Results

Object Name	<i>Equivalent Stress</i>
State	Solved
Scope	
Scoping Method	Geometry Selection
Geometry	All Bodies
Shell	Top/Bottom
Definition	
Type	Equivalent (von-Mises) Stress
By	Time
Display Time	Last
Calculate Time History	Yes
Use Average	Yes
Identifier	
Results	
Minimum	2.3537e-002 MPa
Maximum	305.57 MPa
Minimum Occurs On	Part 6
Maximum Occurs On	Part 6
Information	
Time	1. s

Load Step	1
Substep	1
Iteration Number	1

Material Data

Carbon fiber_2

TABLE 26
carbon fiber_2 > Constants

Density	1.6e-009 tonne mm ⁻³
---------	---------------------------------

TABLE 27
carbon fiber_2 > Isotropic Elasticity

Temperature C	Young's Modulus MPa	Poisson's Ratio
	44236	0.335

TABLE 28
carbon fiber_2 > Tensile Yield Strength

Tensile Yield Strength MPa
449.68

TABLE 29
carbon fiber_2 > Compressive Yield Strength

Compressive Yield Strength MPa
469.67

TABLE 30
carbon fiber_2 > Tensile Ultimate Strength

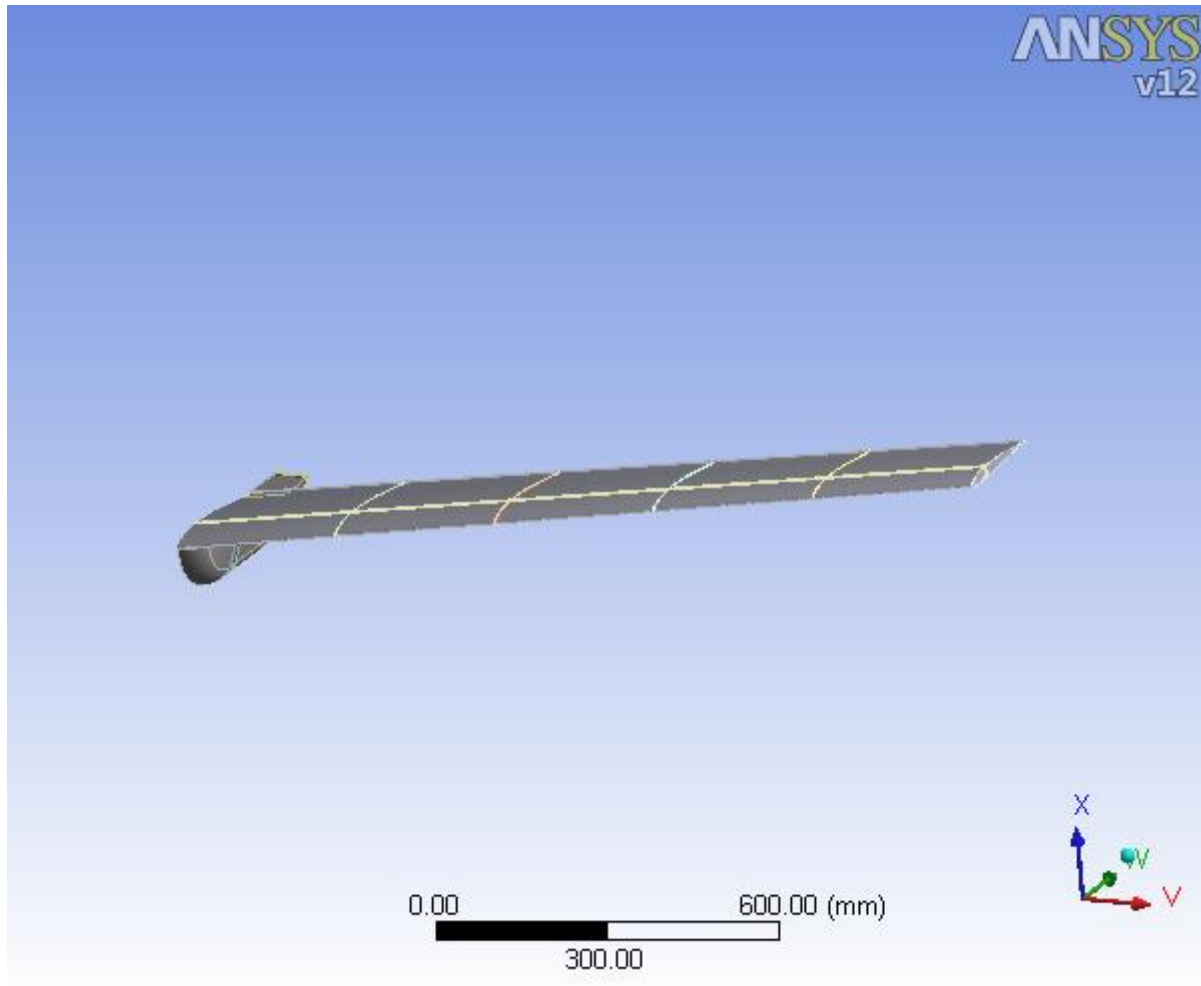
Tensile Ultimate Strength MPa
539.62

TABLE 31
carbon fiber_2 > Compressive Ultimate Strength

Compressive Ultimate Strength MPa
563.6

Appendix B: The ANSYS Report for mode 2

First Saved	Thursday, July 22, 2010
Last Saved	Friday, July 23, 2010
Product Version	12.0.1 Release



Units

TABLE 1

Unit System	Metric (mm, t, N, s, mV, mA) Degrees rad/s Celsius
Angle	Degrees
Rotational Velocity	rad/s

Temperature	Celsius
-------------	---------

Model (B4)**Geometry**

TABLE 2
Model (B4) > Geometry

Object Name	<i>Geometry</i>
State	Fully Defined
Definition	
Source	F:\Data\Ansys\Structural design\The aircraft solid model_2.igs
Type	Iges
Length Unit	Meters
Element Control	Program Controlled
Display Style	Part Color
Bounding Box	
Length X	1250. mm
Length Y	839.54 mm
Length Z	120.65 mm
Properties	
Volume	4.3617e+005 mm ³
Mass	6.9788e-004 t
Scale Factor Value	1.
Statistics	
Bodies	14
Active Bodies	14
Nodes	91115
Elements	27276



Mesh Metric	None
Preferences	
Import Solid Bodies	Yes
Import Surface Bodies	Yes
Import Line Bodies	No
Parameter Processing	Yes
Personal Parameter Key	DS
CAD Attribute Transfer	No
Named Selection Processing	No
Material Properties Transfer	No
CAD Associativity	Yes
Import Coordinate Systems	No
Reader Save Part File	No
Import Using Instances	Yes
Do Smart Update	No
Attach File Via Temp File	Yes
Temporary Directory	C:\Users\Mohamed\AppData\Local\Temp
Analysis Type	3-D
Mixed Import Resolution	None
Enclosure and Symmetry Processing	Yes

TABLE 3
Model (B4) > Geometry > Parts

Object Name	Part 1	Part 2	Part 3	Part 4	Part 5
State	Meshed				
Graphics Properties					
Visible	Yes				

Transparency	1				
Definition					
Suppressed	No				
Stiffness Behavior	Flexible				
Coordinate System	Default Coordinate System				
Reference Temperature	By Environment				
Material					
Assignment	carbon fiber_2				
Nonlinear Effects	Yes				
Thermal Strain Effects	Yes				
Bounding Box					
Length X	1.2192 mm				
Length Y	290.54 mm	274.51 mm	258.49 mm	242.46 mm	226.44 mm
Length Z	30.336 mm	28.824 mm	27.367 mm	25.973 mm	24.652 mm
Properties					
Volume	6846.4 mm³	6111.6 mm³	5418.7 mm³	4767.5 mm³	4158.8 mm³
Mass	1.0954e-005 t	9.7786e-006 t	8.6699e-006 t	7.628e-006 t	6.654e-006 t
Centroid X	0.60954 mm	250.37 mm	500.12 mm	749.88 mm	999.63 mm
Centroid Y	116.98 mm	236.48 mm	355.87 mm	475.17 mm	594.51 mm
Centroid Z	4.5101 mm	4.433 mm	4.394 mm	4.3528 mm	4.3021 mm
Moment of Inertia Ip1	4.7029e-002 t·mm²	3.7493e-002 t·mm²	2.953e-002 t·mm²	2.2832e-002 t·mm²	1.7397e-002 t·mm²
Moment of Inertia Ip2	5.6689e-004 t·mm²	4.4296e-004 t·mm²	3.4806e-004 t·mm²	2.6933e-004 t·mm²	2.0643e-004 t·mm²
Moment of Inertia Ip3	4.6465e-002 t·mm²	3.7053e-002 t·mm²	2.9184e-002 t·mm²	2.2565e-002 t·mm²	1.7192e-002 t·mm²

Statistics					
Nodes	3000	2867	2844	2786	2895
Elements	376	357	353	344	361
Mesh Metric	None				

TABLE 4
Model (B4) > Geometry > Parts

Object Name	Part 6	Part 7	Part 8	Part 9	Part 10
State	Meshed				
Graphics Properties					
Visible	Yes				
Transparency	1				
Definition					
Suppressed	No				
Stiffness Behavior	Flexible				
Coordinate System	Default Coordinate System				
Reference Temperature	By Environment				
Thickness			0.9144 mm		
Thickness Mode			Manual		
Offset Type			Middle(Membrane)		
Material					
Assignment	carbon fiber_2				
Nonlinear Effects	Yes				
Thermal Strain Effects	Yes				
Bounding Box					
Length X	1.2192 mm	1250. mm	70. mm		

Length Y	210.41 mm	616.98 mm	381.9 mm	1.2192 mm	
Length Z	23.419 mm	30.214 mm	100. mm		
Properties					
Volume	3594.2 mm³	1.3205e+005 mm³	49032 mm³	6150.6 mm³	
Mass	5.7507e-006 t	2.1128e-004 t	7.8452e-005 t	9.8409e-006 t	
Centroid X	1249.4 mm	606.43 mm	39.292 mm	27.174 mm	
Centroid Y	713.84 mm	372.43 mm	220.6 mm	108.61 mm	128.61 mm
Centroid Z	4.2787 mm	4.5948 mm	-50.344 mm	-42.267 mm	
Moment of Inertia Ip1	1.2968e-002 t·mm²	2.2518e-002 t·mm²	1.07 t·mm²	7.5809e-003 t·mm²	7.581e-003 t·mm²
Moment of Inertia Ip2	1.5338e-004 t·mm²	33.449 t·mm²	0.1124 t·mm²	9.9696e-003 t·mm²	
Moment of Inertia Ip3	1.2816e-002 t·mm²	33.437 t·mm²	0.99432 t·mm²	2.3911e-003 t·mm²	
Surface Area(approx.)			53622 mm²		
Statistics					
Nodes	2872	2336	1922	12295	12776
Elements	357	340	1832	1696	1764
Mesh Metric	None				

TABLE 5
Model (B4) > Geometry > Parts

Object Name	Part 11	Part 12	Part 13	Part 14
State	Meshed			
Graphics Properties				
Visible	Yes			
Transparency	1			

Definition				
Suppressed	No			
Stiffness Behavior	Flexible			
Coordinate System	Default Coordinate System			
Reference Temperature	By Environment			
Thickness				0.3048 mm
Thickness Mode				Manual
Offset Type				Middle(Membrane)
Material				
Assignment	carbon fiber_2			
Nonlinear Effects	Yes			
Thermal Strain Effects	Yes			
Bounding Box				
Length X	70. mm		65.061 mm	1250. mm
Length Y	1.2192 mm		1.4891 mm	839.54 mm
Length Z	100. mm		91.094 mm	30.321 mm
Properties				
Volume	6150.6 mm³		5371.8 mm³	1.9422e+005 mm³
Mass	9.8409e-006 t		8.5948e-006 t	3.1075e-004 t
Centroid X	27.174 mm	27.173 mm	24.663 mm	591.68 mm
Centroid Y	270.61 mm	289.39 mm	389.41 mm	422.6 mm
Centroid Z	-42.267 mm	-42.222 mm	-36.995 mm	3.9367 mm
Moment of Inertia Ip1	7.5809e-003 t·mm²	7.5613e-003 t·mm²	5.414e-003 t·mm²	1.41 t·mm²
Moment of Inertia Ip2	9.9695e-003 t·mm²	9.947e-003 t·mm²	7.2346e-003 t·mm²	49.378 t·mm²
Moment of Inertia Ip3	2.391e-003 t·mm²	2.3882e-003 t·mm²	1.8229e-003 t·mm²	50.736 t·mm²

Surface Area(approx.)				6.3721e+005 mm²
Statistics				
Nodes	12776	12185	12237	7324
Elements	1764	1681	1687	14364
Mesh Metric	None			

Coordinate Systems

TABLE 6
Model (B4) > Coordinate Systems > Coordinate System

Object Name	<i>Global Coordinate System</i>
State	Fully Defined
Definition	
Type	Cartesian
Ansys System Number	0.
Origin	
Origin X	0. mm
Origin Y	0. mm
Origin Z	0. mm
Directional Vectors	
X Axis Data	[1. 0. 0.]
Y Axis Data	[0. 1. 0.]
Z Axis Data	[0. 0. 1.]

Connections

TABLE 7
Model (B4) > Connections

Object Name	<i>Connections</i>
State	Fully Defined
Auto Detection	



Generate Contact On Update	Yes
Tolerance Type	Slider
Tolerance Slider	0.
Tolerance Value	3.7765 mm
Face/Face	Yes
Face/Edge	No
Edge/Edge	No
Priority	Include All
Group By	Bodies
Search Across	Bodies
Revolute Joints	Yes
Fixed Joints	Yes
Transparency	
Enabled	Yes

TABLE 8
Model (B4) > Connections > Contact Regions

Object Name	Contact Region	Contact Region 2	Contact Region 3	Contact Region 4	Contact Region 5
State	Fully Defined				
Scope					
Scoping Method	Geometry Selection				
Contact	1 Face	2 Faces	1 Face		2 Faces
Target	1 Face				2 Faces
Contact Bodies	Part 1				
Target Bodies	Part 7	Part 8	Part 9	Part 10	Part 11
Target Shell Face		Program Controlled			

Definition	
Type	Bonded
Scope Mode	Automatic
Behavior	Symmetric
Suppressed	No
Advanced	
Formulation	Pure Penalty
Normal Stiffness	Program Controlled
Update Stiffness	Never
Pinball Region	Program Controlled

TABLE 9
Model (B4) > Connections > Contact Regions

Object Name	Contact Region 6	Contact Region 7	Contact Region 8	Contact Region 9	Contact Region 10
State	Fully Defined				
Scope					
Scoping Method	Geometry Selection				
Contact	2 Faces	3 Faces			
Target	2 Faces	3 Faces			
Contact Bodies	Part 1		Part 2	Part 3	Part 4
Target Bodies	Part 12	Part 14			
Target Shell Face		Program Controlled			
Definition					
Type	Bonded				
Scope Mode	Automatic				
Behavior	Symmetric				

Suppressed	No
Advanced	
Formulation	Pure Penalty
Normal Stiffness	Program Controlled
Update Stiffness	Never
Pinball Region	Program Controlled

TABLE 10
Model (B4) > Connections > Contact Regions

Object Name	Contact Region 11	Contact Region 12	Contact Region 13	Contact Region 14	Contact Region 15
State	Fully Defined				
Scope					
Scoping Method	Geometry Selection				
Contact	3 Faces	1 Face	3 Faces	2 Faces	
Target	3 Faces	1 Face	3 Faces	2 Faces	
Contact Bodies	Part 5	Part 6		Part 7	Part 8
Target Bodies	Part 14	Part 7	Part 14		Part 9
Target Shell Face	Program Controlled		Program Controlled		
Contact Shell Face					Program Controlled
Definition					
Type	Bonded				
Scope Mode	Automatic				
Behavior	Symmetric				
Suppressed	No				
Advanced					

Formulation	Pure Penalty
Normal Stiffness	Program Controlled
Update Stiffness	Never
Pinball Region	Program Controlled

TABLE 11
Model (B4) > Connections > Contact Regions

Object Name	Contact Region 16	Contact Region 17	Contact Region 18	Contact Region 19	Contact Region 20
State	Fully Defined				
Scope					
Scoping Method	Geometry Selection				
Contact	2 Faces			3 Faces	1 Face
Target	2 Faces			4 Faces	2 Faces
Contact Bodies	Part 8				
Target Bodies	Part 10	Part 11	Part 12	Part 13	Part 14
Contact Shell Face	Program Controlled				
Target Shell Face					Program Controlled
Definition					
Type	Bonded				
Scope Mode	Automatic				
Behavior	Symmetric				
Suppressed	No				
Advanced					
Formulation	Pure Penalty				
Normal Stiffness	Program Controlled				



Update Stiffness	Never
Pinball Region	Program Controlled

TABLE 12
Model (B4) > Connections > Contact Regions

Object Name	Contact Region 21	Contact Region 22
State	Fully Defined	
Scope		
Scoping Method	Geometry Selection	
Contact	1 Face	
Target	2 Faces	
Contact Bodies	Part 11	Part 12
Target Bodies	Part 14	
Target Shell Face	Program Controlled	
Definition		
Type	Bonded	
Scope Mode	Automatic	
Behavior	Symmetric	
Suppressed	No	
Advanced		
Formulation	Pure Penalty	
Normal Stiffness	Program Controlled	
Update Stiffness	Never	
Pinball Region	Program Controlled	

Mesh

TABLE 13
Model (B4) > Mesh

Object Name	<i>Mesh</i>
-------------	-------------

State	Solved
Defaults	
Physics Preference	Mechanical
Relevance	0
Sizing	
Use Advanced Size Function	On: Curvature
Relevance Center	Fine
Initial Size Seed	Active Assembly
Smoothing	Medium
Transition	Slow
Span Angle Center	Medium
Curvature Normal Angle	Default (45.0 °)
Min Size	Default (0.220520 mm)
Max Face Size	Default (22.0520 mm)
Max Tet Size	Default (44.1050 mm)
Growth Rate	Default (1.20)
Minimum Edge Length	2.3089e-003 mm
Inflation	
Use Automatic Tet Inflation	None
Inflation Option	Smooth Transition
Transition Ratio	0.272
Maximum Layers	5
Growth Rate	1.2
Inflation Algorithm	Pre
View Advanced Options	No

Advanced	
Shape Checking	Standard Mechanical
Element Midside Nodes	Program Controlled
Straight Sided Elements	No
Number of Retries	0
Rigid Body Behavior	Dimensionally Reduced
Mesh Morphing	Disabled
Pinch	
Pinch Tolerance	Default (0.198470 mm)
Generate on Refresh	No
Statistics	
Nodes	91115
Elements	27276
Mesh Metric	None

TABLE 14
Model (B4) > Mesh > Mesh Controls

Object Name	<i>Mapped Face Meshing</i>
State	Ignored
Scope	
Scoping Method	Geometry Selection
Geometry	2 Faces
Definition	
Suppressed	No
Method	Triangles: Best Split
Constrain Boundary	No
Advanced	

Specified Sides	None
Specified Corners	None
Specified Ends	None

Static Structural (B5)

TABLE 15
Model (B4) > Analysis

Object Name	<i>Static Structural (B5)</i>
State	Solved
Definition	
Physics Type	Structural
Analysis Type	Static Structural
Solver Target	ANSYS Mechanical
Options	
Environment Temperature	22. °C
Generate Input Only	No

TABLE 16
Model (B4) > Static Structural (B5) > Analysis Settings

Object Name	<i>Analysis Settings</i>
State	Fully Defined
Step Controls	
Number Of Steps	1.
Current Step Number	1.
Step End Time	1. s
Auto Time Stepping	Program Controlled
Solver Controls	
Solver Type	Program Controlled
Weak Springs	Program Controlled

Large Deflection	Off
Inertia Relief	Off
Nonlinear Controls	
Force Convergence	Program Controlled
Moment Convergence	Program Controlled
Displacement Convergence	Program Controlled
Rotation Convergence	Program Controlled
Line Search	Program Controlled
Output Controls	
Calculate Stress	Yes
Calculate Strain	Yes
Calculate Results At	All Time Points
Analysis Data Management	
Solver Files Directory	F:\Data\Ansys\structural design2\sd_files\dp0\SYS\MECH\
Future Analysis	None
Scratch Solver Files Directory	
Save ANSYS db	No
Delete Unneeded Files	Yes
Nonlinear Solution	No
Solver Units	Active System
Solver Unit System	nmm

TABLE 17
Model (B4) > Static Structural (B5) > Loads

Object Name	Fixed Support	Fixed Support 2	Force
State	Fully Defined		
Scope			

Scoping Method	Geometry Selection		
Geometry	2 Faces	9 Edges	1 Face
Definition			
Type	Fixed Support		Force
Suppressed	No		
Define By			Vector
Magnitude			156. N (ramped)
Direction			Defined

FIGURE 1
Model (B4) > Static Structural (B5) > Force

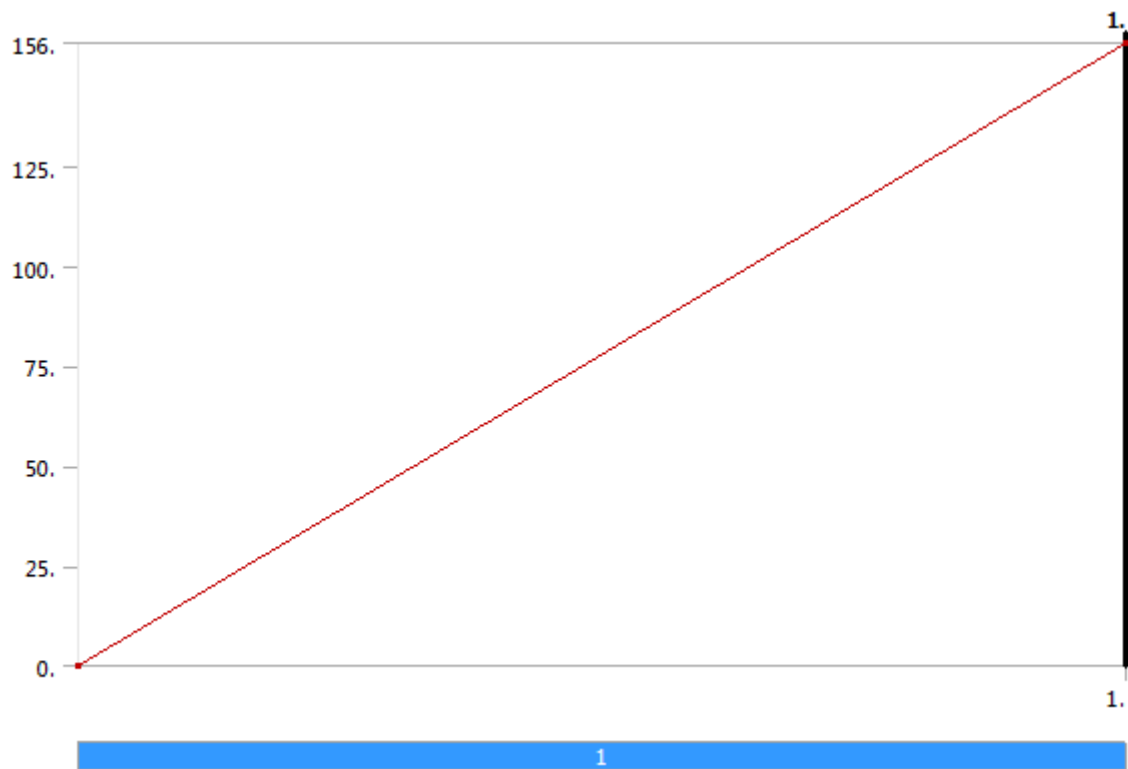


TABLE 18
Model (B4) > Static Structural (B5) > Imported Load (Solution)

Object Name	<i>Imported Load (Solution)</i>
State	Fully Defined

Definition	
Type	Imported Data
Interpolation Type	CFD Results Interpolator
Suppressed	No

TABLE 19

Model (B4) > Static Structural (B5) > Imported Load (Solution) > Imported Pressure

Object Name	<i>Imported Pressure</i>
State	Solved
Scope	
Scoping Method	Geometry Selection
Geometry	9 Faces
Definition	
Type	Imported Pressure
Suppressed	No
Transfer Definition	
CFD Surface	wing
CFD Data	
CFD Results File	F:\Data\Ansys\structural design2\sd_files\dp0\SYS\MECH\Solution\Fluid Flow_001.res

Model (B4) > Static Structural (B5) > Imported Load (Solution) > Imported Pressure > Imported Load Transfer Summary

CFD Load Transfer Summary

CFD Computed Forces from CFD Results File F:\Data\Ansys\structural design2\sd_files\dp0\SYS\MECH\Solution\Fluid Flow_001.res

X-component = 1.1299 N

Y-component = -0.49114 N

Z-component = 22.612 N

Mechanical Mapped Forces for Mechanical Surface File F:\Data\Ansys\structural design2\sd_files\dp0\SYS\MECH\Import_ANSYS_134.cdb

X-component = 1.1112 N

Y-component = -0.5867 N

Z-component = 23.219 N

99% of Mechanical nodes were mapped to the CFD surface, remaining nodes mapped to closest edge or node.

Solution (B6)

TABLE 20
Model (B4) > Static Structural (B5) > Solution

Object Name	<i>Solution (B6)</i>
State	Solved
Adaptive Mesh Refinement	
Max Refinement Loops	1.
Refinement Depth	2.

TABLE 21
Model (B4) > Static Structural (B5) > Solution (B6) > Solution Information

Object Name	<i>Solution Information</i>
State	Solved
Solution Information	
Solution Output	Solver Output
Newton-Raphson Residuals	0
Update Interval	2.5 s
Display Points	All

TABLE 22
Model (B4) > Static Structural (B5) > Solution (B6) > Results

Object Name	Equivalent Stress	Total Deformation	Equivalent Elastic Strain	Equivalent Stress 2
State	Solved			
Scope				
Scoping Method	Geometry Selection			

Geometry	All Bodies			
Shell	Top/Bottom		Top/Bottom	
Definition				
Type	Equivalent (von-Mises) Stress	Total Deformation	Equivalent (von-Mises) Elastic Strain	Equivalent (von-Mises) Stress
By	Time			
Display Time	Last			
Calculate Time History	Yes			
Use Average	Yes		Yes	
Identifier				
Results				
Minimum	1.4056e-004 MPa	0. mm	3.1775e-009 mm/mm	1.4056e-004 MPa
Maximum	252.56 MPa	13.993 mm	5.7093e-003 mm/mm	252.56 MPa
Minimum Occurs On	Part 10	Part 1	Part 10	
Maximum Occurs On	Part 6	Part 14	Part 6	
Information				
Time	1. s			
Load Step	1			
Substep	1			
Iteration Number	1			

TABLE 23
Model (B4) > Static Structural (B5) > Solution (B6) > Stress Safety Tools

Object Name	<i>Stress Tool</i>
State	Solved
Definition	

Theory	Max Shear Stress
Factor	0.5
Stress Limit Type	Tensile Yield Per Material

TABLE 24
Model (B4) > Static Structural (B5) > Solution (B6) > Stress Tool > Results

Object Name	<i>Safety Factor</i>
State	Solved
Scope	
Scoping Method	Geometry Selection
Geometry	All Bodies
Definition	
Type	Safety Factor
By	Time
Display Time	Last
Calculate Time History	Yes
Use Average	Yes
Identifier	
Results	
Minimum	1.5921
Minimum Occurs On	Part 6
Information	
Time	1. s
Load Step	1
Substep	1
Iteration Number	1

Material Data

Carbon fiber_2

TABLE 25
carbon fiber_2 > Constants

Density	1.6e-009 tonne mm ⁻³
---------	---------------------------------

TABLE 26
carbon fiber_2 > Isotropic Elasticity

Temperature C	Young's Modulus MPa	Poisson's Ratio
	44236	0.335

TABLE 27
carbon fiber_2 > Tensile Yield Strength

Tensile Yield Strength MPa
449.68

TABLE 28
carbon fiber_2 > Compressive Yield Strength

Compressive Yield Strength MPa
469.67

TABLE 29
carbon fiber_2 > Tensile Ultimate Strength

Tensile Ultimate Strength MPa
539.62

TABLE 30
carbon fiber_2 > Compressive Ultimate Strength

Compressive Ultimate Strength MPa
563.6



References:

- Karl Nickel, Michael Wohlfahrt, "Tailless Aircraft".
- John D. Anderson, "Aircraft Performance and design".
- John D. Anderson, "Introduction to Flight".
- B.C. Hoskin, and A.A. Baker, "Composite Materials for Aircraft Structures".
- Alan Baker, "Composite Materials for Aircraft Structures".
- Ever J. Barbero, "Introduction to Composite Materials Design".
- Mike Niu, "Airframe Structural Design".
- Michael Chun-yung Niu, "Composite Airframe Structure".
- Brian L. Stevens, Frank L. Lewis, "Aircraft Control and simulation".
- MATLAB Program.
- J. E. ASHTON, J. C. HALPIN, P. H. PETIT, "PRIMER ON COMPOSITE MATERIALS ANALYSIS".
- Engineering Materials Handbook, Volume 1.
- Jan Roskam, "Airplane Design", Level 3.